Invited Speaker

115 Electron Videography and Machine Learning of Soft Matter
Prof. Qian Chen[1], Lehan Yao
[1]Department of Materials Science and Engineering, University of Illinois, Urbana, United States
42 Nanoparticle size estimation by HR-STEM and generative AI

Oral Presentation

Henrik Eliasson[1], Mr. Angus Lothian[2], Mr Ivan Surin[3], Dr. Sharon Mitchell[3], Professor Javier Pérez-Ramírez[3], Professor Rolf Erni[1]
[1]Electron Microscopy Center, Empa – Swiss Federal Laboratories for Materials Science and Technology, Dübendorf, Switzerland, [2]Computer Vision Laboratory, Department of Electrical Engineering, Linköping University, Linköping, Sweden, [3]Department of Chemistry and Applied Biosciences, ETH Zürich, Zürich, Switzerland
406 NP-SAM: Implementing the Segment Anything Model for Easy Nanoparticle Segmentation and Analysis in Electron Microscopy
Rasmus Larsen[1], Mr. Torben L. Villadsen[1], Ms. Jette K. Mathiesen[2], Ms. Kirsten M. Ø. Jensen[3], Mr. Espen D. Bøjesen[1]
[1]Interdisciplinary Nanoscience Center & Aarhus University Centre for Integrated Materials Research, Aarhus University, Aarhus, Denmark, [2]Surface Physics & Catalysis (SURFCAT), Department of Physics, Technical University of Denmark, Kongens Lyngby, Denmark, [3]Department of Chemistry, University of Copenhagen, Copenhagen, Denmark
410 Characterization of structure and mixing in nanoparticle hetero-aggregates using convolutional neural networks: 3D-reconstruction versus 2D-projection
Dr. Christoph Mahr[1], Dr. Florian Krause[1], Jakob Stahl[2], Beeke Gerken[1], Dr. Marco Schowalter[1], Dr. Tim Grieb[1], Prof. Dr.-Ing. Lutz Mädler, Prof. Dr. Andreas Rosenauer
[1]Universität Bremen, Bremen, Germany, [2]Leibniz Institut für Werkstofforientierte Technologien, Bremen, Germany
661 Deep convolutional neural networks for atomic imaging in STEM
Mr Alex Williams[1], Mr Jack Wells[1,2], Dr Alex Robinson[3], Dr Daniel Nicholls[3], Dr Amirafshar Moshtaghpour[2,4], Prof Angus Kirkland[4,5], Dr Konstantinos Tsakalidis[6], Prof Yao-chun Shen[7], Prof Nigel Browning[2,3]
[1]Distributed Algorithms Centre of Doctoral Training, University of Liverpool, Liverpool, United Kingdom, [2]Mechanical Materials and Aerospace Engineering, University of Liverpool, Liverpool, United Kingdom, [3]SenseAI Innovations Ltd., Brodie Tower, University of Liverpool, Liverpool, United Kingdom, [4]Rosalind Franklin Institute, Harwell Science & Innovation Campus, Didcot, United Kingdom, [5]Department of Materials, University of Oxford, Oxford, United Kingdom, [6]Department of Computer Science, University of Liverpool, Liverpool, United Kingdom, [7]Department of Electrical Engineering and Electronics, University of Liverpool, Liverpool, United Kingdom
672 Unsupervised Machine Learning-based STEM diffraction pattern denoising for enhanced grain visualization in phase change materials
Karina Ruzaeva[1], Dr. Dieter Weber[2], Jonas Werner[3], Prof. Stefan Sandfeld[1]
[1]IAS-9, Forschungszentrum Jülich, Jülich, Germany, [2]ERC-1, Forschungszentrum Jülich, Jülich, Germany, [3]GFE, RWTH Aachen University, Aachen, Germany
1134 Unsupervised and supervised machine learning for feature classification in atomic resolution images
Christian Liebscher[1,2], Andreas Leitherer[3], Byung Chul Yeo[4], Christoph Freysoldt[5], Luca Ghiringhelli[6]
[1]Faculty of Physics and Astronomy, Ruhr University Bochum, Bochum, Germany, [2]Research Center Future Energy Materials and Systems, Ruhr University Bochum, Bochum, Germany, [3]ICFO-Institut de

Ciencies Fotoniques, The Barcelona Institute of Science and Technology, 08860 Castelldefels (Barcelona), Spain, [4]Department of Energy Resources Engineering, Pukyong National University, Busan, Republic of Korea, [5]Max-Planck-Institute for Sustainable Materials, Düsseldorf, Germany, [6]Department of Materials Science and Engineering, Friedrich-Alexander Universität, Erlangen-Nürnberg, Germany

152 Synthetic data generation and Mask-RCNN for Transmission Electron Microscope Image Segmentation

Natalia Da Silva De Sa[1], Dr. Andrew Stewart[2]
[1]University of Limerick, Limerick, Ireland, [2]University College London, London, United Kingdom

221 Unsupervised learning assisted secondary electron hyperspectral imaging for high-throughput cheminformatics analysis of materials

Jinggiong Zhang[1], James Nohl[2], Nicholas Farr[3], Cornelia Rodenburg[3], Lyudmila Mihaylova[1]
[1]Department of Automatic Control and Systems Engineering, The University of Sheffield, Sheffield, UK, [2]Department of Materials Science and Engineering, The Faraday Institution, The University of Sheffield, Sheffield, UK, [3]Department of Materials Science and Engineering, The University of Sheffield, Sheffield, UK

286 3D fruit microstructure characterization using micro-CT imaging and deep learning-based panoptic segmentation

Leen Van Doorselaer[1], Dr. Pieter Verboven[1], Prof. Bart Nicolaï[1,2]
[1]BIOSYST-MeBioS, Postharvest group, KU Leuven, Leuven, Belgium, [2]VCBT, Leuven, Belgium

367 Blockwise Processing of Hyperspectral Analytical Scanning Transmission Electron Microscopy Data for Enhanced Analysis

Sebastian Cozma[1], Dr. Pau Torruella[1], Dr. Duncan T.L. Alexander[1], Prof. Dr. Cécile Hébert[1]
[1]Electron Spectrometry and Microscopy Laboratory, Institute of Physics, École Polytechnique Fédérale de Lausanne (EPFL), Lausanne, Switzerland

441 Deep orientation estimation of macromolecules in cryo-electron tomography

Dr. Noushin Hajarolasvadi[1], Phd Harold Phelippeau[2], Phd Robert Brandt[2], MSc. Pierre Nicolas Suau[3], Phd Antonio Martinez-Sanchez[3], Phd Daniel Baum[1]
[1]Zuse Institute Berlin, Berlin, Germany, [2]Thermo Fisher Scientific, Bordeaux, France, [3]Universidad de Murcia, Murcia, Spain

507 Revolutionizing Electron Microscopy Through Intuitive Language-Driven Interfaces: The Emergence of the EM CoPilot

Remco Geurts[1], Pavel Potocek[1], Remco Schoenmakers[1], Giovanni Mariotta[1]
[1]ThermoFisher Scientific, Eindhoven, Netherlands

598 3D visualization of in situ nanoscale dynamics in transmission electron microscopy via self-supervised deep learning

Mr. Timothy Craig[1], Dr. Ajinkya Kadu[1], Prof. Dr. Kees Batenburg[2], Prof. Dr. Sara Bals[1]
[1]Electron Microscopy for Materials Science and NANOlab Center of Excellence University of Antwerp, Antwerp, Belgium, [2]Leiden Institute of Advanced Computer Science, Leiden University, Leiden, The Netherlands

628 Self-supervised deep learning method for in-cell cryo-electron tomography

Frosina Stojanovska[1,2], Anna Kreshuk[3], Julia Mahamid[1,3], Judith Zaugg[1,4]
[1]Structural and Computational Biology Unit, European Molecular Biology Laboratory, Heidelberg, Germany, [2]Collaboration for Joint PhD Degree between EMBL and Heidelberg University, Heidelberg, Germany, [3]Cell Biology and Biophysics Unit, European Molecular Biology Laboratory, Heidelberg, Germany, [4]Genome Biology Unit, European Molecular Biology Laboratory, Heidelberg, Germany

77 SEMNet: Deep Synthetic Training for Unprecedented SEM Image Denoising and Super-Resolution

Junghun Cha[1], Ph.D Doohyun Cho[1], Ph.D SeungJae Lee[1]
[1]D.notitia Inc., Seoul, Republic of Korea

126 Physics-based synthetic data model for automated segmentation in catalysis microscopy

Maurits Vuijk[1,2], Dr. Gianmarco Ducci[1], Dr. Luis Sandoval[2], Dr. Thomas Lunkenbein[2], Dr. Christoph Scheurer[1], Prof. Dr. Karsten Reuter[1]
[1]Fritz-Haber-Institut, Theory Department, Berlin, Germany, [2]Fritz-Haber-Institut, AC Department, Berlin, Germany

145 Data Reduction and Clustering Approaches for a Comprehensive Phase Analysis inside Na-ion battery Cathode Materials

PhD student Fayçal ADRAR[1,2], Dr. Nicolas Folastre[1,2], PhD student Chloe Pablo[1,2], Dr. Stefan STANESCU[3], Dr. Sufal SWARJ[3], Dr. Antonella Iadecola[2,3], Pr. Christian MASQUELIER[1,2], Dr. Laurence Croguennec[4], Dr. Matthieu BUGNET[5], Dr. Arnaud DEMORTIERE[1,2]
[1]Laboratoire de Réactivité et Chimie des Solides (LRCS), CNRS UMR 7314, 80009 Amiens, France, [2]Réseau sur le Stockage Electrochimique de L'énergie (RS2E), CNRS FR 3459, 80009 Amiens, France, [3]Synchrotron SOLEIL, L'Orme des Merisiers, Départementale 128, 91190 Saint-Aubin, France , [4]ICMCB-CNRS (UPR-9048), Université de Bordeaux, IPB-ENSCBP, Pessac Cedex 33608, France, [5]CNRS, INSA-Lyon, Université Claude Bernard Lyon 1, MATEIS, UMR 5510, 69621 Villeurbanne, France

242 Contrast Optimization Aided by Machine Learning Applied to Virtual 4D-STEM Images

Daniel Stroppa[1], Dr. Roberto dos Reis[2,3,4]
[1]DECTRIS, Baden-Daettwil, Switzerland, [2]Department of Materials Science and Engineering, Northwestern University, Evanston, USA, [3]Northwestern University Atomic and Nanoscale Characterization Experimental (NUANCE) Center, Evanston, USA, [4]International Institute for Nanotechnology, Northwestern University, Evanston, USA

395 A Robust Toolkit to Correlate High Dimensional Multimodal Microscopy

Mr Thomas Selby[1], Mr Cullen Chosy[1,3], Dr Simon Fairclough[2], Mr Taeheon Kang[1], Dr Terry Chien-Jen Yang[1,3], Ms Hayley Gilbert[1,4], Mr Kieran Orr[1,3], Dr Tiarnan Doherty[2], Prof Paul Midgley[2], Prof Samuel Stranks[1,3]
[1]Department of Chemical Engineering and Biotechnology, University of Cambridge, Cambridge, UK, [2]Department of Materials Science and Metallurgy, University of Cambridge, Cambridge, UK, [3]Cavendish Laboratory, University of Cambridge, Cambridge, UK, [4]Diamond Light Source, Harwell Science and Innovation Campus, Didcot, UK

435 Data Augmentation and Innovative Machine Learning Approaches for Classifying EEL Spectra of Transition Metals Oxides

Daniel Del Pozo Bueno[1], Dr. Demie Kepaptsoglou[2], Prof. Quentin M. Ramasse[3], Prof. Francesca Peiró[1], Prof. Sònia Estradé[1]
[1]LENS-MIND, Dept. d'Enginyeria Electrònica i Biomèdica and Institute of Nanoscience and Nanotechnology (IN2UB), Universitat de Barcelona, Barcelona, , [2]School of Physics, Engineering and Technology, University of York & SuperSTEM Laboratory, Heslington - Daresbury, North Yorkshire - Cheshire, [3]Schools of Chemical and Process Engineering & Physics and Astronomy, University of Leeds & SuperSTEM Laboratory, Leeds - Daresbury, West Yorkshire - Cheshire

462 Denoising of 4D-STEM Dataset using Pix2Pix GAN Algorithm and Artifact Reduction Strategy

Junhao Cao[1,2], Dr. Arnaud Demortière[1,2,3,4], Dr. Nicolas Folastre[1,2], Dr. Gozde Oney[5], Dr. Partha Pratim Das[6], Dr. Stavros Nicolopoulos[6]
[1]Centre national de la recherche scientifique (CNRS), Amiens, France, [2]Laboratoire de Réactivité et Chimie des Solides (LRCS, Amiens, France, [3]Réseau sur le Stockage Electrochimique de l'Energie (RS2E) , Amiens, France, [4]ALISTORE-European Research Institute, CNRS , Amiens, France, [5]Institute of Condensed Matter Chemistry of Bordeaux (ICMCB), CNRS , Pessac, France, [6]NanoMEGAS SPRL company, Brussels, Belgium

1152 Introducing a FAIR RDM infrastructure for electron microscopy and other materials science data

Prof. Christoph Koch[1], Dr. Markus Kühbach[1], Sherjeel Shabih[1], Dr. Sandor Brockhauser[1], Prof. Dr. Erdmann Spiecker[2], Markus Scheidgen[1], Lauri Himanen[1], Ádám Fekete[1], Dr. José A. Márquez[1], Prof. Dr. Heiko Weber[3], Prof. Dr. Claudia Draxl[1]

[1]Department of Physics and CSMB at Humboldt-Universität zu Berlin, Berlin, Germany, [2]Department of Materials Science and Engineering, FAU Friedrich-Alexander-Universität, Erlangen, Germany, [3]Institute of Condensed Matter Physics, FAU Friedrich-Alexander-Universität, Erlangen, Germany

Poster Presentation

18 Miniaturized material testing devices for multimodal in situ microscopic studies
Matthias Weber[1], Dr. Julian Müller[1], Dr. Rainer Steinheimer[2], Prof. Robert Brandt[3], Prof. Axel von Hehl[4], Prof. Benjamin Butz[1]
[1]Micro- and Nanoanalytics Group, University of Siegen, Siegen, Germany, [2]Lehrstuhl für Umformtechnik, University of Siegen, Siegen, Germany, [3]Lehrstuhl für Werkstoffsysteme für den Fahrzeugleichtbau, University of Siegen, Siegen, Germany, [4]Lehrstuhl für Materialkunde und Werkstoffprüfung, University of Siegen, Siegen, Germany

36 An advanced smart counting mode for pixelated direct electron detectors based on semiconductors
Dr. Björn Eckert[1], Mr. Stefan Aschauer[1], Mr. Martin Huth[1], Mrs. Petra Majewski[1], Mrs. Heike Soltau[1], Mr. Lothar Strüder[2]
[1]PNDetector, München, Germany, [2]PNSensor, München, Germany, [3]University of Siegen, Siegen, Germany

58 Fractal: An open-source framework for reproducible bioimage analysis at scale using OME-Zarrs
Dr. Joel Lüthi[1]
[1]BioVisionCenter, University of Zurich, Zurich, Switzerland

61 Comprehensive 3D Characterization Workflow for Solid Oxide Cells
Dr Bartlomiej Winiarski[1], Patrick Barthelemy[2], Chengge Jiao[3], Dirk Laeveren[3], Dalton Cox[4], SA Barnett[4]
[1]Thermo Fisher Scientific, Brno, Czech Republic, [2]Thermo Fisher Scientific, Waltham, USA, [3]Thermo Fisher Scientific, Eindhoven, The Netherlands, [4]Northwestern University, Evanston, USA

71 FFT denoising methodology through CNN for the study of WS2 vacancies
Ivan Pinto[1], Mr. Marc Botifoll[1], Mr. Yuki Wang[3], Pf. Chen Wang[3], Pf. Jordi Arbiol[1,2]
[1]Catalan Institute of Nanoscience and Nanotechnology (ICN2), CSIC and BIST, Barcelona, Spain, [2]ICREA, Pg. Lluis Companys 23, Barcelona, Spain, [3]MSE, Tsinghua University, Beijing, China

108 MIPAR Spotlight: Shedding Light on Next-Generation Detection for Microscopists
CEO Sammy Nordqvist[1], Mr Sammy Nordqvist[2], Dr John Sosa[1], Mr Michael Kudlinski[1]
[1]MIPAR Image Analysis Software, Columbus, United States, [2]SciSpot, Stenungsund, Sweden

226 Unlocking 3D nanoparticle shapes from 2D HRTEM images: a Deep Learning breakthrough
Romain Moreau[1], Dr. Hakim Amara[1], Dr. Maxime Moreaud[2], Dr. Jaysen Nelayah[3], Mr. Adrien Moncomble[3], Dr. Damien Alloyeau[3], Pr. Christian Ricolleau[3], Dr. Riccardo Gatti[1]
[1]Université Paris-Saclay, ONERA, CNRS, Laboratoire d'Études des Microstructures, Châtillon, France, [2]IFP Énergies Nouvelles, Solaize, France, [3]Université Paris Cité, CNRS, Laboratoire Matériaux et Phénomènes Quantiques (MPQ), Paris, France

237 Application of reinforcement learning to aid the alignment of an electron microscope
Richard Konstantin Jinschek[1], Dr. Mounib Bahri[2], Dr. Mario Gianni[3], Dr. Yao-Chun Shen[4], Dr. Nigel D. Browning[2,5]
[1]Distributed Algorithms Centre for Doctoral Training, University of Liverpool, Liverpool, UK, [2]Department of Mechanical, Materials and Aerospace Engineering, University of Liverpool, Liverpool, UK, [3]Department of Computer Science, University of Liverpool, Liverpool, UK, [4]Department of Electrical Engineering and Electronics, University of Liverpool, Liverpool, UK, [5]SenseAI Innovations Ltd., Brodie Tower, University of Liverpool, Liverpool, UK

371 Mapping of interstitial atoms using super-resolution and optimized machine-learning techniques
Dr. Cyril Guedj[1]

[1]Univ. Grenoble Alpes, CEA, LETI, Grenoble, France

448 Multi-scale cements and concrete characterization using X-ray Microscopy, automated phase classification, and machine learning

Ria Mitchell[1], Prof John Provis[2], Dr Giacomo Torelli[3], Mr Kajanan Selvaranjan[3], Dr Antonia Yorkshire[3], Dr Sarah Kearney[3], My Andy Holwell[1]

[1]ZEISS Microscopy, Cambridge, UK, [2]Paul Scherrer Institut, Villigen, Switzerland, [3]University of Sheffield, Sheffield, UK

494 Event-responsive Beam-modulated STEM with Multi-frame and Sparse Scanning

Dr Jonathan Peters[1,2,3], Matthew Mosse[1,2], Bryan Reed[4], Daniel Masiel[4], Michele Conroy[5], Lewys Jones[1,2,3]

[1]Advanced Microscopy Laboratory (CRANN), Trinity College Dublin, Dublin, Ireland, [2]School of Physics, Trinity College Dublin, Dublin, Ireland, [3]turboTEM Ltd., , Ireland, [4]Integrated Dynamic Electron Solutions, Inc., Pleasanton, USA, [5]Department of Materials, London Centre of Nanotechnology, Imperial Henry Royce Institute, Imperial College London, London, UK

569 Coupling Clustering and Channeling Contrast in the Scanning Electron Microscope

Dr. Sudeep Kumar Sahoo[1,2], M. Thierry Douillard[1], Dr. Bianca Frincu[2], Mme Christine Nardin[2], Dr. Hdr Cyril Langlois[1]

[1]INSA Lyon, MATEIS Laboratory, Lyon, France, [2]Constellium Technology Center (C-TEC), , France

650 Image Restoration from Subsampled STEM Measurements using Deep Learning

Amirafshar Moshtaghpour[1], Dr. Matthieu Terris[2], Prof. Mike Davies[3], Prof. Angus Kirkland[1,4], Abner Velazco Torrejón

[1]Rosalind Franklin Institute, Didcot, United Kingdom, [2]Université Paris-Saclay, Palaiseau, France, [3]University of Edinburgh, , United Kingdom, [4]University of Oxford, Oxford, United Kingdom

652 pyEELSMODEL: python library for model-based EELS quantification

Daen Jannis[1,2], Mr. Jo Verbeeck[1,2]

[1]EMAT, Universiteit Antwerpen, Antwerpen, Belgium, [2]NANOlab, Universiteit Antwerpen, Antwerpen, Belgium

654 Cellular in-situ Assessment of Complex Tissue Environments in 3D

Dr. Ralph Palmisano[1], MSc Vasco F Fontes[1,2,3], Prof. Stefan Uderhardt[1,2,3]

[1]Optical Imaging Competence Centre Erlangen (OICE), Friedrich-Alexander University Erlangen-Nürnberg (FAU) , Erlangen, Germany, [2]Department of Internal Medicine 3, Friedrich-Alexander University Erlangen-Nürnberg (FAU) and Universitätsklinikum Erlangen, Erlangen, Germany, [3]Deutsches Zentrum für Immuntherapie (DZI), Friedrich-Alexander University Erlangen-Nürnberg (FAU) and Universitätsklinikum Erlangen, Erlangen, Germany

666 Comparative Analysis of Self-Supervised Learning Techniques for Electron Microscopy Images

Dr.-ing. Bashir Kazimi[1], Prof. Dr. Stefan Sandfeld[1,2]

[1]Forschungszentrum Jülich, Institute for Advanced Simulation – Materials Data Science and Informatics (IAS-9), Aachen, Germany, [2]RWTH Aachen University, Chair of Materials Data Science and Informatics, Aachen, Germany

667 EDX-based annotation of biological features in large-scale EM

Peter Duinkerken[1], Dr. Ahmad Alsahaf[1], Dr. Jacob Hoogenboom[2], Dr. Ben Giepmans[1]

[1]Department of Biomedical Sciences, University Groningen, University Medical Center Groningen, Groningen, the Netherlands, [2]Department of Imaging Physics, Delft University of Technology, Delft, the Netherlands

668 Improving segmentation of FIB tomography data

Dr.-Ing. Martin Ritter[1], M.sc. Trushal Sardhara[2], Prof. Dr. med. Roland Aydin[2], Prof. Dr.-Ing. Christian Cyron[2]

[1]Electron Microscopy Unit, Hamburg University of Technology, Hamburg, Germany, [2]Institute for Continuum and Material Mechanics, Hamburg University of Technology, Hamburg, Germany

688 Deep Learning assisted denoising of in situ liquid STEM-movies of nanoparticle nucleation and growth
Adrien Moncomble[1], Damien Alloyeau[1], Guillaume Wang[1], Hakim Amara[1,2], Riccardo Gatti[2], Maxime Moreaud[3], Christian Ricolleau[1], Jaysen Nelayah[1]
[1]Université Paris Cité, CNRS, Paris, France, [2]Université Paris-Saclay, ONERA-CNRS, Chatillon, France, [3]IFP Energies Nouvelles, Solaize, France
847 TEMsuite – A Matlab-based software platform for TEM data analysis
Simon Hettler[1,2]
[1]Instituto de Nanociencia y Materiales de Aragón (INMA), CSIC-Universidad de Zaragoza, Zaragoza, Spain, Zaragoza, Spain, [2]Laboratorio de Microscopías Avanzadas (LMA), Universidad de Zaragoza. Zaragoza, Spain, Zaragoza, Spain
874 Leveraging AutoScript for Cross-Platform Deep Learning Solutions in Electron Microscopy
Remco Geurts[1], Pavel Potocek[1], Noopur Jain[1], Ricardo Egoavil[1], Bert Freitag[1], Maurice Peemen[1], Yuri Rikers[1]
[1]ThermoFisher Scientific, Eindhoven, Netherlands
893 A high-throughput compositional study of nanocrystals using a machine learning-assisted algorithm for STEM hyperspectral datasets
Mr. Basem Qahtan[1,3], Dr. Yurii P. Ivanov[1], Mr. Nikolaos Livakas[2,3], Mr. Francesco Di Donato[2], Prof. Liberato Manna[2], Dr. Giorgio Divitini[1]
[1]Electron Spectroscopy and Nanoscopy, Istituto Italiano di Tecnologia, Genoa, Italy, [2]Nanochemistry, Istituto Italiano di Tecnologia, Genoa, Italy, [3]Dipartimento di Chimica e Chimica Industriale, Università degli Studi di Genova, Genoa, Italy
934 Automatic signal clasification of the Low-Loss Region in Electron Energy Loss Spectroscopy
Vanessa Costa-Ledesma[1], Daniel del-Pozo-Bueno[1], Catalina Coll Benejam[2], Josep Nogués[2], Borja Sepulveda[3], Laura Bocher, Mathieu Kociak[4], Javier Blanco-Portals[1], Sònia Estradé Albiol[1], Francesca Peiró[1]
[1]LENS-MIND, Dept. d'Enginyeria Electrònica i Biomèdica and Institute of Nanoscience and Nanotechnology (IN2UB), Universitat de Barcelona, Barcelona, Spain, [2]2Catalan Institution for Research and Advanced studies, ICREA Academia, Bellaterra, Spain, [3]3Instituto de Microelectrónica de Barcelona (IMB-CNM, CSIC)Campus UAB, Bellaterra, Spain, [4]4Laboratoire de Physique des Solides (LSP), Microscopie électronique STEM, Orsay, France
973 Interpretable evaluation of STEM images of nanostructures via homology analysis
Mr. Ryuto Eguchi[1,2], Dr. Yu Wen[1,2], Dr. Ayako Hashimoto[1,2]
[1]National Institute for Materials Science, Tsukuba, Japan, [2]University of Tsukuba, Tsukuba, Japan
990 From volume electron microscopy datasets to segmentation models, feature quantification, and data reuse
Dr. Ilya Belevich[1], Kirk Czymmek[2], Johanna Bischof[3], Aastha Mathur[3], Lucy Collinson[4], Eija Jokitalo[1]
[1]University of Helsinki, Helsinki, Finland, [2]Donald Danforth Plant Science Center, Saint Louis, USA, [3]Euro-BioImaging ERIC Bio-Hub, EMBL, Heidelberg, Germany, [4]Francis Crick Institute, London, UK
1019 Quantitative Elemental Mapping Of Bimetallic Nanoparticles From Atomic Scale STEM-HAADF Images
Adrien Moncomble[1], Damien Alloyeau[1], Guillaume Wang[1], Nathaly Ortiz-Peña[1], Hakim Amara[1,2], Riccardo Gatti[2], Maxime Moreaud[3], Christian Ricolleau[1], Jaysen Nelayah[1]
[1]Université Paris Cité / CNRS, Paris, France, [2]Université Paris-Saclay / CNRS, Chatillon, France, [3]IFP Énergies Nouvelles, Solaize, France
1031 U-NET Enhanced 4D-STEM/PNBD: Advancing Microscopy Image Reconstruction
Pavlina Sikorova[1], Miroslav Slouf[2], Radim Skoupy[1], Ewa Pavlova[2], Vladislav Krzyzanek[1]
[1]Institute of Scientific Instruments, Czech Academy of Sciences, Brno, Czech Republic, [2]Institute of Macromolecular Chemistry, Czech Academy of Sciences, Prague, Czech Republic
1074 Label-free biological composition predictions in EM images

Msc Stijn Karaçoban[1], PhD Ryan Lane[1], MSc Daniel Spengler[2], BSc Anouk Wolters[3], Associate Professor Carlas, S. Smith[2], Associate Professor Jacob, P. Hoogenboom[1]
[1]Imaging Physics, Delft University of Technology, Delft, The Netherlands, [2]Delft Center for Systems and Control, Delft University of Technology, Delft, The Netherlands, [3]Cell Biology, University Medical Center Groningen, Groningen, The Netherlands

1099 Deep learning-based single cell volume segmentation for soft X-ray microscopy data

Valentina Alberini[1,2], Aurélie Dehlinger[1,2], Dr. Christian Seim[1,2], Dr. Holger Stiel[2,3], Dr. Antje Ludwig[4], Prof. Dr. Birgit Kanngießer[1,2]
[1]Technische Universität Berlin, Berlin, Germany, [2]Berlin Laboratory for innovative X-ray technologies (BLiX), Berlin, Germany, [3]Max-Born-Institute (MBI), Berlin, Germany, [4]Charité Universitätsmedizin Berlin, Berlin, Germany

Late Poster Presentation

1173 Development of an automated pipeline for segmenting and analyzing organelle contacts in Volume Electron Microscopy.

Miss Analle Abuammar[1], Miss Odara Medagedara[1], Mr Aaran Vijayakumaran[1], Mr Vito Mennella[1], Mr Kedar Narayan[2]
[1]University of Cambridge, Cambridge, United Kingdom, [2]National Cancer Institute at NIH center for cancer research, Bethesda , United States

1284 AI-driven microscopy for analysis of xenotransplantation models

Dr Courtney Wright[1], Professor Deniz Kirik[1]
[1]Brain Repair and Imaging in Neural Systems (B.R.A.I.N.S), Department of Experimental Medicine, Lund University, Sweden, Lund, Sweden

1315 DELiVR: An end-to-end deep-learning pipeline for cleared-brain cell annotation

Moritz Negwer[1], Doris Kaltenecker[2], Rami Al-Maskari[2], Ali Ertürk[2]
[1]Radboudumc Nijmegen, Donders Institute for Brain, Behavious and Cognitionn, Nijmegen, Netherlands, [2]Institute for Tissue Engineering and Regenerative Medicine, Helmholtz Munich, Neuherberg, Germany

1318 A pipeline for classification and segmentation of 3D quasi-ordered patterns rmormo

Dr. Luca Curcuraci[2], Konrad Handrich[1], Dr. Ronald Seidel[1], Dr. Peter Fratzl[2], Dr. Richard Weinkammer[2], Dr Luca Bertinetti[1]
[1]Technische Universität Dresden, Dresden, Germany, [2]Max Planck Institute of Colloids and Interfaces, Potsdam, Germany

1324 Advancements in Quantifying Neuroinflammation: Leveraging AI-Based Microscopy for Enhanced In Vivo Analysis in pharmaceutical studies

Dr Emilie Tresse-Gommeaux[1], Franziska Wichern[1], Lotte Frederiksen[1], Marie Barkai[1], Dr Morten Skott Thomsen Lindskov[1]
[1]Lundbeck, Valby, Denmark

1336 High throughput automated SEM imaging and feature identification using AI/ML models

Mr. Aloshious Lambai[1], Mr. Zeb Akhtar[1], Dr. Araujo Cesar[1], Dr. Supriya Nandy[1], Dr. Elina Huttunen-Saarivirta[1], Dr. Marko Mäkipää[1]
[1]VTT Technical Research Centre of Finland Ltd, , Finland

115

Electron Videography and Machine Learning of Soft Matter

Prof. Qian Chen[1], Lehan Yao
[1]Department of Materials Science and Engineering, University of Illinois, Urbana, United States

IM-10 (1), Lecture Theater 3, august 29, 2024, 10:30 - 12:30

Background
New methods of materials synthesis and processing with various accelerated discovery strategies have led to huge libraries of functional materials systems. Examples include morphology-controlled nanoparticles as catalysts, nanoparticle superstructures as metamaterials, polymer films with multiscale porosity as separation membranes, to composite energy storage systems. These materials are spatiotemporally heterogeneous in composition, structure, and function, which call for three aspects of advancements in materials characterization. The first is the need for real-space, non-ensemble averaged characterization methods which map the heterogeneity, at least in space, and if possible, over time to capture changes during the synthesis, application, and functioning of materials. The ever-improving toolbox of electron microscopy can meet this requirement by providing atomic to nanometer resolution mapping of the composition, structure, and phase of nanomaterials. Yet, depending on the specific materials systems, different factors still need to be considered in the imaging protocols, such as beam sensitivity, substrate effect, and in-situ stimulation. The second is the need for descriptors to describe heterogeneity. For example, low-dimensional descriptors of symmetry and lattice constants for crystalline solids do not apply for random, or mixed phase systems. Even when it comes to merely the shape (not composition or microstructure), in three dimensions (3D), irregular shapes can be hard to quantify. The third is the need for automated data analysis and reduction methods as high volumes of multi-modal experimental and simulation data are required to describe the heterogeneity and infer the structure−property relationship. Specific to electron microscopy studies, with the cutting-edge detectors, the data collected in one single in-situ experimental session can be 100,000 frames which are extremely laborious to be analyzed manually, let alone the introduction of human bias in the manual analysis process. Mapping properties such as composition and modulus at a similar resolution will only further increase the volume and dimension of the datasets.

Here we will discuss our group's efforts on developing different machine learning strategies to accommodate the data analysis requirements for two different electron microscopy methods, liquid-phase transmission electron microscopy (TEM) and electron tomography, both involving taking series of images and thus referred to collectively as "electron videography". Several materials applications will be discussed, including nanoparticle reaction, self-assembly, and polymer membranes.

Methods
We first introduced the method of U-Net based segmentation for liquid-phase TEM videos1. For liquid-phase TEM videos, they are usually of low signal-to-noise ratio, and thus make manual annotations difficult. To address this challenge, we devised a workflow to generate simulated liquid-phase TEM videos, where the noise levels were captured as dependent on the dose rates to maximally mimic the practical experimental complications. These simulated liquid-phase TEM videos were used as training datasets for the U-Net, with well-defined ground truth, and thus can enable high fidelity and high throughout training of the U-Net, to be used for practical experimental liquid-phase TEM videos.

As to quantification of complex morphologies, we defined a mathematical fingerprint function2 that considers all the coordinates in the shape contours (two-dimensional or 3D) but stays as a one-

dimensional function, which can be used as input for principal component analysis (PCA) and then for machine-learning based Gaussian mixture model for grouping of different morphologies and yield analysis. This method works both for TEM images of nanoparticles and electron tomographs of polymer membranes.

Lastly, to facilitate high throughput electron tomography of complex materials3, we developed an unsupervised sinogram inpainting for nanoparticle electron tomography (UsiNet) to correct the missing wedge effects. UsiNet is the first sinogram inpainting method that can be realistically used for experimental electron tomography by circumventing the need for ground truth.

Results
For the U-Net based segmentation of nanoparticles in liquid-phase TEM videos, we were able to achieve high throughput analysis of the nanoparticle reaction kinetics, self-assembly dynamics, and internanoparticle potentials through the statistics accumulated from the liquid-phase TEM videos. For the application of fingerprint functions, they were useful to differentiate the desired tetrahedral nanoparticles from impurities, enabling yield analysis and the investigation of reaction mechanism. They were also capable of differentiating nanoparticles of different patterned polymer coatings, as well as membranes of four different shape categories, which aid the understanding of synthesis-morphology-property relationship. As to the UsiNet method, we apply it to experimental tomographs, where >100 decahedral nanoparticles and vastly different byproduct nanoparticles are simultaneously reconstructed without missing wedge distortion. The reconstructed nanoparticles are sorted based on their 3D shapes to understand the growth mechanism.

Conclusion
We show collectively the usage of machine learning to liquid-phase TEM and electron tomography for understanding the dynamics and synthesis-morphology relationships of complex materials. The experimental and analysis workflow can extend to other in-situ studies of time-series and tomography studies of complex materials, as well as the potential integration of liquid-phase TEM with electron tomography to study 3D morphological evolution of materials important for applications in self-assembly, nanoparticle synthesis, polymer morphing, and energy storage and conversion.

References:
1. L. Yao, Z. Ou, B. Luo, C. Xu, Q. Chen. ACS Central Science 6, 1421 (2020).
2. L. Yao, H. An, S. Zhou, A. Kim, E. Luijten, Q. Chen. Nanoscale 14, 16479 (2022).
3. L. Yao, Z. Lyu, J. Li, Q. Chen. npj Computational Materials 10, 28 (2024).

Keywords:

Machine learning, electron videography

Reference:

1. L. Yao, Z. Ou, B. Luo, C. Xu, Q. Chen. ACS Central Science 6, 1421 (2020).
2. L. Yao, H. An, S. Zhou, A. Kim, E. Luijten, Q. Chen. Nanoscale 14, 16479 (2022).
3. L. Yao, Z. Lyu, J. Li, Q. Chen. npj Computational Materials 10, 28 (2024).

42

Nanoparticle size estimation by HR-STEM and generative AI

Henrik Eliasson[1], Mr. Angus Lothian[2], Mr Ivan Surin[3], Dr. Sharon Mitchell[3], Professor Javier Pérez-Ramírez[3], Professor Rolf Erni[1]
[1]Electron Microscopy Center, Empa – Swiss Federal Laboratories for Materials Science and Technology, Dübendorf, Switzerland, [2]Computer Vision Laboratory, Department of Electrical Engineering, Linköping University, Linköping, Sweden, [3]Department of Chemistry and Applied Biosciences, ETH Zürich, Zürich, Switzerland

IM-10 (1), Lecture Theater 3, august 29, 2024, 10:30 - 12:30

Background incl. aims
Scanning transmission electron microscopy (STEM) is commonly used to estimate the particle size distribution in heterogeneous catalysts. A problem with the conventional approach of manually measuring particle diameters in STEM images is that it is labor-intensive and disregards the actual particle structure, making particle size prediction with atomic precision impossible. To overcome these limitations, we propose a machine learning approach based on the CycleGAN architecture. The model learns to map between simulated and experimental images, and a subsequent network is trained to estimate the size of an imaged nanoparticle in terms of number of atoms. This technique is fully automatic and could form the basis for a modern characterization method when combined with automated data acquisition. As catalysts should ideally be studied under reaction conditions, we also explore the possibility of extending this workflow to gas-cell measurements.

Methods
Triggered by our recent experimental results, we have developed a structure generator which can generate realistic but random atomic models of Pt nanoparticles supported on ceria. These models have been used to generate a dataset of 3500 HAADF STEM multislice image simulations. A second dataset of high resolution HAADF STEM images of Pt nanoparticles supported on ceria was recorded on a probe-corrected Titan Themis operated at 300 keV. All experimental images were recorded under identical conditions. Images in both datasets are 128x128 with a pixel size in the range 10-50 pm. The simulated and experimental dataset were used to train a CycleGAN to map between the two sets. We use 2 U-Net generators and 2 PatchGAN discriminators for the CycleGAN. With the trained CycleGAN, we then send the simulated dataset through the "simulation-to-experimental" generator, thus obtaining a new dataset of 3500 fake experimental images with a corresponding particle size ground truth. Another U-Net with a fully connected layer at the end to output a scalar size prediction was then trained on the fake experimental dataset. The trained size-estimator was applied to the experimental dataset and the particle size distribution was compared with that of the manual technique of measuring the particle diameters and assuming a hemispherical particle shape.

Results
We have successfully trained a cycle-consistent generative adversarial network to map between physical image simulations and experimental HR-STEM images of small Pt nanoparticles supported on cerium dioxide. Passing raw multislice simulated images through the network yields realistic-looking experimental images with noise profile matching that of the real experimental dataset. In the same way, passing an experimental image through the network can be compared to applying a potent denoising algorithm to the image.
We apply our size estimation network to a set of 118 experimentally observed nanoparticles in a Pt/CeO2 catalyst to get the particle size distribution. Most predictions are reasonable and the particle size distribution obtained by the size-estimator network follows that of the manual hemisphere estimation technique. We find that the mean Pt particle size in the catalyst is 117 atoms with our

technique, and 154 with the hemisphere estimation technique. Typical fail-cases of our model includes images of particles larger than 500 atoms and particles oriented along a major zone axis. This is likely due to a lack of large particles in the simulated data, as well as a lack of particles in zone axis in the experimental set. This could be addressed by generating more data.

Conclusion

In conclusion, our machine learning approach establishes a connection between physical image simulations and experimental images, making it possible to train supervised machine learning techniques on realistic-looking data with a known atomic model ground truth. We have showcased this by developing a size-estimation network which proves to output reasonable size estimates when applied to experimental images. Combined with automated data acquisition, we envision techniques like this will lead to more comprehensive and accurate characterization of nanoparticle-based heterogeneous catalysts.

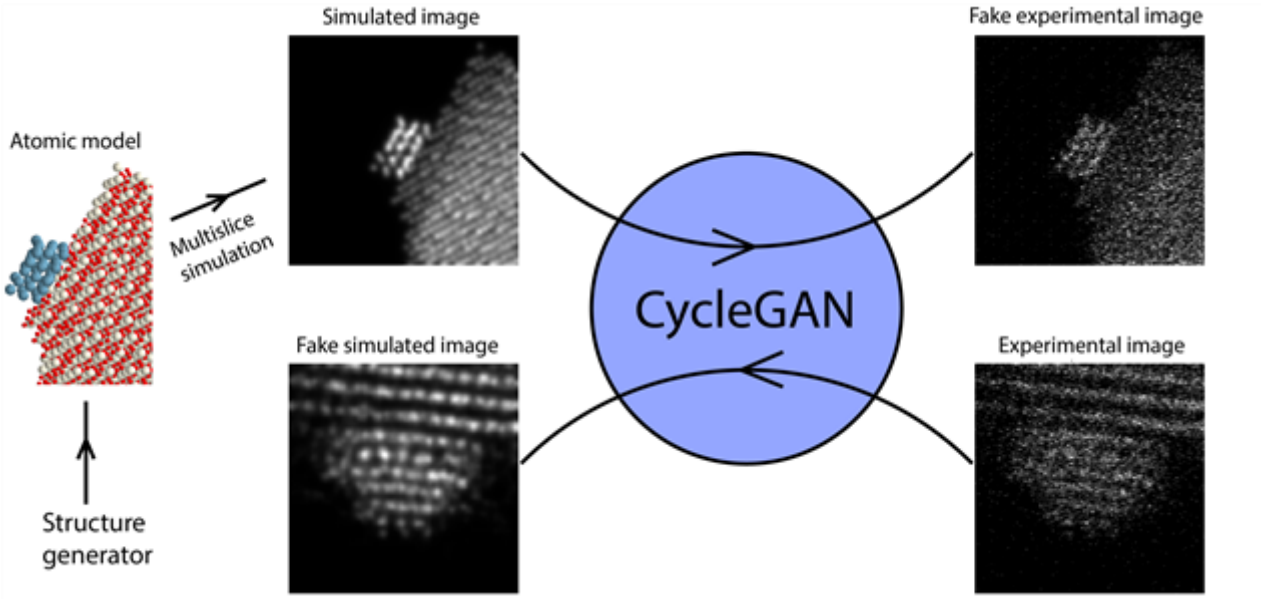

Keywords:

Nanoparticles, Generative AI, Catalysis, Simulations

Reference:

Zhu et al., Unpaired Image-to-Image Translation using Cycle-Consistent Adversarial Networks, ICCV, 2017.

Ronneberger et al., U-Net: Convolutional Networks for Biomedical Image Segmentation, MICCAI, 2015.

Khan et al., npj Computational Materials 9, 85 (2023).

Eliasson et al., Nanoscale 15, 19091-19098 (2023).

406

NP-SAM: Implementing the Segment Anything Model for Easy Nanoparticle Segmentation and Analysis in Electron Microscopy

Rasmus Larsen[1], Mr. Torben L. Villadsen[1], Ms. Jette K. Mathiesen[2], Ms. Kirsten M. Ø. Jensen[3], Mr. Espen D. Bøjesen[1]
[1]Interdisciplinary Nanoscience Center & Aarhus University Centre for Integrated Materials Research, Aarhus University, Aarhus, Denmark, [2]Surface Physics & Catalysis (SURFCAT), Department of Physics, Technical University of Denmark, Kongens Lyngby, Denmark, [3]Department of Chemistry, University of Copenhagen, Copenhagen, Denmark

IM-10 (1), Lecture Theater 3, august 29, 2024, 10:30 - 12:30

Background incl. aims
Nanoparticles (NPs) have important use cases in catalysis, nanomedicine, photonics and plasmonics, and their properties are very dependent on elemental composition, structure, size, and shape. Reliable characterization methods are, therefore, very important in developing these technological areas. With X-ray-based scattering methods, large volumes of NPs can be probed, which gives volume-averaged ensemble characteristics. (Scanning) transmission electron microscopy ((S)TEM) on the other hand can give detailed information about the individual particles, but thousands of NPs must be analyzed to get statistically significant information about the sample. This calls for automatic NP characterization. Although numerous approaches exist, many require choosing the right combination of segmentation parameters or training machine learning algorithms. Here, we present NP-SAM [1], an easy-to-use segmentation and analysis software for NP characterization with advanced filtering based on NP characteristics and with the ability to run with varying degrees of human intervention.
Methods
NP-SAM is based on the Segment Anything Model (SAM) developed by Meta AI Research [2]. We have implemented SAM into NP-SAM and added extra functionalities such as a user-friendly mask filtering mechanism, overlap handling, core-shell analysis, and automatic generation of different types of useful output. The figure shows the general workflow of NP-SAM. Electron microscopy image(s) are first segmented with SAM, resulting in a mask for every segmented particle in different colors. Unlike most other segmentation methods, masks can overlap the same regions, making it possible to analyze neighboring NPs that overlap to a certain degree. An optional graphical user interface (GUI) allows undesired masks to be easily filtered based on the most relevant characteristics such as area, intensity, overlap, etc. For advanced users, even more advanced filtering is possible. Finally, NP-SAM produces different kinds of output: 1) Histograms and statistics of user-chosen characteristics, 2) an overview .pdf file for quick sharing that contains the histograms and summarizes the segmentation and filtering parameters (for reproducibility), 3) a .csv file with the particle characteristics, e.g. area, perimeter, orientation, etc., 4) a flattened binary mask image of all the particles found, and 5) a mask for every individual particle enabling further advanced workflows of i.e. core-shell particles or hyperspectral data.
Results
We have tested NP-SAM on various electron microscopy images including high-angle annular dark-field (HAADF) and bright-field TEM images. 24 HAADF images of PdCu NPs were analyzed, and 2352 NPs were analyzed in about 11 minutes. The size distribution found with NP-SAM agrees with manually measured sizes. NP-SAM's segmentation can be adjusted depending on the accuracy needed and the computer power available. Four segmentation model weights are available: Huge, large, base, and fast, with huge being the most accurate but also computationally heaviest and fast being lightweight and less accurate [3]. Segmenting the 24 HAADF images with the fast model

weights took 3 minutes, and 1925 NPs were found to give a size distribution that again resembles the manually measured one.
The segmentation is based on a grid of points determining where the segmentation model searches for objects. For a HAADF image of very polydisperse Ag NPs and with many small NPs, a finer grid helped find more NPs. We have also implemented a feature called crop and enlarge that can help detect small NPs by dividing the image into four enlarged and segmented sections individually.
One of the exciting features of NP-SAM is its ability to handle overlapping NPs. The overlap between masks is calculated since masks are allowed to occupy the same pixels. This overlap is an important filter parameter, and the user can freely choose the amount of overlap tolerated. This is shown with a HAADF image of AgCuIrPdPt NPs with complicated HAADF contrast.
NP-SAMs sensitivity and ability to handle overlapping masks also enable advanced analysis of core-shell NPs. With core-shell NPs being segmented as two masks, one being the entire particle and the other being the core within the particle, the core and shell can be analyzed individually, and their characteristics can be linked. For example, we can plot shell thickness as a function of core diameter.
NP-SAM is available at our GitLab at https://gitlab.au.dk/disorder/np-sam with installation instructions, source code and user-friendly example notebooks. It is written in Python and can easily be installed using pip after installing PyTorch. A CUDA-compatible GPU speeds up computations significantly, and 8 GB of VRAM is recommended for the huge model weights. NP-SAM can also be run in a cloud-based Google Colab notebook where GPUs are often available. The segmented masks can then be downloaded and filtered locally using the GUI. Finally, we have also developed NP-SAM as a .exe file that runs NP-SAM through a user-friendly interface, not requiring any Python knowledge.
Conclusion
NP-SAM is a powerful tool for quick, user-friendly, and semi-automatic NP segmentation and analysis. Several images can be segmented in less than a minute per image, facilitating quick and reproducible analysis of thousands of NPs. In general, the size distributions found with NP-SAM resemble those found manually. Because NP-SAM can handle overlap, this allows for useful filtering and advanced analysis workflows such as the analysis of core-shell particles.

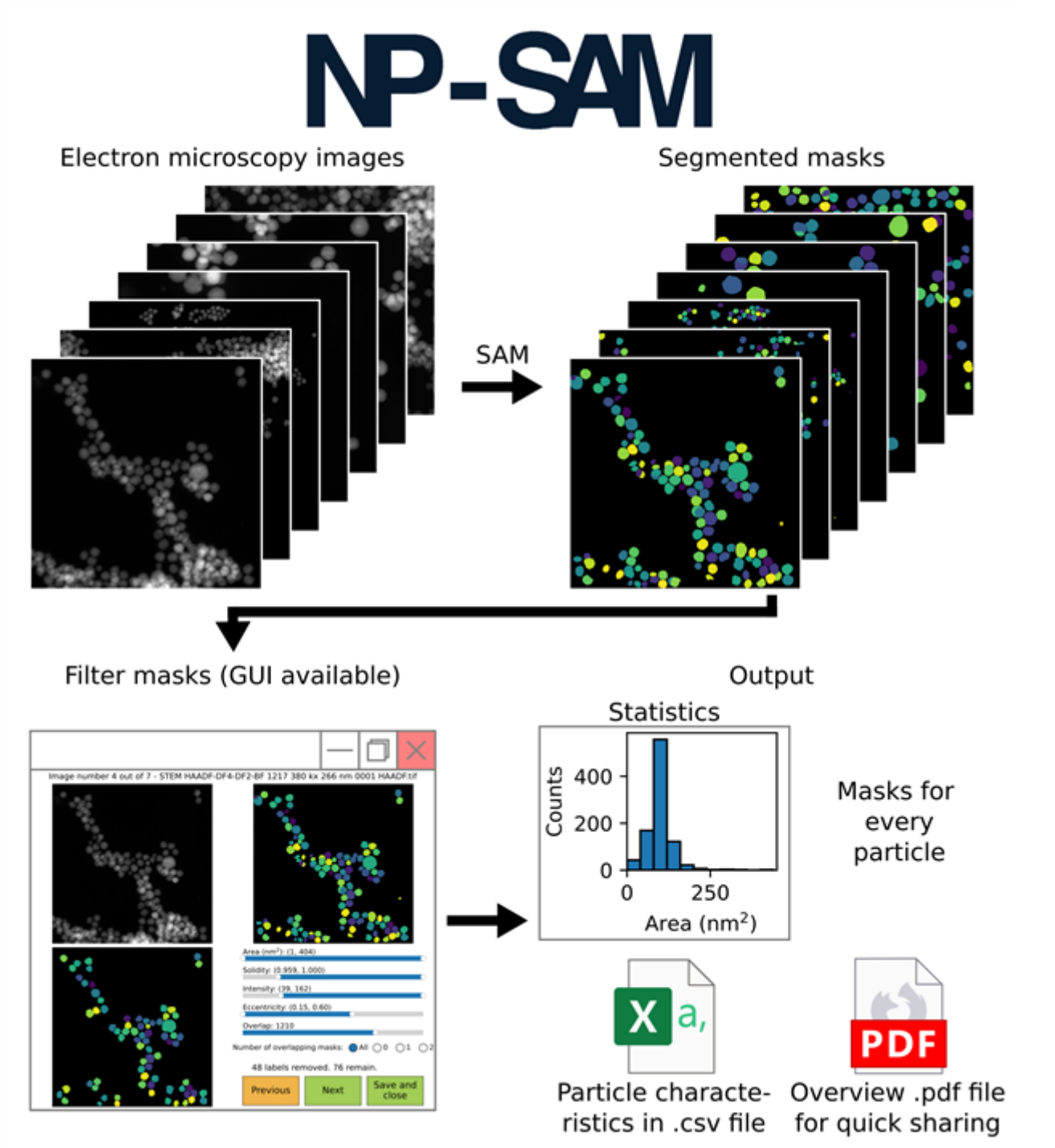

Keywords:

segmentation, automatization, machine learning, nanoparticles

Reference:

[1] R. Larsen, T. L. Villadsen, E. D. Bøjesen et al., NP-SAM: Implementing the Segment Anything Model for Easy Nanoparticle Segmentation in Electron Microscopy Images. ChemRxiv, (2023). https://doi.org/10.26434/chemrxiv-2023-k73qz-v2
[2] A. Kirillov et al., Segment Anything. arXiv, (2023). https://doi.org/10.48550/arXiv.2304.02643
[3] X. Zhao et al., Fast Segment Anything. arXiv, (2023). https://doi.org/10.48550/arXiv.2306.12156

410

Characterization of structure and mixing in nanoparticle hetero-aggregates using convolutional neural networks: 3D-reconstruction versus 2D-projection

Dr. Christoph Mahr[1], Dr. Florian Krause[1], Jakob Stahl[2], Beeke Gerken[1], Dr. Marco Schowalter[1], Dr. Tim Grieb[1], Prof. Dr.-Ing. Lutz Mädler, Prof. Dr. Andreas Rosenauer
[1]Universität Bremen, Bremen, Germany, [2]Leibniz Institut für Werkstofforientierte Technologien, Bremen, Germany

IM-10 (1), Lecture Theater 3, august 29, 2024, 10:30 - 12:30

Background
Functional properties of nanomaterials depend to a large extent on the underlying structure and chemical composition. An example are hetero-aggregates in which nanoparticles of two different materials are mixed. The mixture of titanium-dioxide (TiO2) and tungsten-trioxide (WO3) nanoparticles shows enhanced functionality if applied as a photo-catalyst compared to pure TiO2[1]. The performance of the material depends on the mixing. Best photo-catalytic activity is achieved in completely mixed hetero-aggregates[1].
Improvement of functional properties requires a characterization of structure and mixing. In conventional STEM, two-dimensional (2D) projection images of the samples are acquired, information about the third dimension is lost. This drawback can be overcome by STEM tomography, where the three-dimensional (3D) structure is reconstructed from a series of projection images acquired using various projection directions. However, 3D measurements are expensive with respect to acquisition and evaluation time. Hence, the measurement of 3D-reconstruction can only be done for a limited number of hetero-aggregates.

Methods
TiO2-WO3 hetero-aggregates are generated in a double-flame spray pyrolysis setup. Precursors of the two materials are sprayed and combusted in the two separate flames. Nanoparticles form by nucleation and coagulation and aggregate to clusters of the same material. After a certain distance both flames intersect and clusters of both materials form hetero-contacts. The length of the intersection distance has an influence on the mixing.
To obtain statistically relevant results, information on many hetero-aggregates has to be gathered. Positions of many nanoparticles have to be determined in 2D and 3D data. This can be challenging especially in regions where many particles overlap in crowded regions in 2D-projection data. In recent years, it was demonstrated that the application of artificial intelligence (i.e. convolutional neural networks, CNNs) outperforms a manual measurement or classical object detection algorithms[2,3]. The application of CNNs requires a training of the network first. To this end, many training images in which particle positions and material types are known are required. In the present contribution, we simulate realistic 2D-projection and 3D-reconstruction data of computer-generated virtual hetero-aggregates, in which particle positions and material types are known. We evaluate the trained CNNs using simulated data that has not been used during the training process and apply the networks to experimental 2D-projection and 3D-reconstruction data. For evaluations of 2D-projection data we train a Mask R-CNN[4], for evaluation of 3D-reconstructions we train a StarDist-3D network[5].

Results
An example evaluation is shown in the figure. Part (a) shows a STEM image of a TiO2-WO3 hetero-aggregate. Part (b) shows particles detected by the Mask R-CNN, where TiO2 and WO3 are represented in red and green, respectively. The material discrimination shows a good agreement

with the energy dispersive X-ray spectroscopy (EDXS) map in (c). The nanoparticles as detected by the StarDist-3D network in the STEM tomography reconstruction is shown in (d). The material discrimination is in good agreement with the EDXS map in (c) again.
To correlate structure and chemical composition with functional properties it is required to obtain quantitative information from 2D-projections and/or 3D-reconstructions. In the present contribution, we evaluate the number of particles, the WO3 mass fraction, particle size distributions and the fractal dimension, which is a measure for the hetero-aggregate structure. To quantify the mixing, we measure the heterogeneous coordination number, i.e. the average number of neighbour particles of a different material. A higher heterogeneous coordination number indicates better mixing. We show that for a measurement of mass fractions and for the characterization of mixing, the evaluation of less expensive 2D-projection data is sufficient, whereas for a measurement of the fractal dimension a 3D-reconstruction is required.

Conclusion
Results of the present contribution will help for future characterization of nanoparticle hetero-aggregates, if only the less expensive 2D-projection data is available. In these cases, results of this contribution will provide the possibility to relate 2D-projection evaluations with the 3D structure of the samples.

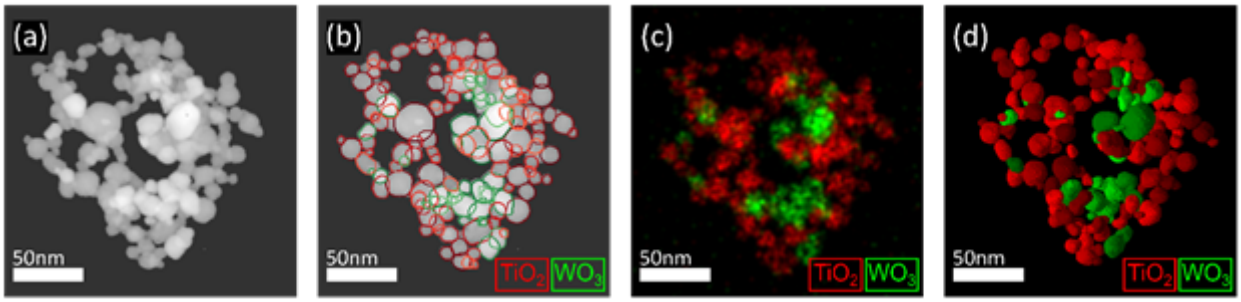

Keywords:

nanoparticle-mixing
object-detection
neural networks
tomography

Reference:

[1] Yan et al., Progress in Natural Science: Materials International 22 (2012), p.654.
[2] Frei et al., Powder Technology 360 (2020), p.324.
[3] Mahr et al., Nano Select (2024), p.2300128.
[4] He et al., IEEE International Conference on Computer Vision (ICCV) (2017).
[5] Weigert et al., IEEE Winter Conference on Applications of Computer Vision (WACV) (2020), p.3655.

661

Deep convolutional neural networks for atomic imaging in STEM

Mr Alex Williams[1], Mr Jack Wells[1,2], Dr Alex Robinson[3], Dr Daniel Nicholls[3], Dr Amirafshar Moshtaghpour[2,4], Prof Angus Kirkland[4,5], Dr Konstantinos Tsakalidis[6], Prof Yao-chun Shen[7], Prof Nigel Browning[2,3]
[1]Distributed Algorithms Centre of Doctoral Training, University of Liverpool, Liverpool, United Kingdom, [2]Mechanical Materials and Aerospace Engineering, University of Liverpool, Liverpool, United Kingdom, [3]SenseAI Innovations Ltd., Brodie Tower, University of Liverpool, Liverpool, United Kingdom, [4]Rosalind Franklin Institute, Harwell Science & Innovation Campus, Didcot, United Kingdom, [5]Department of Materials, University of Oxford, Oxford, United Kingdom, [6]Department of Computer Science, University of Liverpool, Liverpool, United Kingdom, [7]Department of Electrical Engineering and Electronics, University of Liverpool, Liverpool, United Kingdom

IM-10 (1), Lecture Theater 3, august 29, 2024, 10:30 - 12:30

Scanning Transmission Electron Microscopy (STEM) is a well-established method for looking into the physical properties of complex nanostructures. However, a major drawback is that acquiring very high-resolution images may lead to negative effects such as radiolysis and knock-on damage [1]. It has been shown that by lowering the electron beam dose, sample damage is reduced, however this leads to a lower signal-to-noise ratio (SNR) reducing the final quality of the image [2].
Convolutional Neural Networks (CNN) are a type of feed-forward neural network that is used as a powerful tool for improving image SNR through methods such as denoising. Recently, aberration-corrected STEM using CNNs has shown promising results, achieving resolutions below 0.1 nm. Specifically, improved SNR without using high-dose electron beams has been achieved by using CNNs trained on large datasets of microscopy data [3]. These methods have demonstrated the capability of CNNs to reduce damage to samples by improving image quality of low-dose STEM below 0.1 nm.
Inspired by the successful use of deep learning-based convolution for noise reduction [4] outside of STEM, we propose the use of self-supervised deep CNNs trained on both real and synthetic high-dose data to improve the SNR of low-dose data. We aim to create a robust network that is portable to methods outside of denoising by using the high-dose data to retrain the network for a variety of conditions [5] (such as hysteresis, defocus, and image blur).
This talk will present the results of utilizing self-supervised deep learning CNNs to improve the quality of low-dose data below 0.1 nm. We will also compare our proposed method to the STEM neural network autoencoder [3] and SDnDTI for Magnetic Resonance Imaging (MRI) [4] and discuss the potential of our method to improve upon on current methods within STEM as well as other domains by analyzing the SNR with the final image structural similarity (SSIM).

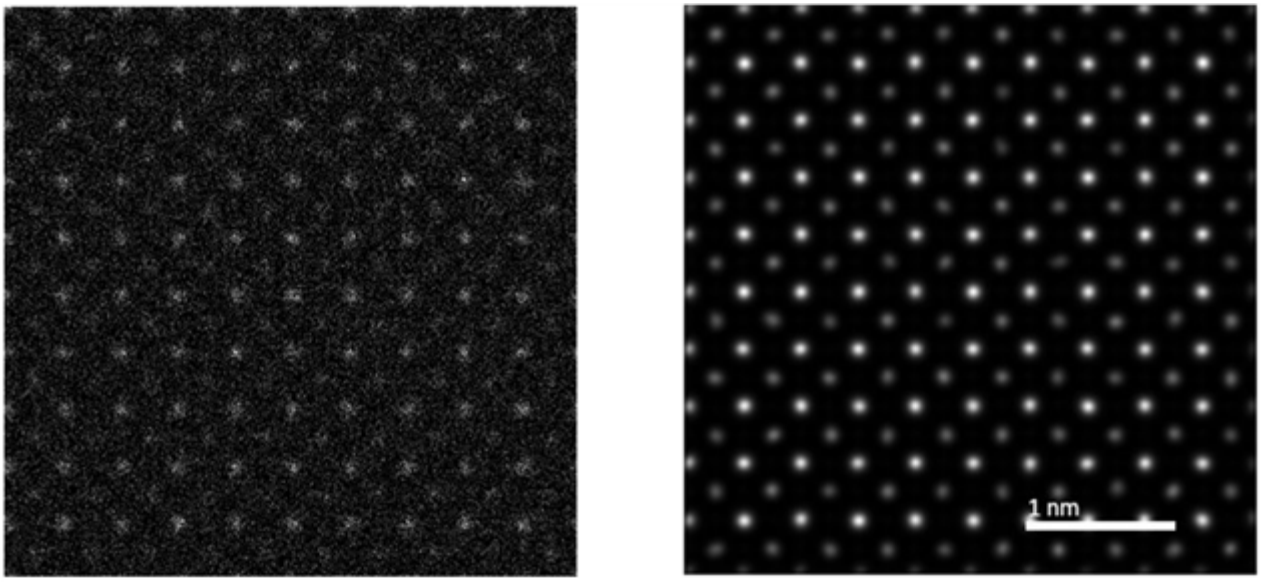

Fig 1. Example of simulated STEM noise with a beam current of 50pA, dwell time of 1.4µs, and a general noise bias of 0.2 which strengthens the generated noise in dark regions (left), showing a PSNR of 18.244 and SSIM of 0.157. Denoised by an 8-layer reverse-hourglass CNN, which works by increasing feature filters the closer you get to the middle of the network (right). Resulting in a PSNR of 28.123 and an SSIM of 0.85.

Keywords:

STEM, Deep Learning, Aberration Correction

Reference:

1. D. Nicholls et al, Nanoscale, 12.41 (2020), p. 21248-21254. 10.1039/D0NR04589F
2. M. R. Libera et al, Polymer Reviews 50:3 (2010), p. 321-339. 10.1080/15583724.2010.493256
3. L. Gambini et al, Machine Learning: Science and Technology, 4 (2023), 10.1088/2632-2153/acbb52
4. Q. Tian et al, NeuroImage, 253 (2022), p. 1053-8119. 10.1016/j.neuroimage.2022.119033.
5. G. Bertoni et al, Ultramicroscopy, 245 (2023), p. 0304-3991. 10.1016/j.ultramic.2022.113663.

672

Unsupervised Machine Learning-based STEM diffraction pattern denoising for enhanced grain visualization in phase change materials

Karina Ruzaeva[1], Dr. Dieter Weber[2], Jonas Werner[3], Prof. Stefan Sandfeld[1]
[1]IAS-9, Forschungszentrum Jülich, Jülich, Germany, [2]ERC-1, Forschungszentrum Jülich, Jülich, Germany, [3]GFE, RWTH Aachen University, Aachen, Germany

IM-10 (1), Lecture Theater 3, august 29, 2024, 10:30 - 12:30

Background
Phase change materials (PCM) are an emerging class of materials in which different phases of the same material may have different optical, electric, or magnetic properties and can be used as a phase change memory [1]. Phase-change memory materials, exemplified by (Ag, In)-doped Sb2Te (AIST) in this research, have several advantages, including high-speed read and write operations, non-volatility, and a long lifespan [2]. PCMs are able to switch between amorphous and crystalline phases when subjected to heat or electrical current. However, the full understanding of PCMs depends heavily on accurate characterization, often through techniques such as scanning transmission electron microscopy (STEM).
In the field of materials science and nanotechnology, the analysis of STEM diffraction patterns is crucial for understanding the structural characteristics of materials, especially in the context of PCMs. Accurate interpretation of diffraction patterns is essential for crystallographic analysis, phase identification, and grain visualization during an in-situ switching experiment. However, the analysis of STEM diffraction patterns in PCMs can be challenging due to the presence of noise and weak signals (Fig.1 left).
Methods
In this study, we present a solution to address the challenge of grain visualization in PCMs. We propose an unsupervised machine learning (ML) approach that employs an autoencoder to denoise STEM diffraction patterns.
Autoencoders are neural network architectures that have the ability to learn in an unsupervised manner and that are able to represent complex data in a lower-dimensional, noise-reduced form [3]. By applying this technique, we enhance the quality of diffraction patterns, improving the signal-to-noise ratio, which is highly beneficial for further analysis and visualization.
Results
Our results demonstrate a significant enhancement in the clustering and visualization [4] of crystalline grains within STEM diffraction patterns of phase change materials. By reducing noise and enhancing signal clarity, the unsupervised ML-based denoising technique allows for more precise discrimination between different crystallographic orientations and refines the identification of grain boundaries.
Furthermore, we employed clustering based on the non-zero order peak position. Nnotably, this approach yielded significantly improved results for the denoised data (Fig. 2).
Additionally, the proposed denoising enhances pattern-matching quality in commercial orientation mapping software (ACOM ASTAR), indicated by higher average index values and more visible structure in index maps, as illustrated in Fig. 3), facilitating precise analysis of crystallographic orientations and grain boundaries.
Conclusion
The proposed approach paves the way for a deeper understanding of phase change behavior, aiding in designing and optimizing PCMs for various applications, from thermal energy storage to non-volatile memory technology.
As an unsupervised method, it does not require the laborious production of specific training data and, therefore, can serve as a universal tool for STEM diffraction pattern denoising and signal

enhancement. Last but not least, the proposed denoising technique is not limited to PCMs; therefore, our work can be understood as a general strategy for enhancing diffraction patterns.

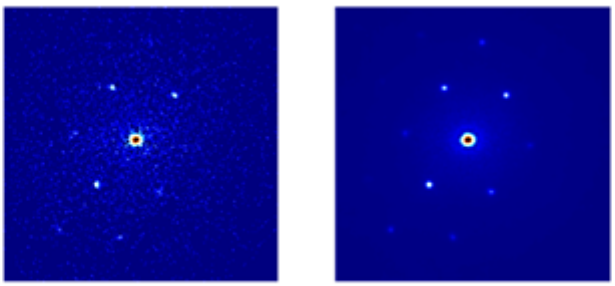

Fig. 1: The diffraction pattern before (left) and after (right) the denoising

Fig. 2: The clustering using the original (left) and the denoised (right) STEM dataset

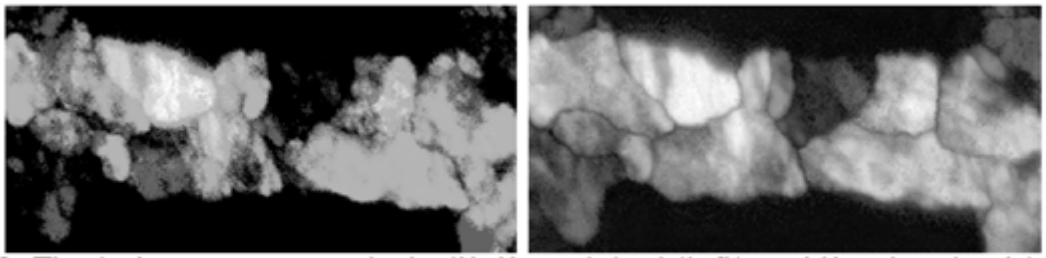

Fig. 3: The index map generated with the original (left) and the denoised (right) STEM dataset

Keywords:

4D-STEM, Denoising, Machine Learning

Reference:

[1] Rehn, D., Li, Y., Pop, E., & Reed, E., 2018, npj Computational Materials, 4, pp. 1-9.
[2] Zhai, et al., 2013, Physica B-condensed Matter, 408, pp. 12-15.
[3] Pawar, K.& Attar, V., Deep Learning: Concepts and Architectures, 2019, 866, pp. 101-132
[4] Clausen et al., Journal of Open Source Software, 2020, 5, pp. 2006

1134

Unsupervised and supervised machine learning for feature classification in atomic resolution images

Christian Liebscher[1,2], Andreas Leitherer[3], Byung Chul Yeo[4], Christoph Freysoldt[5], Luca Ghiringhelli[6]
[1]Faculty of Physics and Astronomy, Ruhr University Bochum, Bochum, Germany, [2]Research Center Future Energy Materials and Systems, Ruhr University Bochum, Bochum, Germany, [3]ICFO-Institut de Ciencies Fotoniques, The Barcelona Institute of Science and Technology, 08860 Castelldefels (Barcelona), Spain, [4]Department of Energy Resources Engineering, Pukyong National University, Busan, Republic of Korea, [5]Max-Planck-Institute for Sustainable Materials, Düsseldorf, Germany, [6]Department of Materials Science and Engineering, Friedrich-Alexander Universität, Erlangen-Nürnberg, Germany

IM-10 (1), Lecture Theater 3, august 29, 2024, 10:30 - 12:30

Background
High resolution scanning and transmission electron microscopy (S/TEM) enable the observation and exploration even of complex materials and interfaces down to the atomic level. It is often desired to uncover the atomic scale building blocks of materials, which is pivotal in understanding their physical nature and to tailor material properties. Identifying local features of the nanostructure of a material and deciphering latent attributes of them is of vital importance to discover new material phenomena. However, the increasing rate at which atomic resolution data is generated in modern electron microscopes makes human-based analysis tedious and renders it nearly impossible in the near future. This requires the development of automatic data analysis approaches to automatically extract meaningful physical information from local image features.

Methods
We present unsupervised and supervised machine learning approaches to classify phases and interfaces in atomic resolution microscopy images. An unsupervised image segmentation approach based on local symmetry descriptors to detect crystallographic features without prior knowledge of the underlying crystal structure is introduced [1]. The segmentation algorithm relies on self-similarity measures based on local symmetry operators that map the image into a symmetry score vector space. The dimensionality of the local descriptor is reduced by principal component analysis and the pattern labels are assigned by K-means clustering. We then show a supervised image classification framework that automatically labels crystal symmetries and orientations as well as interface regions in atomic resolution STEM images [2]. The underlying convolutional neural network is trained on simulated images of pristine crystal structures, while using the fast Fourier transform of local window regions as the descriptor. Typical noise sources, lattice distortions and rotations are taken into account by augmenting the training data.

Results
We show that the unsupervised segmentation approach can identify the different crystalline regions across a grain boundary in atomic resolution STEM images. By including rotational symmetry, it is even possible to segment the interface itself in an automatic fashion. We then apply the segmentation to atomic scale compositional faults in tetrahedrally complex phases and demonstrate its robustness on noisy data. In a final example, we show that the approach is even capable to segment image regions in an in situ atomic resolution video sequence. The supervised image classification is demonstrated on atomic resolution STEM images of grain boundaries in fcc, bcc and hcp systems of pure metals. By adopting a Bayesian neural network, the uncertainty estimates of the prediction are considered, which provides information even on structures not contained in the training data. To test the model, we first apply it to synthetic polycrystalline images and demonstrate

that amorphous regions can be indirectly identified by high uncertainty estimates. We then show the applicability to experimental STEM images of grain boundaries, where the mutual information is used to identify the interface regions automatically. The higher-dimensional neural network representations are explored via unsupervised learning and we find that it does not only provide information on the different crystal symmetries, but also the interface types.

Conclusions
We developed unsupervised and supervised machine learning approaches to automatically segment and classify image regions in atomic resolution images. It is demonstrated that the supervised segmentation is robust against noise in images and can be applied to image video sequences for in situ experimentation. The supervised learning provides quantitative classification of atomic resolution images of crystalline phases and is even capable to identify structural features not contained in the training data.

Keywords:

Atomicßresolution, machine learning, segmentation, classification

Reference:

[1] Wang, Ning, et al. “Segmentation of Static and Dynamic Atomic-Resolution Microscopy Data Sets with Unsupervised Machine Learning Using Local Symmetry Descriptors”, Micr. Microanal. 27 (2021) 1454-1464

[2] Leitherer, Andreas, et al. “Automatic Identification of Crystal Structures and Interfaces via Artificial-Intelligence-based Electron Microscopy”, npj Comp. Mater. 9 (2023) 179

152

Synthetic data generation and Mask-RCNN for Transmission Electron Microscope Image Segmentation

Natalia Da Silva De Sa[1], Dr. Andrew Stewart[2]
[1]University of Limerick, Limerick, Ireland, [2]University College London, London, United Kingdom

IM-10 (2), Lecture Theater 3, august 29, 2024, 14:00 - 16:00

Background incl. aims
The rapid advancement of neural networks (NN) has led to a diverse array of innovations, including autonomous driving, image and text generation. Notably, within image processing, object detection and classification has been significantly improving with a variety of NNs leading the way, particularly U-Net, Fast-RCNN, Mask-RCNN. A significant challenge while training a NN is the substantial volume of training data required to achieve satisfactory results. ImageNet or COCO are typical datasets, with 14M and 200K labelled images (image and ground truth pairs), respectively, used to train NNs to detect everyday objects, people and animals within images. The Transmission Electron Microscope (TEM) field stands to benefit from machine learning image analysis techniques, which can reduce the time and effort of researchers analysing images, especially for particle size and morphology. Furthermore, automation of image analysis will lead to an increase in reproducibility when compared to manual analysis, however, there is a lack of publicly available data which is segmented and labelled appropriately for such applications. Here we present an alternative approach using synthetic data as a method for overcoming the lack of segmented and labelled data, which differs from simulated data and is a pictorial representation rather than a specifically generated simulation of a TEM image and use Mask-RCNN for instance segmentation, a form of image segmentation that detects individual objects in an image. The application shown here is for nanoparticle analysis. The principles can be generalised to all image data produced in a transmission or scanning electron microscopes.
Methods
Our research introduces an innovative approach to generating synthetic images for training machine learning algorithms in nanoparticle detection and classification. Unlike traditional simulation methods (multislice, Bloch waves), our method utilises Python packages to generate images, bypassing the need for costly computing resources. We illustrate this approach through two distinct examples: the creation of polylatex spheres and silica particles on holey carbon substrates with ultra-thin continuous carbon layers and expand to gold nanoparticles. By randomising various parameters such as magnification, particle size, illumination, and contrast, we generate synthetic data for training an instance segmentation machine learning algorithm.
Specifically, we employ a Mask-RCNN model pretrained on the COCO dataset and refine it using our synthetic transmission electron microscopy (TEM) images, a technique known as transfer learning. This approach significantly improves the model's performance by leveraging knowledge from a broader dataset for a specialised task. Subsequently, we apply the trained model to segment experimental TEM images sourced from Certified Reference Materials (CRMs), which are industry standards used for analytical validation and microscope calibration within the PAT4Nano standardization project. To enhance the algorithm's segmentation accuracy and reduce false positives, we explore augmenting the training data with synthetic particles overlaid on experimental TEM grid substrate images. The efficacy of this approach is demonstrated through comparative analysis and visualisation.
Expanding our data generation efforts, we simulate various scenarios including continuous carbon structures and diverse shapes of gold nanoparticles. Additionally, we adjust intensity values to fall within the 1-99 percentile range, further enriching the dataset. This augmented dataset is utilised to

train a secondary Mask-RCNN model, which is then deployed for predicting segmentation of experimental images.

Results

Our evaluation of the models was conducted separately, utilising the Mean Average Precision (mAP) metrics. The Average Precision (AP) is quantified as the area under the precision-recall curve (PR curve), where precision denotes the ratio of true positive predictions to all predictions, and recall represents the proportion of correct positive predictions to all true positive cases. The mAP aggregates all AP values across various classes or categories. The initial model, trained on the polylatex/silica dataset with approximately 500 synthetic images, achieved a mAP of 0.40 when tasked with predicting 90 experimental images. Subsequent augmentation of the training dataset with an additional 500 synthetic images of particles overlaid on experimental backgrounds resulted in a notable improvement, raising the mAP to 0.80 for the same set of 90 experimental images. In parallel, the second model, trained on the gold nanoparticles dataset, attained a mAP of 0.84 when predicting 19 experimental images. Both model predictions were subjected to a minimum detection confidence threshold of 0.9. The graphics section visually depict the predictions generated by models 1 and 2, respectively, providing tangible insights into their performance.

Conclusion

Our research demonstrates the successful training of an instance segmentation algorithm using synthetic data generation, with notable enhancements are achieved by incorporating experimental backgrounds into the training process. Additionally, our findings illustrate the adaptability of the algorithm across diverse datasets characterised by varied backgrounds and particle shapes. Moving forward, our focus will centre on refining particle edge detections to achieve pixelwise accuracy and advancing nanoparticle measurement techniques. Furthermore, we aim to develop an open-source, user-friendly interface for the generation of synthetic data adaptable to a wide variety of transmission electron microscopy (TEM) data. This interface will include a built-in trainable model which can be tuned and refined with user generated synthetic data, facilitating broader accessibility to automated image segmentation for researchers with electron microscope data.

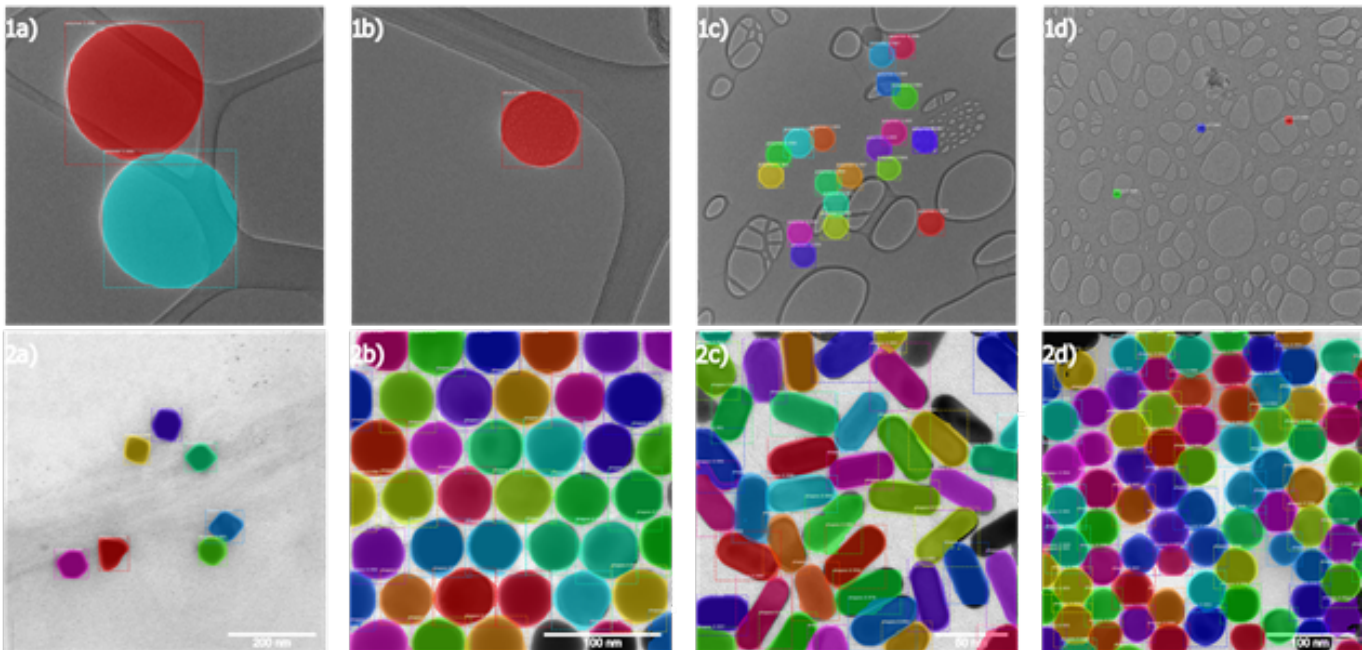

Keywords:

ML, Instance Segmentation, Synthetic Data

Reference:

He, Kaiming, et al. "Mask r-cnn." IEEE international conference on computer vision. 2017.
Janique Hupperetz, at al. (2023). Database on Certified Reference Materials measured with PAT tools for validation and verification purposes. Zenodo.
Salley, D., et al. A nanomaterials discovery robot for the Darwinian evolution of shape programmable gold nanoparticles. (2020).

221

Unsupervised learning assisted secondary electron hyperspectral imaging for high-throughput cheminformatics analysis of materials

Jingqiong Zhang[1], James Nohl[2], Nicholas Farr[3], Cornelia Rodenburg[3], Lyudmila Mihaylova[1]
[1]Department of Automatic Control and Systems Engineering, The University of Sheffield, Sheffield, UK, [2]Department of Materials Science and Engineering, The Faraday Institution, The University of Sheffield, Sheffield, UK, [3]Department of Materials Science and Engineering, The University of Sheffield, Sheffield, UK

IM-10 (2), Lecture Theater 3, august 29, 2024, 14:00 - 16:00

Background
As a powerful instrumentation tool, scanning electron microscopy (SEM) has been increasingly used to perform analysis on a wide range of minerals, metals, biological specimens, nanostructured materials, polymers, composites, and electronic components [1]. By integrating hyperspectral imaging techniques into SEM, secondary electron hyperspectral imaging (SEHI) technology is able to offer detailed and comprehensive spatial-spectral information of the materials, making it versatile for analysing chemical properties and surface morphology at micro- to nano-scale [2].
However, effectively visualizing spatial-spectral information can still be challenging, especially when changes in spectra are subtle due to spectral mixing or occur only in a very small percentage of the area analysed. To address this problem, we propose a novel analytical workflow for SEHI data using unsupervised learning, which can automatically identify chemical bonds or elements present in the imaged materials and additionally segment the materials surfaces into corresponding chemical groups.
Methods
The proposed automated analytical workflow includes the following steps:
(1) Microscopy image data is processed by traversing the whole field of view of the image, through small block-based or pixel-wise methods. For block-based processing, the entire image is divided into smaller, predetermined units (e.g., blocks of 3*3 pixels).
(2) For each small block, the peaks in the corresponding spectral curve, also known as spectral peaks, are identified and gathered. This allows for the collection of the overall distribution of all spectral peaks across the image.
(3) The distribution of spectral peaks is learned by using unsupervised clustering approaches. In this work, the Gaussian mixture model (GMM) approach is adopted to perform probabilistic clustering. The centroid of each GMM component reflects the location of the corresponding spectral peak, which can be used to deduce the associated chemical bonds or elements in the material sample.
(4) Image blocks that fall into the same cluster are then identified. Accordingly, the spectra of these image blocks from the same cluster are extracted. These extracted spectral signatures then act as reference spectra, or like "endmembers" in spectral unmixing processes.
(5) By evaluating spectral similarity using spectral angle mapper (SAM), the image regions, sharing similar spectral properties with these reference spectra obtained in (4), are distinguished.
Results
We implemented this framework into analysing a complex metal alloy (palladium & silver, PdAg) and carbon film, imaged using a Helios Nanolab G3 UC microscope [3]. Firstly, the raw hyperspectral image slices are registered through a template-matching algorithm [4]. By dividing the entire image into smaller blocks and identifying the localized spectral peaks from these blocks, we obtain the distribution of spectral peaks. To figure out the predominant spectral peaks within this distribution, unsupervised clustering by the GMM is applied. As shown in Fig.1, the GMM outcomes reveal 5 components with peak locations at 0.83, 1.98, 3.57, 4.75, and 5.60 eV, respectively. According to the literature, the spectral peaks at 0.83 and 1.98 eV are likely attributed to metals Pd and Ag [3]. The

peaks observed in 3-6 eV range are thought to be linked to the contributions from sp^2-like, a-CH and sp^3-like carbon bond types. Intuitively, image blocks that fall into the same cluster, primarily contribute to a particular spectral peak. Thus, the reference spectra, or endmembers-like spectra, can be extracted from the image blocks belonging to the same cluster. The SAM is utilized to assess spectral similarity against these reference spectra for image segmentation.

Conclusion

Conventional and manual microscopy data analysis methods, due to their limitations in processing efficiency and accuracy, could hinder the applications of SEHI in advanced characterization of materials. Machine learning-based approaches, especially unsupervised learning, offer promising automated analytical solutions for tackling these challenges effectively. The automated analytical workflow proposed here well identifies the chemical bonds and elements present in the imaged materials. The unsupervised clustering method, GMM, perform well in modelling the overall distribution of all spectral peaks and uncovering the chemical bonding types. According to the clustering outcomes, the materials surfaces can then be segmented into the corresponding chemical groups. This novel workflow can facilitate comprehensive cheminformatics analysis of materials, particularly complex carbon material systems.

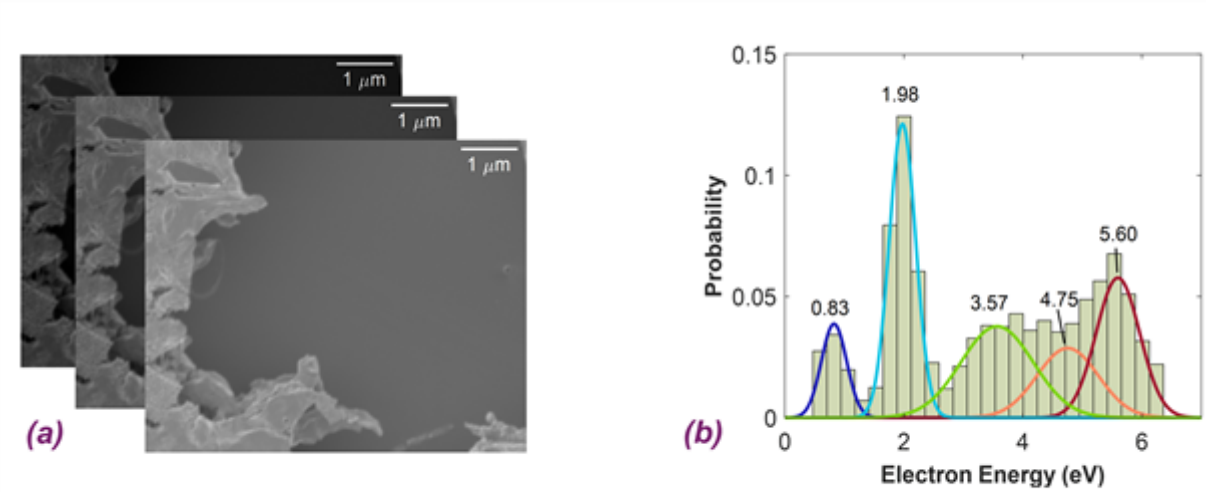

Fig1. (a) Raw SEHI data, collected with a thin *PdAg* metal alloy and carbon film. (b) Probability histogram with GMM results showing the distribution of all spectral peaks derived from (a).

Keywords:

SEHI, clustering, material cheminformatics, segmentation

Reference:

[1] M. Abd Mutalib et al., Membrane characterization, 2017, 161-179. DOI: 10.1016/B978-0-444-63776-5.00009-7
[2] J. Nohl et al., Micron, 2022 (156), 103234. DOI: 10.1016/j.micron.2022.103234
[3] K. J. Abrams et al., Advanced Science, 2019 (19), 1900719. DOI: 10.1002/advs.201900719
[4] J. Nohl et al., Materials Today Advances, 2023 (19), 100413. DOI: 10.1016/j.mtadv.2023.100413

286

3D fruit microstructure characterization using micro-CT imaging and deep learning-based panoptic segmentation

Leen Van Doorselaer[1], Dr. Pieter Verboven[1], Prof. Bart Nicolaï[1,2]
[1]BIOSYST-MeBioS, Postharvest group, KU Leuven, Leuven, Belgium, [2]VCBT, Leuven, Belgium
IM-10 (2), Lecture Theater 3, august 29, 2024, 14:00 - 16:00

Background
Metabolic processes in plants involving transport of water, metabolic gasses, and nutrients are controlled by the three-dimensional (3D) microscopic morphology of the plant tissues. However, imaging and quantifying this microstructure, including the spatial layout of cells, pores (intercellular spaces) and vascular bundles, is a challenging task.
X-ray micro-computed tomography (micro-CT) has been proposed for 3D plant tissue imaging. This advanced imaging technique requires little preparation and resolves easily pore and cell phases due to differences in attenuation. X-ray micro-CT also covers a large field of view compared to other microscopy techniques, thus rendering more representative volumes of interest.
To quantify plant tissue morphology, the tomographic images require extensive image processing, which can become time-consuming and labor-intensive. Cell segmentation in particular is a difficult task because of low contrast in X-ray attenuation at cell-to-cell interfaces.
Deep learning (DL) is increasingly being used for complex image processing tasks in various fields. DL models can be trained to predict semantic labels where each pixel or voxel is assigned to a class label. Cell segmentation, however, is an instance segmentation task, where pixels or voxels of the same class are assigned to separate instances.
This work aims to speed up and improve 3D plant tissue microstructure characterization using X-ray micro-CT imaging and DL-based models for panoptic segmentation, which combines semantic and instance segmentation tasks. The method was developed and validated for pome fruit tissue samples.
Methods
An X-ray micro-CT dataset was collected to develop panoptic segmentation models. This dataset consisted of pairs of conventional and contrast-enhanced X-ray micro-CT images of the same tissue sample. Pear and apple fruit were sampled at three different radial positions. Different cultivars were compared. X-ray projections were acquired using a UniTom HR micro-CT system (Tescan XRE nv, Ghent, Belgium) with voxel resolution of 3 µm for apple and 2.5 µm for pear. For the contrast-enhanced scan after the conventional scan, the tissue sample was carefully unwrapped and incubated in a 10% (w/v) cesium iodide solution for 1 (all pear cultivars and ‘Jonagold’) or 2 h (‘Braeburn’ and ‘Kizuri’) while agitating every 15 min.
After reconstruction, the corresponding 3D images were registered. From the conventional scan, the binary of the cell matrix and pore space were extracted using Otsu’s thresholding. From the contrast-enhanced scan, the individual cell labels were extracted using a semi-automated cell segmentation workflow; the vasculature and stone cells were semi-manually segmented if present. Labeled images were used as ground truth for training the DL algorithm. Data was split into test, training and validation sets making sure datasets were from different fruit. Following the state-of-the art method for cell segmentation, the marker-based watershed algorithm was applied to the binary of the cell matrix as benchmark. As additional benchmark, an instance segmentation model trained on 2D data and enabling 3D prediction by averaging the 2D predictions in all orientations was included, to evaluate the cell segmentation accuracy.
Results
The panoptic segmentation model was able to segment following semantic labels: pore spaces, cell matrix, vascular bundles and clusters of stone cells (brachysclereids, only in pear tissue) and at the

same time to predict intermediate representations of the instance labels, i.e. the cells, that allow cell reconstruction in a post-processing step. Thereto, it exploited the 3D extended version of the public domain Cellpose instance segmentation model, which in this study was adapted to a panoptic model after optimizing instance segmentation performance. The original instance segmentation model uses a 3D U-Net architecture to predict gradient map representations of cell instances. Following changes to this network architecture improved the instance segmentation accuracy: addition of long skip connections with direct summation, replacement of the standard building blocks with residual blocks whereby two consecutive residual blocks were implemented per layer, resulting in double the depth of the original 3D U-Net architecture, and retrieval of a style vector using global average pooling on the convolutional maps of the smallest dimension. The 3D model achieved Aggregated Jaccard Indices of 0.788 ± 0.061 and 0.889 ± 0.030 for pear and apple tissue, respectively, compared to 0.732 ± 0.075 and 0.861 ± 0.028 for the 2D model and 0.631 ± 0.134 and 0.715 ± 0.034 for the watershed-based benchmark.

The 2D instance segmentation model was able to recognize vascular bundles and stone cell clusters and exclude them from the volume-of-interest. This demonstrated the potential to expand to panoptic segmentation combining semantic and instance segmentation tasks for the 3D model. However, prediction of the semantic labels was difficult as the dataset was highly imbalanced. From the 810 training samples, 308 contain vasculature and/or stone cell clusters and if these labels were present, the occurrence based on the amount of voxels was much lower compared to the cell matrix and pore space labels. Focal loss was the most appropriate loss functions that learned the model to focus on the vascular bundles and stone cell clusters.

Conclusion

The 3D model succeeded in improving the cell segmentation accuracy over the 2D model and watershed-based benchmark. Cell segmentation remains more difficult for dense pear tissue compared to apple, but the 3D model showed greater improvement for pear tissue segmentation, reducing the difference between tissue types. The prediction of semantic labels is hindered by the large imbalance in the data. Therefore, further training wit data augmentation techniques have yet to confirm how much the focal loss can improve segmentation accuracy of vascular bundles and stone cells.

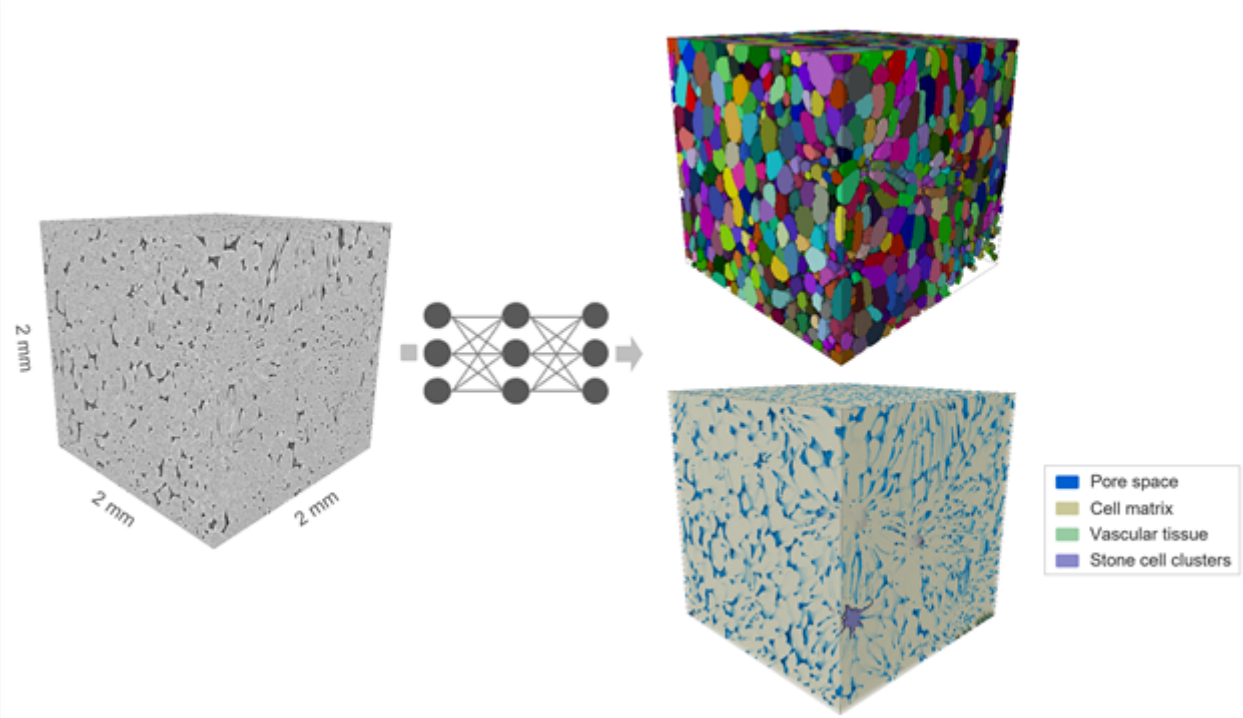

Keywords:

X-ray micro-CT
Image processing

AI

Reference:

Stringer C, Wang T, Michaelos M, Pachitariu M. Cellpose: a generalist algorithm for cellular segmentation. Nat Methods. 2021;18:100–6.
Eschweiler D, Smith RS, Stegmaier J. Robust 3D Cell Segmentation: Extending the View of Cellpose. In: IEEE International Conference on Image Processing. 2022. p. 191–5.
Van Doorselaer L, Verboven P, Nicolai B. Automatic 3D cell segmentation of fruit parenchyma tissue from X-ray micro CT images using deep learning. Plant Methods. 2024;20:1–19
Herremans E, Verboven P, Verlinden BE, Cantre D, Abera M, Wevers M, et al. Automatic analysis of the 3-D microstructure of fruit parenchyma tissue using X-ray micro-CT explains differences in aeration. BMC Plant Biol. 2015;15:1–15.

367

Blockwise Processing of Hyperspectral Analytical Scanning Transmission Electron Microscopy Data for Enhanced Analysis

Sebastian Cozma[1], Dr. Pau Torruella[1], Dr. Duncan T.L. Alexander[1], Prof. Dr. Cécile Hébert[1]
[1]Electron Spectrometry and Microscopy Laboratory, Institute of Physics, École Polytechnique Fédérale de Lausanne (EPFL), Lausanne, Switzerland

IM-10 (2), Lecture Theater 3, august 29, 2024, 14:00 - 16:00

Processing the vast amounts of data generated by STEM spectroscopy techniques, particularly hyperspectral data obtained through energy dispersive X-ray spectroscopy (EDXS), poses significant computational challenges. Current approaches based on machine learning algorithms of the family of multivariate statistical analysis often struggle with the monolithic analysis of very large datasets that exceed available computer memory. A second challenge with very large datasets is that minority phases might be discarded with the noise if the dataset is treated in one block. Our research addresses these challenges by extending a monolithic, in-house, non-negative matrix factorisation (NMF) method specifically tailored for model-based treatment of EDXS data[1], called ESpM-NMF – that enables meaningful interpretation of the resulting spectral and spatial components – into a new tool where the dataset can be treated blockwise before a global reconstruction is performed.
First, we split the hyperspectral data into spatial blocks, the optimal size of which is based on the spatial structure of the initial dataset. Next, we perform principal component analysis (PCA) utilising singular value decomposition (SVD) to identify the number of relevant components within each block, by visual inspection of the SVD output. Subsequently, an initial NMF decomposition is performed with our ESpM-NMF algorithm on a blockwise basis, to estimate spectral components. In the following post-processing stage, we integrate a priori information concerning elemental composition, phase details, and chemical compound identification. The resultant spectral components are correlated using a custom spectral clustering algorithm to identify shared features across the different data blocks. With this step, we are able to reduce the number of spectral components to the exact total number of components to be expected for the whole dataset. Finally, we use the definitive spectral components relevant to the entire dataset to derive the corresponding spatial components capable of monolithically representing the input dataset by solving the least squares problem in a blockwise manner and concatenating the resulting blocks.
For the purpose of testing our algorithm, we generated a synthetic dataset with 5 spatially-separated phases using a previously-developed EDXS dataset simulation algorithm[2]. We use four spherical particles sitting on a silicon substrate. The substrate corresponds to a thickness of 10 nm, the sphere sizes are 10, 10, 20 and 50 nm for W, Pd, $ScVO_4$ and $SrTiO_3$, respectively. As shown by the comparison of monolithic to blockwise dataset decomposition in the figure below, our methodology shows clear improvements for processing large hyperspectral EDXS datasets. Through the integration of prior knowledge and the utilisation of blockwise NMF-based decomposition, we attain enhanced accuracy in separating spectral and spatial components, while also enabling the identification of minority phases that are not adequately detected in the monolithic approach. Leveraging spectral clustering aids in identifying shared spectral features across blocks with remarkable noise resilience, thereby improving results consistency, reliability and interpretability. Crucially, our approach enables efficient out-of-core processing, surmounting memory constraints and enabling the analysis of datasets previously deemed impractical without access to high-performance computing clusters.
In summary, we introduce a new tool for out-of-core hyperspectral data processing. Our NMF-based methodology not only overcomes memory constraints but also enables the detection of minority phases that are not successfully retrieved using monolithic processing. This advancement opens avenues for more comprehensive and detailed analyses in STEM spectroscopy, paving the way for

deeper insights into material structures and compositions. Progress is under way to publish the tool in an open-source format.

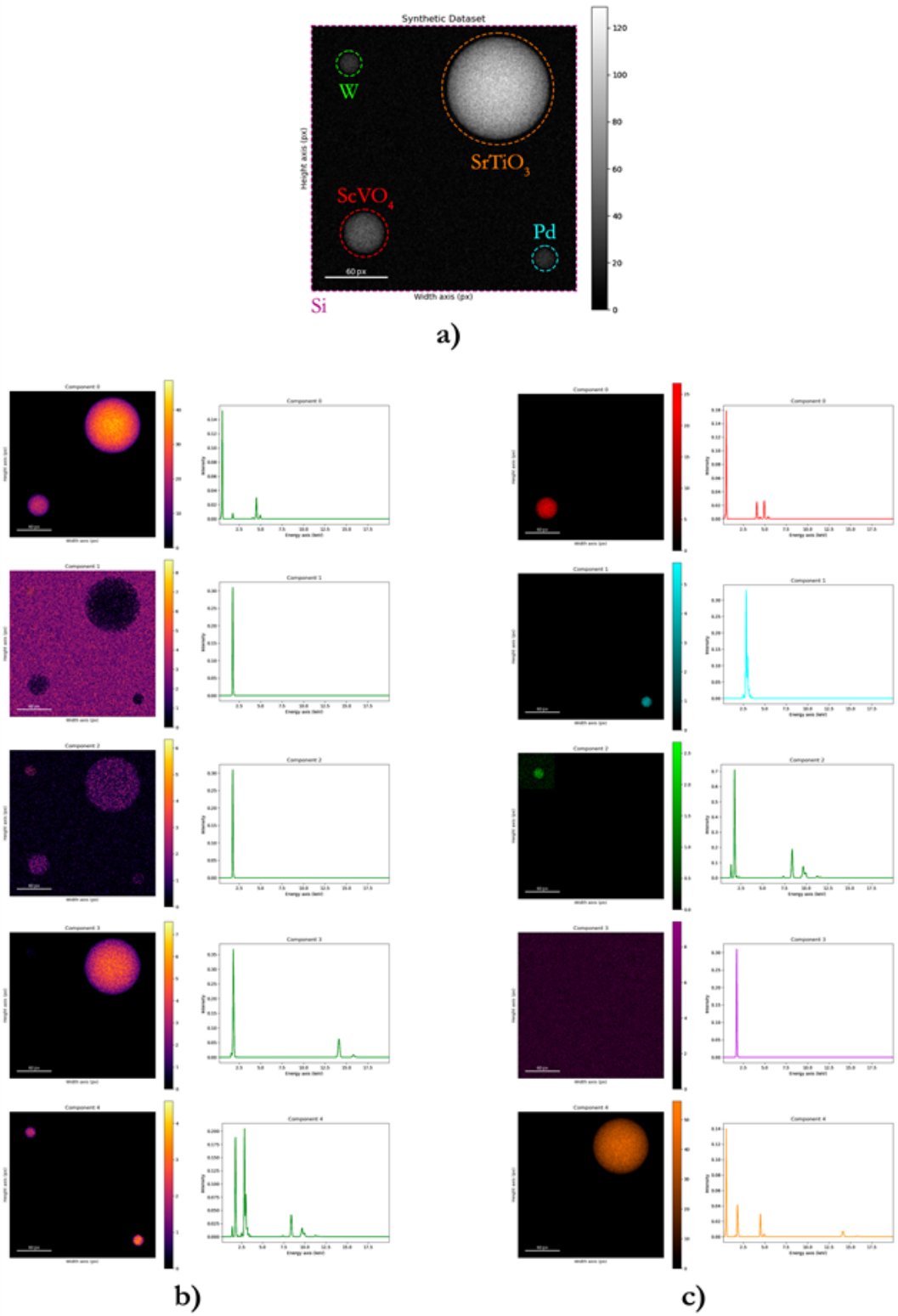

Figure. *a)* Spatial representation of the synthetic dataset used with the ground truth phases highlighted.
Phase unmixing results for *b)* monolithic approach and *c)* blockwise approach. To assess the accuracy of the phase unmixing with respect to the ground truth, the spectral angle (SA) metric and the mean square error (MSE) metric were used for the spectral and spatial components, respectively. By using the blockwise approach, the mean SA was improved by a factor of 5.3 (from 33.85° to 6.38°) and the mean MSE was improved by a factor of 3.74 (from $1.22 \cdot 10^{-5}$ to $3.26 \cdot 10^{-6}$) compared to the monolithic approach.

Keywords:

Physics-guided NMF, Out-of-core Processing

Reference:

[1] Adrien Teurtrie et al., “From STEM-EDXS data to phase separation and quantification using physics-guided NMF”, under preparation.
[2] Adrien Teurtrie, Nathanaël Perraudin, Thomas Holvoet, Hui Chen, Duncan T.L. Alexander, Guillaume Obozinski and Cécile Hébert, “espm: A Python library for the simulation of STEM-EDXS Datasets”, Ultramicroscopy 249, 113719, 2023, https://doi.org/10.1016/j.ultramic.2023.113719.

441

Deep orientation estimation of macromolecules in cryo-electron tomography

Dr. Noushin Hajarolasvadi[1], Phd Harold Phelippeau[2], Phd Robert Brandt[2], MSc. Pierre Nicolas Suau[3], Phd Antonio Martinez-Sanchez[3], Phd Daniel Baum[1]
[1]Zuse Institute Berlin, Berlin, Germany, [2]Thermo Fisher Scientific, Bordeaux, France, [3]Universidad de Murcia, Murcia, Spain

IM-10 (2), Lecture Theater 3, august 29, 2024, 14:00 - 16:00

Background incl. aims

The standard method for detecting macromolecules in cryo-electron tomography (cryo-ET) images is template matching (TM), which suffers from high computational complexity and difficulties in identifying particles with similar structures. In TM, one uses template density maps of a specific macromolecular particle and computes the cross-correlation score at every voxel across the whole tomogram. The highest-ranked cross-correlation scores correspond to possible particle locations. In addition to the particle location, one also obtains an estimation of the particle orientation. As a final step, sub-volumes are extracted at those locations which can be used in turn for other tasks like classification and segmentation.

Recently, the investigation of crowded cell environments using cryo-ET has been attempted with deep learning (DL) methods. Models like DeepFinder [1] improve particle picking by being much faster while at the same time providing a reasonable accuracy. Prediction of the particle orientation using DL methods, however, has, to the best of our knowledge, not yet been achieved. This, we believe, is mainly because learning based on representations like Euler angles or quaternions fails due to discontinuities of the representation space [2].

Here, we investigate DL-based particle orientation estimation using a continuous representation with six degrees of freedom (6DoF) that empowers neural networks for the optimal estimation. Input to the neural network is a 3D image patch containing the particle. Since for experimental data, usually no ground truth is available, we generate test data using the PolNet software that was recently published [3]. We evaluate the accuracy of the orientation estimation using an end-to-end model on this test data. Our promising results suggest that particle orientation using DL methods is indeed feasible.

Methods

Different rotation representations may be used to train a machine learning model for orientation estimation. Inspired by the work of Zhou et al. [2] , we address the problem of orientation estimation as a regression problem. We use M =[a1, …, an] and SO(n) to denote a rotation matrix and the space of n-dimensional rotations, respectively, and ai represents a column vector. In consequence, having a set of 3D rotations, one can define the original space X=SO(3). Zhou et al. [2] showed that representations for 3D rotations are discontinuous in four or lower dimensions; hence, representation spaces for rotations based on Euler angles and quaternions are discontinuous.

Let R and X be the representation space and the original space of rotations; then the neural network should predict an intermediary representation in R that can be mapped into the original space X. In other words, we are looking for a representation (f, g) such that f:R→X maps from the representation space to the original space and g:X→R maps back to R, preserving the continuity. Figure 1 illustrates

these definitions. However, the problem is that the limit of g is undefined for zero rotation, i.e. limit of g in one direction gives 0 and in the other 2π.

One possible solution is to employ identity mapping. Although this guarantees that the network output is back in SO(3), it results in matrices of size 3 × 3 which can be computationally exhaustive due to orthogonalization. As a result, we perform the orthogonalization in the representation space. Having the original space X=SO(3), a representation space $R=R^{3\times2}\backslash D$, and a rotation matrix M, the mapping g is simply defined as dropping the last column of the rotation matrix, resulting in [a1, a2], as suggested by Zhou et al. Here, the set D represents that part of the space that f cannot map to SO(3) [2].

In addition to these challenges, designing a network structure that can reduce the computational cost while accurately estimating the orientation is a profound task. One such structure is a multi-layer perceptron (MLP). We use a four-layer fully connected network with 32 nodes per layer and a regression layer with tanh activation function. The number of output nodes in the regression layer equals the dimension of the orientation representation, i.e. 3, 4, and 6 for Euler angles, quaternions, and 6DoF, respectively.

Results

We performed experiments on a synthetic dataset generated by PolNet [3] that for uniform random sampling of the rotations uses the Algorithm S2 in [4]. We generated 150 tomograms of resolution 10A° containing the ribosomal complex (4v4r) and Thermoplasma acidophilum 20S proteasome (3j9i). We extracted centred patches of size 40^3 for all 4v4r particles, leading to 26703 samples. 130 tomograms (23128 samples) were used for training and validation, and 20 tomograms (3575 samples) for testing. Note that the synthesized tomograms contain the missing-wedge artifact and noise.

We trained our network for 50 epochs using Adam optimization, batch size 32, learning rate 0.0001, and patch size of 40^3. We used Huber loss to calculate differences between ground truth and predicted orientation representation. Our experimental results suggest that the continuous representation performs much better in practice. Figure 2, left, shows the ground truth and predicted orientations on a test tomogram for the 6DoF representation. Green and red colors represent ground truth and prediction, respectively. Our model predicted 81% of the test samples correctly using the Crowther criterion [5] with an angle difference threshold of 20 degrees. Visual analysis shows that most incorrect predictions occur in regions where the particles form a cluster. While training time was about 1 hour, inference time was only approximately 25 seconds on a single GPU. We achieved an R2 score of 0.96 on training data and 0.87 on test data for the 6DoF representation. These values downgrade to 0.76, -0.07 on training and -0.47, -0.07 on test data for the quaternion and Euler representations, respectively. Figure 2, right, shows a histogram chart of the angle differences for all three representations.

Conclusion

We studied the use of MLP to estimate macromolecule orientation using various representation spaces, namely Euler angles, quaternions, and a 6DoF-continuous. The continuous representation space shows a huge advantage over the others. Our future work includes developing more complex models to perform multiple downstream tasks along rotation estimation.

Figure1: Illustration of MLP network trained using a continuous representation space

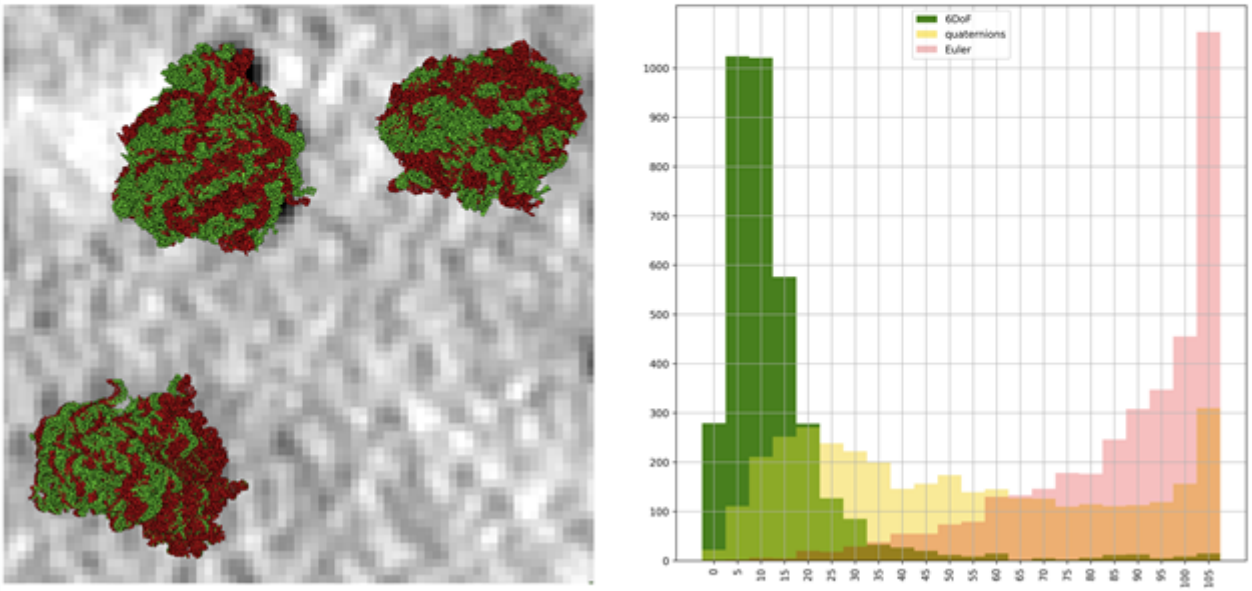

Figure 2: Visualization of ground truth and predicted orientations using 6DoF for a test tomogram (left) histogram chart of the angle differences with a 20° bin width and a 10 step Crowther criterion (right)

Keywords:

machine learning, cryo-electron tomography, orientation

Reference:

[1] E. Moebel, A. Martinez-Sanchez, L. Lamm, R. D. Righetto, W. Wietrzynski, S. Albert and D. Larivière, "Deep learning improves macromolecule identification in 3D cellular cryo-electron tomograms," Nature methods, pp. 1386-1394, 2021.

[2] Y. Zhou, C. Barnes, J. Lu and J. Yang, "On the Continuity of Rotation Representations in Neural Networks," Long Beach, CA, USA, 2019.

[3] A. Martinez-Sanchez, M. Jasnin, H. Phelippeau and L. Lamm, "Simulating the cellular context in synthetic datasets for cryo-electron tomography," bioRxiv, 2023.

[4] A. Martinez-Sanchez, W. Baumeister and a. V. Lučić, "Statistical spatial analysis for cryo-electron tomography," Computer methods and programs in biomedicine, 2022.

[5] M. L. Chaillet, G. v. d. Schot, I. Gubins, S. Roet, R. C. Veltkamp and F. Förster, "Extensive angular sampling enables the sensitive localization of macromolecules in electron tomograms," International Journal of Molecular Sciences, 2023.

507

Revolutionizing Electron Microscopy Through Intuitive Language-Driven Interfaces: The Emergence of the EM CoPilot

Remco Geurts[1], Pavel Potocek[1], Remco Schoenmakers[1], Giovanni Mariotta[1]
[1]ThermoFisher Scientific, Eindhoven, Netherlands

IM-10 (2), Lecture Theater 3, august 29, 2024, 14:00 - 16:00

The field of electron microscopy (EM) has long been constrained by the complexity of its operating systems, which require extensive training and expertise to navigate. Traditional graphical user interfaces (GUIs) provide a layer of abstraction that, while useful, can distance the operator from the most efficient and intuitive interaction with the instrument. This study introduces the EM CoPilot, an innovative application of Large Language Models (LLMs) [1-4]. designed to transform the operation of electron microscopes by enabling control through intuitive language commands. This paradigm shift signifies a new era in microscopy, where accessibility, efficiency, and user-friendliness are paramount.

Methodology involved the development of an LLM capable of understanding and translating natural language commands into specific function calls for electron microscopes. The system supports a wide range of commands. The code was integrated into an EM control system, equipped with voice and text recognition capabilities, supporting multiple languages to cater to a global user base.

Key findings demonstrate that the EM CoPilot significantly reduces the learning curve for new users, while enhancing the operational efficiency and flexibility for seasoned experts. Users can execute complex sequences of operations with simple commands, automate routine tasks, and receive operational guidance, thereby reducing operational errors and increasing throughput. Furthermore, the system's ability to handle complex sequence function calls and integrate basic classical image processing tasks directly through language commands opens new avenues for advanced microscopy techniques.

The implications of this study are profound, signaling a move towards more user-centric approaches in the design and operation of scientific instruments. By bridging the gap between advanced technology and user interface design, the EM CoPilot not only democratizes access to high-level electron microscopy but also sets a precedent for the application of LLMs in scientific instrumentation. The integration of LLMs into EM operation paves the way for future innovations in instrument control, potentially revolutionizing how scientific research is conducted across multiple disciplines.

This abstract encapsulates the essence of the EM CoPilot study, highlighting its innovative approach, methodology, key findings, and the broader implications for the field of electron microscopy and beyond.

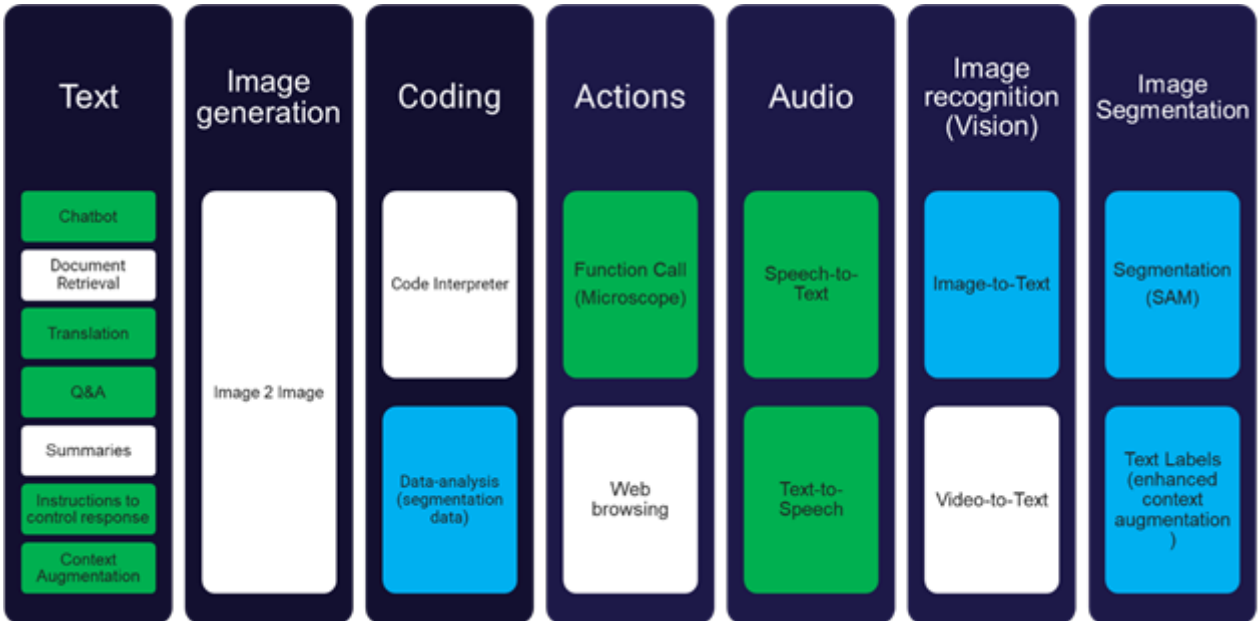

Keywords:

EM Automation, Large Language Models

Reference:

[1] OpenAI. ChatGPT can now see, hear, and speak. https://openai.com/blog/chatgpt-can-now-see-hear-and-speak/ (2023).
[2] 1. Ren Z, Zhang Z, Tian Y, Li J. CRESt – Copilot for Real-world Experimental Scientist. ChemRxiv. July 11, 2023; https://doi.org/10.26434/chemrxiv-2023-tnz1x (pre-print)
[3] Jianwei, Yang et. Al. Set-of-Mark Prompting Unleashes Extraordinary Visual Grounding in GPT-4V. Oct 17, 2023. https://doi.org/10.48550/arXiv.2310.11441
[4] Feng Liang et al. Open-Vocabulary Semantic Segmentation with Mask-adapted CLIP, Oct 8, 2022. https://doi.org/10.48550/arXiv.2210.04150

598

3D visualization of in situ nanoscale dynamics in transmission electron microscopy via self-supervised deep learning

Mr. Timothy Craig[1], Dr. Ajinkya Kadu[1], Prof. Dr. Kees Batenburg[2], Prof. Dr. Sara Bals[1]
[1]Electron Microscopy for Materials Science and NANOlab Center of Excellence University of Antwerp, Antwerp, Belgium, [2]Leiden Institute of Advanced Computer Science, Leiden University, Leiden, The Netherlands

IM-10 (2), Lecture Theater 3, august 29, 2024, 14:00 - 16:00

Background
In recent years, nanomaterials have seen widespread usage in fields as diverse as biomedicines, energy storage and catalysis due to their unique properties. The efficacy of nanomaterials for an application are significantly dependent on their physical and chemical properties. Electron tomography is an invaluable technique, which allows researchers to determine these properties in 3D by reconstructing a series of 2D projections collected at various angles (tilt series).1 However, the 3D spatial properties alone are insufficient to fully characterize nanomaterials and their application. In real world conditions, material properties are rarely static and they change as a result of environmental conditions such as pressure, heat and chemical reactions.2,3 To fully characterize the dynamic behaviour of materials, researchers must move towards 3D volume + time characterizations. Unfortunately, collecting a single tilt series for electron tomography can take about an hour, resulting in loss of temporal information and motion blurring artefacts in the resulting reconstructed volume. Herein, we propose a novel reconstruction method that uses a deep image prior self-supervised neural network (DIP-NN)4 to determine the 3D volume as a function of time. This allows researchers to collect a series of 3D volumes with a temporal resolution of less than a minute.

Methods
To reconstruct a volume time series, 1D slices of the tilt series were used as an input to the DIP-NN. Each slice was mapped to a depth and time coordinate. A 2D orthoslice of the reconstructed volume-time series was predicted for the specified coordinates. To train the network, the orthoslice was forward projected and compared back to the original tilt series. During the reconstruction, the volume-time series is reconstructed slice-by-slice, until the full volume-time series is acquired (Figure 1). Hence, for every 2D image collected in the tilt series a full 3D volume was acquired at the same time of acquisition. This methodology was used to reconstruct simulated nanoparticles with morphological and compositional changes and experimental Au/Ag nanoparticles that were subject to changes in both shape and alloying as a result of in situ heating during electron tomography.

Results
In both the simulated and experimental cases, a significant improvement was observed in temporal resolution compared to conventional tomography. In the simulated case, a set of 100 images in the tilt series was used to reconstruct a set of 100 volumes, where only one would be acquired using conventional electron tomography. In the experimental case, we were able to obtain a frame rate of approximately 1 volume per minute, far outpacing even fast tomography. In both experimental and simulated cases, the reconstruction quality, determined based on the signal-to-noise ratio and the structural similarity index, were comparable to conventional tomography.

Conclusions
Herein, a machine learning method is presented which allows the reconstruction of a series of 3D volumes with a temporal resolution of less than a minute. Unlike supervised machine learning

approaches, this method can be trained solely from the acquired tilt series. This method was validated with both simulated and experiment studies on Au and Ag nanoparticles during heating.

Figure 1. DIP-NN algorithm takes in 1D slices of the tilt series using the coordinates for the depth (z) and time (t) to predict a 2D orthoslice of the reconstruction at the same coordinates. For training, this 2D orthoslice is forward projected and compared back to the tilt series. To reconstruct a full volume time series, the 2D orthoslices are stacked slice by slice for every z and t value.

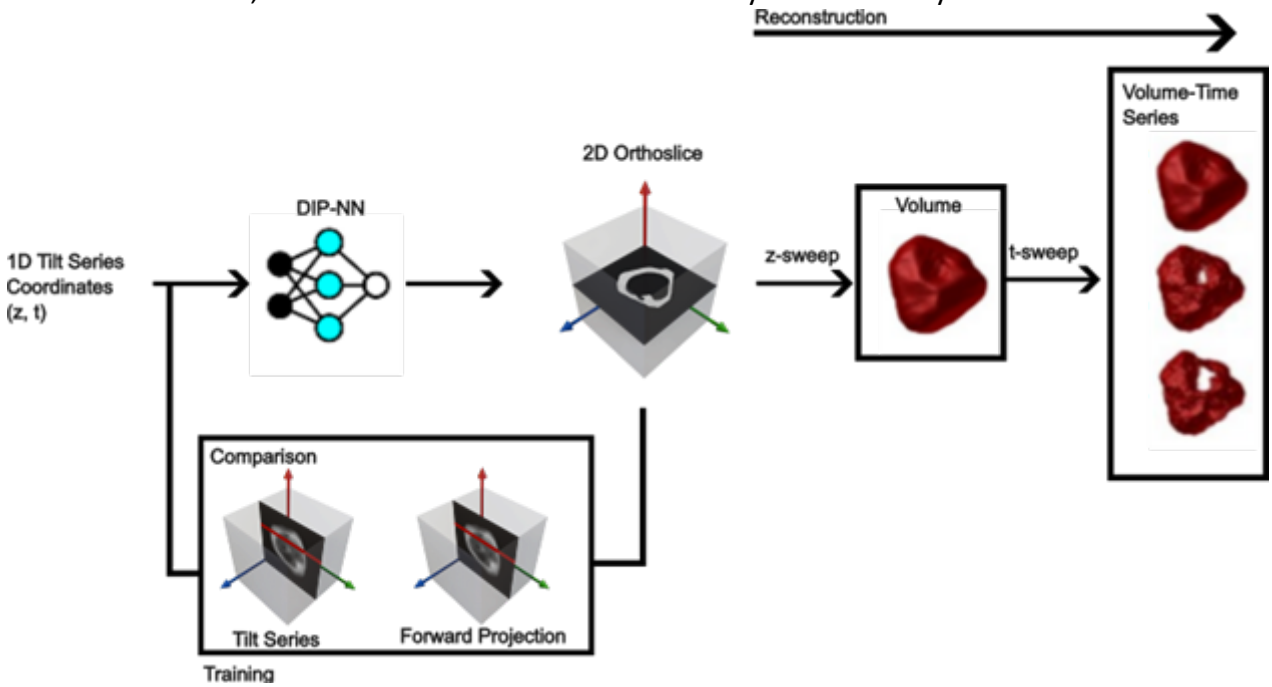

Keywords:

Tomography, Deep Image Prior, Dynamics

Reference:

(1) Weyland, M. Electron Tomography of Catalysts. Top. Catal. 2002, 21 (4), 175–183.
(2) Mychinko, M.; Skorikov, A.; Albrecht, W.; Sánchez-Iglesias, A.; Zhuo, X.; Kumar, V.; Liz-Marzán, L. M.; Bals, S. The Influence of Size, Shape, and Twin Boundaries on Heat-Induced Alloying in Individual Au@Ag Core–Shell Nanoparticles. Small 2021, 17 (34), 2102348. https://doi.org/https://doi.org/10.1002/smll.202102348.
(3) Vanrompay, H.; Bladt, E.; Albrecht, W.; Béché, A.; Zakhozheva, M.; Sánchez-Iglesias, A.; Liz-Marzán, L. M.; Bals, S. 3D Characterization of Heat-Induced Morphological Changes of Au Nanostars by Fast: In Situ Electron Tomography. Nanoscale 2018, 10 (48), 22792–22801. https://doi.org/10.1039/c8nr08376b.
(4) Yoo, J.; Jin, K. H.; Gupta, H.; Yerly, J.; Stuber, M.; Unser, M. Time-Dependent Deep Image Prior for Dynamic MRI. IEEE Trans. Med. Imaging 2021, 40 (12), 3337–3348. https://doi.org/10.1109/TMI.2021.3084288.

628

Self-supervised deep learning method for in-cell cryo-electron tomography

Frosina Stojanovska[1,2], Anna Kreshuk[3], Julia Mahamid[1,3], Judith Zaugg[1,4]
[1]Structural and Computational Biology Unit, European Molecular Biology Laboratory, Heidelberg, Germany, [2]Collaboration for Joint PhD Degree between EMBL and Heidelberg University, Heidelberg, Germany, [3]Cell Biology and Biophysics Unit, European Molecular Biology Laboratory, Heidelberg, Germany, [4]Genome Biology Unit, European Molecular Biology Laboratory, Heidelberg, Germany

IM-10 (2), Lecture Theater 3, august 29, 2024, 14:00 - 16:00

Cryo-electron tomography (cryo-ET) is a powerful technique for visualizing and analyzing macromolecular complexes within their native cellular context. However, cryo-ET analysis is hindered by the low signal-to-noise ratio (SNR) inherent to cryo-ET data and the lack of ground truth data, which pose significant challenges for supervised automated mining of molecular patterns within the cellular environment. As a result, the accurate localization and identification of macromolecular structures of interest, particularly those that are small and less abundant, continue to be a major challenge in the analysis of cryo-ET data.
To address these challenges, we developed a new self-supervised deep learning approach tailored for the dense (voxel-wise) representation of in-cell cryo-ET data. This method generates high-resolution representations of cellular information at the voxel level, facilitating precise segmentation of structural details within tomograms, including particles (globular macromolecular complexes) and filaments (for example, DNA). To evaluate the performance of the model, we created an extensive simulated dataset (Purnell, 2023) that closely mimics a crowded cellular environment, featuring membranes, actin and microtubule filaments, and over 100 PDB protein structure entries of varying sizes. Additionally, we enhanced the dataset by simulating the presence of DNA structures.
Experimental results from the simulated data from the 2021 SHREC competition (Gubins, 2020) and our new simulated crowded dataset demonstrate the efficiency of our method in extracting detailed information about membranes, actin, microtubules, particles, and filaments on a voxel level. To achieve further separation of different types of particles, we conducted an experiment in which we extracted subtomograms for each detected particle and generated embedding representations for every subtomogram. This approach resulted in a new representation space, where distinct clusters were formed using unsupervised clustering, effectively separating different types of particles. The ability to distinguish and separate different types of structural information highlights the potential of our method for advancing the analysis of complex cellular structures in cryo-ET data.
Furthermore, we applied our method to tomograms of Mycoplasma pneumoniae (O'Reilly, 2020), which capture the entire cell in a single tomogram. We successfully extracted structural information of the membrane, particles, and putative DNA filaments, creating a comprehensive 3D structural cell model.
In conclusion, our novel self-supervised deep learning approach demonstrates significant potential in overcoming challenges associated with ground truth generation and accelerating biological discoveries from cryo-ET data. By enabling accurate segmentation and extraction of macromolecular and filament information, even in cases with limited or missing annotations, our method advances the analysis of cryo-ET data. Furthermore, the proposed approach can be utilized to construct a comprehensive 3D Mycoplasma pneumoniae cell model from in situ tomograms, showcasing its potential for diverse applications in the field.

Keywords:

self-supervised deep learning, cryo-ET, segmentation

Reference:

Purnell, C., Heebner, J., Swulius, M. T., Hylton, R., Kabonick, S., Grillo, M., ... & Swulius, M. T. (2023). Rapid synthesis of cryo-ET data for training deep learning models. bioRxiv.
Gubins, I., Chaillet, M. L., van Der Schot, G., Veltkamp, R. C., Förster, F., Hao, Y., ... & Bunyak, F. (2020). SHREC 2020: Classification in cryo-electron tomograms. Computers & Graphics, 91, 279-289.
O'Reilly, F. J., Xue, L., Graziadei, A., Sinn, L., Lenz, S., Tegunov, D., ... & Rappsilber, J. (2020). In-cell architecture of an actively transcribing-translating expressome. Science, 369(6503), 554-557.

77

SEMNet: Deep Synthetic Training for Unprecedented SEM Image Denoising and Super-Resolution

Junghun Cha[1], Ph.D Doohyun Cho[1], Ph.D SeungJae Lee[1]
[1]D.notitia Inc., Seoul, Republic of Korea

IM-10 (3), Lecture Theater 5, august 30, 2024, 14:00 - 16:00

The Scanning Electron Microscope (SEM), an essential tool in electron microscopy, excels in delivering detailed visuals by directing an electron beam over a specimen's surface. Its widespread use in material science, biology, and various industrial fields stems from its ability to provide high-resolution, in-depth focus, and three-dimensional imagery.

Despite these advantages, acquiring high-quality SEM images can be challenging. This is due to inherent resolution limitations and noise factors that impair image clarity. Addressing these issues, our study introduces a method to enhance SEM image quality through advanced deep-learning algorithms, focusing on both denoising and super-resolution (SR) to refine image details and clarity effectively.

We introduce SEMNet, a Convolutional Neural Network (CNN) specifically designed for SEM image restoration with an upscale factor of 2. Inspired by the successes of the RRDBNet [1] in real-world image restoration, our model innovatively applies this architecture to SEM imagery, overcoming typical denoising and SR challenges. Fig. 1 illustrates our SEMNet.

SEMNet's core consists of 6 Residual-in-Residual Dense Blocks (RRDBs), a sophisticated structure pivotal for meticulously refining image details. Within each RRDB, we embed 3 Residual Dense Blocks (RDBs) characterized by their densely connected convolutional layers (denoted as Conv in Fig. 1). This design ensures a seamless flow of data and gradients throughout the network, significantly boosting feature extraction performance. The RDBs each consist of 5 convolutional layers paired with LeakyReLU activation functions (denoted as LeakyReLU in Fig. 1), having a negative slope coefficient of 0.2. Overall, SEMNet comprises 94 convolutional layers and 19 LeakyReLU activation functions, considering the additional convolutional layers outside the RRDBs as well. The network concludes with an up-sampling convolutional layer (denoted as Upsample in Fig. 1) that utilizes nearest neighbor interpolation to achieve SR, enhancing the quality and resolution of SEM images.

To effectively tackle the challenges posed by diverse noise types and low-resolution issues in SEM images, we devise a degradation modeling strategy specialized to producing synthesized low-quality (LQ) images from high-quality (HQ) counterparts. Specifically, our methodology concentrates on simulating two primary noise types frequently observed in SEM images: Gaussian noise, with a mean of 0 and a standard deviation ranging from 2 to 25, and Poisson noise, with a lambda value (λ) between 10^2 and 10^4. Moreover, we integrated additional degradations into our datasets, such as Gaussian blurring effects and up-downscaling processes. This comprehensive approach is designed to bolster the robustness of our SEM image restoration model by broadening its exposure to a variety of noise and other degradation scenarios. Note that it serves as a form of data augmentation, dedicately aimed at enhancing image restoration performance.

We trained the model for 5.44×10^5 iterations using Adam optimizer, with a batch size of 4. The learning rate starts at 0.0001 and is halved when the iteration reaches a multiple of 2.0×10^5. The training utilizes the following loss functions with respective weights: L1 loss (1.0), Histogram loss [2] (0.1), and Total Variation loss (0.01). The L1 loss effectively minimizes absolute pixel differences, playing a crucial role in image restoration. Histogram loss targets the reduction of pixel distribution disparities, ensuring the restored image faithfully mirrors the statistical characteristics of the original. Total Variation loss focuses on diminishing noise and maintaining fine details, like edges, enhancing the overall quality of restored images. Our model is trained with 1300 real SEM images and 1300

images sampled from Flickr2K [3], which is the public dataset that has high-resolution real-world images from multiple categories such as nature, cityscape, human, animal, etc.

To quantitatively evaluate the performance of SEM image SR, we employ two metrics: Peak Signal-to-Noise Ratio (PSNR) and Structural Similarity Index (SSIM). PSNR measures the pixel-level accuracy between the reconstructed and the original images, while SSIM assesses the perceptual quality by considering changes in luminance, contrast, and structural similarity. For both metrics, higher values indicate better performance. A testing set of 25 SEM images was used to calculate both metrics.

Compared to the classical restoration using bicubic interpolation (for SR) and Gaussian blurring (for denoising), SEMNet achieved an increase of 0.212dB in average PSNR and 0.1379 in average SSIM. These results suggest that deep learning-based image restoration methods surpass classical image processing techniques in enhancing the quality of SEM images. Fig.2 shows the qualitative results of classical restoration and the SEMNet. The original sizes of the LQ and HQ images are 640×480 and 1280×960, respectively. Our SEMNet demonstrates superior visual performance compared to the classical restoration method.

In conclusion, we introduce SEMNet, a new deep-learning model for restoring LQ SEM images to HQ ones. With a diverse training dataset, SEMNet effectively removes multiple types of noises and upscales the image resolution through detailed degradation modeling and specialized loss functions. It surpasses classical restoration methods in improving SEM image quality, both quantitatively and qualitatively. Our work will contribute to the field of microscopy image restoration by introducing innovative deep-learning architecture designs and training strategies, specifically tailored to handle highly complex and diverse degradations in SEM images.

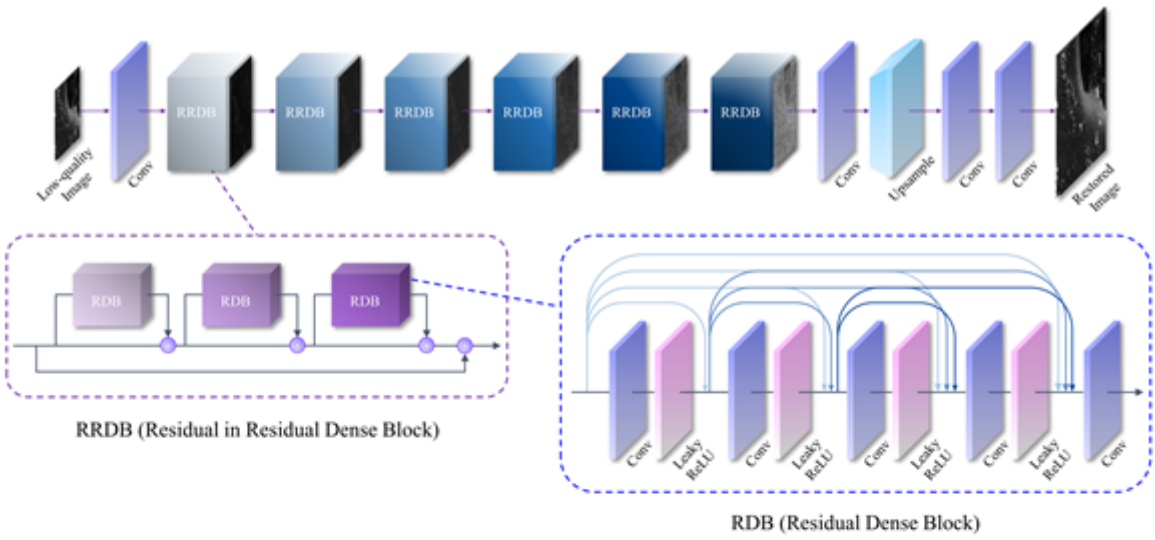

Fig 1. Overview of our SEMNet. It is consisted of 6 Residual-in-Residual Dense Blocks (RRDBs). Within each RRDB, we embed 3 Residual Dense Blocks (RDBs) characterized by their densely connected convolutional layers (denoted as Conv). The RDBs each consist of 5 convolutional layers paired with LeakyReLU activation functions (denoted as LeakyReLU). Overall, SEMNet comprises 94 convolutional layers and 19 LeakyReLU activation functions, considering the additional convolutional layers outside the RRDBs as well. Also, the network concludes with an up-sampling convolutional layer.

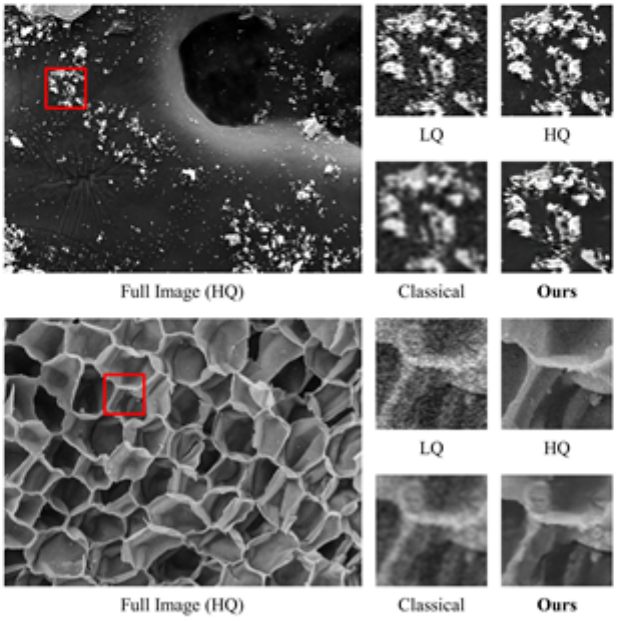

Fig 2. Qualitative results of our proposed methods. Our SEMNet demonstrates superior visual performance compared to the classical restoration method.

Keywords:

SEM, Image Restoration, Deep Learning

Reference:

[1] Wang et al., "Real-ESRGAN: Training Real-World Blind Super-Resolution with Pure Synthetic Data", ECCVW, 2018
[2] Afifi et al., "HistoGAN: Controlling Colors of GAN-Generated and Real Images via Color Histograms", CVPR, 2021
[3] Lim et al., "Enhanced Deep Residual Networks for Single Image Super-Resolution", CVPRW, 2017

126

Physics-based synthetic data model for automated segmentation in catalysis microscopy

Maurits Vuijk[1,2], Dr. Gianmarco Ducci[1], Dr. Luis Sandoval[2], Dr. Thomas Lunkenbein[2], Dr. Christoph Scheurer[1], Prof. Dr. Karsten Reuter[1]
[1]Fritz-Haber-Institut, Theory Department, Berlin, Germany, [2]Fritz-Haber-Institut, AC Department, Berlin, Germany

IM-10 (3), Lecture Theater 5, august 30, 2024, 14:00 - 16:00

Background:
In catalysis research, the amount of microscopy data acquired when imaging dynamic processes is typically too vast for non-automated analysis. Consistent image segmentation is a common first step to obtain data that can be correlated with time-dependent chemical observable. Developing machine learned segmentation models is challenged by the requirement of more high-quality annotated training data than is available in most cases. In our approach, we thus substitute expert-annotated data with a physics-based sequential synthetic data model.
We study environmental SEM (ESEM) data collected from the process of propanol oxidation to acetone over cobalt oxide. After raising the temperature to 350 °C during the reaction a phase transition occurs, reducing the selectivity of the catalyst towards acetone. This phase transition manifests in the µm-scale ESEM data as the formation of cracks between the pores of the catalyst surface. The aim is to generate synthetic data to train a neural network capable of performing semantic segmentation (pixel-wise labelling) of this ESEM data. Statistical analysis of this data will lead to greater insights into this phase transition.

Method:
To generate synthetic image data that approximates the observed transition, our algorithm composes ESEM images of the pristine room-temperature catalyst with dynamically evolving synthetic cracks satisfying two physical construction principles, gathered from empirical knowledge about the phase transition. First, crack growth propagates along surface paths which avoid close vicinity to nearby pores in the surface. Second, each growing path successively widens and is rendered with increasing contrast over short sequences of frames, allowing the algorithm to mimic the growth of the crack features on the surface. The synthetic dataset generated using this algorithm is then used to train a U-NET-LSTM recurrent convolutional neural network. This network architecture consists of a U-NET component with a convolutional Long Short-Term Memory cell appended.
Results:
To evaluate the quality of the neural network, and by extension the synthetic data generation algorithm, two neural networks were trained. The physics-based network was trained on a synthetic dataset generated as described above, and the random network was trained on a similar synthetic dataset, with the restriction that the crack growth paths avoid close vicinity to pores removed. These models were then benchmarked against each other using a synthetic test set to evaluate the importance of this physics-based component of the synthetic dataset. The results show that the physics-based network has a much lower rate of false positives than the random network, at a cost of a slightly lower rate of true positives. This is reflected in the resulting Dice-coefficients of 0.76 (physics-based) and 0.64 (random).
The physics-based network was then applied to the original ESEM movie, giving a fully semantically segmented dataset as the result. From this, statistics about the evolution of crack features could be extracted. Their analysis revealed that the crack feature is first visible to the ESEM about 100 minutes after the acetone selectivity loss event.

Conclusions:
By integrating physical characteristics of the features on the catalyst surface into a synthetic training data generation algorithm, we obtained a network with superior accuracy and a greatly decreased false positive rate. By taking advantage of the temporal nature of the data through the use of a recurrent Long Short-Term Memory layer, we improved the confidence and accuracy of the model further.

Keywords:

computer vision synthetic data ESEM

Reference:

Trampert P, Rubinstein D, Boughorbel F, Schlinkmann C, Luschkova M, Slusallek P, Dahmen T, Sandfeld S. Deep Neural Networks for Analysis of Microscopy Images—Synthetic Data Generation and Adaptive Sampling. Crystals. 2021; 11(3):258. https://doi.org/10.3390/cryst11030258

145

Data Reduction and Clustering Approaches for a Comprehensive Phase Analysis inside Na-ion battery Cathode Materials

PhD student Fayçal ADRAR[1,2], Dr. Nicolas Folastre[1,2], PhD student Chloe Pablo[1,2], Dr. Stefan STANESCU[3], Dr. Sufal SWARJ[3], Dr. Antonella Iadecola[2,3], Pr. Christian MASQUELIER[1,2], Dr. Laurence Croguennec[4], Dr. Matthieu BUGNET[5], Dr. Arnaud DEMORTIERE[1,2]
[1]Laboratoire de Réactivité et Chimie des Solides (LRCS), CNRS UMR 7314, 80009 Amiens, France, [2]Réseau sur le Stockage Electrochimique de L'énergie (RS2E), CNRS FR 3459, 80009 Amiens, France, [3]Synchrotron SOLEIL, L'Orme des Merisiers, Départementale 128, 91190 Saint-Aubin, France , [4]ICMCB-CNRS (UPR-9048), Université de Bordeaux, IPB-ENSCBP, Pessac Cedex 33608, France, [5]CNRS, INSA-Lyon, Université Claude Bernard Lyon 1, MATEIS, UMR 5510, 69621 Villeurbanne, France

IM-10 (3), Lecture Theater 5, august 30, 2024, 14:00 - 16:00

In the field of battery electrode materials, the presence of multiple phases undergoing structural modifications poses a significant challenge, as it can drastically impact battery performance and durability. These phases introduce complexity to the electrochemical processes that occur during charge and discharge cycles. As Na ions transfer between the positive and negative electrodes, structural transformations within the electrode materials take place. The spatial distribution of Na ion occupancy inside the crystal host leads to phase transitions and structural rearrangements, a phenomenon exacerbated by the co-existence of multiple phases related to multiple electrochemical activations. Each phase exhibits distinct electrochemical properties and undergoes different structural modifications during cycling, collectively influencing overall battery performance1. Therefore, it is imperative to characterize and understand the individual contributions of these phases and their spatial distribution.

For this purpose, we employed scanning transmission X-ray microscopy (STXM), offering a spatial resolution of 30 nm, coupled with X-ray absorption spectroscopy technique (XAS) at the HERMES beamline of the SOLEIL Synchrotron. Our focus was on the chemical evolution of Na3V2(PO4)2F3 (NVPF) upon charge/discharge cycles. These NVPF cathode samples underwent electrochemical cycling (versus hard carbon) processes to achieve various Na contents, specifically Na2.5V2(PO4)2F3, Na2V2(PO4)2F3, Na1V2(PO4)2F3, and Na0.3V2(PO4)2F3. NVPF is a promising material for the next generation of sodium batteries, but its complex phase behavior makes it difficult to characterize using traditional methods2. Therefore, the main objective of our study is to develop a novel approach for processing STXM-XANES data to obtain phase maps within individual crystals of the NaxV2(PO4)2F3 (x = 0.3, 1.0, 2.0, 2.5, 3.0) cathode material.

To achieve our objective, we developed a Python-based solution that leverages machine learning algorithms, i.e. non-negative matrix factorization (NMF) and the Pearson correlation coefficient (PCC). This approach enabled us to identify various sodium occupancy phases within individual Na3V2(PO4)2F3 crystals, providing detailed phase maps based on X-ray absorption edges of V and O modifying with the state of charge. With indirect observation in variations in sodium content inside individual crystals, our study offers fundamental insights into sodium-ion diffusion processes, which are essential for guiding the development of advanced cathode materials for the next generation of Na-ion batteries.

In parallel, we conducted a structural study based on electron diffraction using four-dimensional scanning transmission electron microscopy (4D-STEM) automated crystal orientation mapping (ACOM), on the same individual crystals as in STXM3. To facilitate this process, we developed the ePattern4 code to index diffraction spots and reduce the noise in large datasets. By combining

ePattern with the software ASTAR (Nanomegas), a pattern matching approach for crystal orientation and phase determination, we generated phase maps based on the structural information of our sample. The close lattice parameters of the de-sodiated phases raise questions about the phase map reliability.

In this study, we developed a Python solution that allowed us to obtain phase maps and reliability maps for the STXM-XANES data, offering insights into the confidence level of our phase mapping results. These maps provide valuable information about the accuracy and reliability of the identified phases within the sample. Our study demonstrates the effectiveness of combining advanced analytical techniques with machine learning algorithms to characterize phase heterogeneities within battery electrode materials. By developing a novel approach for processing STXM-XANES data, we were able to gain detailed insights into the phase behavior of Na3V2(PO4)2F3 cathode material. These insights are crucial for advancing the development of sodium-ion batteries, paving the way for the design and optimization of electrode materials with improved performance and durability.

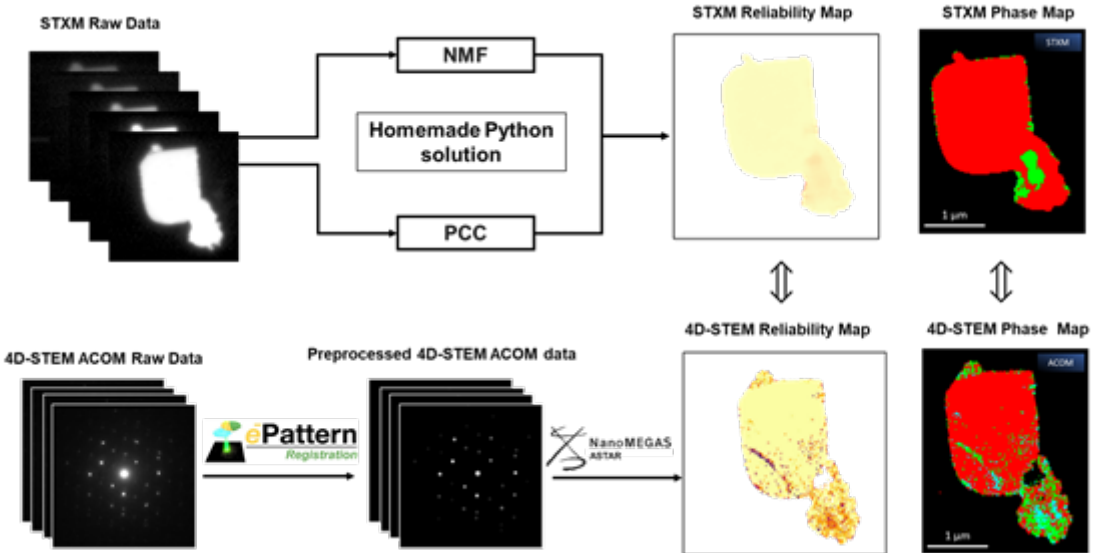

Keywords:

STXM, 4D-STEM, Battery material,NMF, PCC

Reference:

[1] Li, J., Hwang, S., Guo, F., Li, S., Chen, Z., Kou, R., Sun, K., Sun, C., Gan, H., Yu, A., Stach, E. A., Zhou, H., & Su, D. (2019). Phase evolution of conversion-type electrode for lithium ion batteries. Nature Communications, 10(1). https://doi.org/10.1038/s41467-019-09931-2

[2] Yan, G., Mariyappan,S., Rousse,G., Jacquet,Q., Deschamps,M., Rooney,D., Mirvaux,B., Freeland,J. W., & Tarascon, J. (2019). Higher energy and safer sodium ion batteries via an electrochemically made disordered Na3V2(PO4)2F3 material. Nature Communications, 10(1). https://doi.org/10.1038/s41467-019-08359-y

[3] Folastre, N., Cherednichenko, K., Cadiou, F., Bugnet, M., Rauch, E., Olchowka, J., Croguennec, L. , Masquelier, C., Demortière, A. (2021). Multimodal study of dis-sodiation mechanisms within individual Na3V2 (PO4) 2F3 cathode crystals using 4D-STEM-ASTAR and STXM-XANES. Microscopy and Microanalysis, 27(S1), 3446-3447.

[4] Folastre, N., Cao,J., Oney,G., Park,S., Jamali, A., Masquelier,C., Croguennec, L., Véron, M., Rauch, E., & Demortière, A. (2023). Adaptive Diffraction Image Registration for 4D-STEM to optimize ACOM Pattern Matching. arXiv (doi.org/10.48550/arxiv.2305.02124).

242

Contrast Optimization Aided by Machine Learning Applied to Virtual 4D-STEM Images

Daniel Stroppa[1], Dr. Roberto dos Reis[2,3,4]
[1]DECTRIS, Baden-Daettwil, Switzerland, [2]Department of Materials Science and Engineering, Northwestern University, Evanston, USA, [3]Northwestern University Atomic and Nanoscale Characterization Experimental (NUANCE) Center, Evanston, USA, [4]International Institute for Nanotechnology, Northwestern University, Evanston, USA

IM-10 (3), Lecture Theater 5, august 30, 2024, 14:00 - 16:00

Scanning Transmission Electron Microscopy (STEM) has revolutionized imaging due to its high spatial resolution and easy interpretation due to varied contrast mechanisms, such as atomic number (Z) contrast at high-angle scattering and phase contrast from the bright-field disk. The enhanced flexibility in terms of scattering range detection in comparison with STEM is one of the reasons that led to the increased interest in 4D-STEM [1]. Supported by the recent evolution of pixelated detectors, 4D-STEM currently allows for the recording of the complete electron scattering range at speeds commensurate with traditional STEM experiments [2]. With the possibility of flexible reconstruction of virtual STEM images with arbitrary detector shapes, contrast optimization for sample regions with different scattering cross-sections is envisioned. This study delves into the optimization of contrast in virtual 4D-STEM images, employing both user-guided and machine-learning (ML) optimization approaches.

Reference samples from semiconductor devices and supported catalysts were measured with fast 4D-STEM under experimental conditions mirroring standard STEM imaging practices, with 1024x1024 scan positions and 10 us dwell time. The resultant datasets comprised 106 diffraction patterns with 96x96 pixels each, presenting a great challenge for manual contrast optimization due to the vast data volumes and nuanced contrast differences within the areas of the specimens. Figure 1 shows manual contrast optimization applied to virtual 4D-STEM images, serving as a foundational comparison point for our machine learning (ML)-aided methodology. The left panel reveals a virtual Bright Field (BF) STEM image, with an inset in the upper left corner illustrating a typical example of electron scattering and the application of a virtual mask overlay, highlighting the initial manual approach to contrast enhancement. The center panel demonstrates a virtual STEM image that has been collected utilizing an optimized annular mask, reflecting the outcomes of manual contrast optimization efforts. In the right panel, a line profile from these virtual images is presented, with indications of contrast levels, offering a quantitative perspective on the enhancements achieved through manual methods. This figure effectively sets a benchmark for the subsequent introduction of our ML-aided approach, illustrating the initial state of contrast optimization against which the improvements facilitated by automated, ML-driven processes can be measured. By providing a clear depiction of manual optimization efforts, Figure 1 underscores the necessity and impact of transitioning towards more sophisticated, automated methodologies for contrast enhancement in 4D-STEM imaging

In the current study, we develop an innovative computational framework designed to automate the enhancement of contrast in similar regions within 4D-STEM data. Our methodology integrates the advanced deep learning architecture, ResNet101 [3], for feature extraction, followed by Principal Component Analysis (PCA) for dimensionality reduction, and the application of hierarchical clustering techniques (Figure 2). The utilization of ResNet101, distinguished for its deep residual learning capabilities, is strategically chosen to adeptly capture the nuanced, hierarchical features inherent in 4D-STEM datasets, which are pivotal for identifying similarities across various regions. The initial phase of our analysis involves processing the 4D-STEM diffraction patterns through the ResNet101 model, which has been pre-trained on extensive image datasets. This step is

instrumental in extracting comprehensive high-dimensional feature vectors that encapsulate the essential attributes of each pattern. Such a transformation of raw diffraction data into a quantitative form surpasses traditional manual feature identification methods, which are often subjective and labor-intensive, by leveraging automated, objective feature extraction. Following feature extraction, we employ PCA to transform the high-dimensional feature space into a lower-dimensional one, effectively reducing the computational complexity while preserving the variance critical for subsequent analysis. This dimensionality reduction is crucial for enhancing the tractability and interpretability of the dataset, allowing for a focused examination of the significant variances among diffraction patterns. The analysis concludes with hierarchical clustering, an agglomerative method that iteratively merges data points based on their similarity, thereby organically identifying clusters of similar regions without the need for predefining the number of clusters. This method is selected for its adaptability in uncovering the inherent groupings within the data, thereby facilitating an intuitive understanding of similarities across the dataset. The dendrogram generated in this process serves as a pivotal tool for visually determining the grouping of similar regions, thereby informing the selection of clusters for targeted contrast enhancement.

This integrated approach—merging deep learning-based feature extraction, PCA, and hierarchical clustering—presents a robust strategy for automatically enhancing the contrast of similar regions within 4D-STEM data. By doing so, it significantly advances the automation of contrast enhancement, ensuring more efficient, accurate, and objective analysis of material structures. This methodology helps to streamline the process of identifying and enhancing similar regions within complex materials.[4]

Fig. 1. (left) Virtual BF STEM image, inset (upper left) indicates an example scattering and with the virtual mask overlay. (center) Virtual STEM image collected with an optimized annular mask. (right) Line profile from virtual images with the relative contrast level calculated from normalized intensities, with an An contrast increase from 28% to 39% is observed between images reconstructed from virtual BF and with an optimized annular mask.

Fig 1. B) Workflow applied for the ML-based contrast optimization.

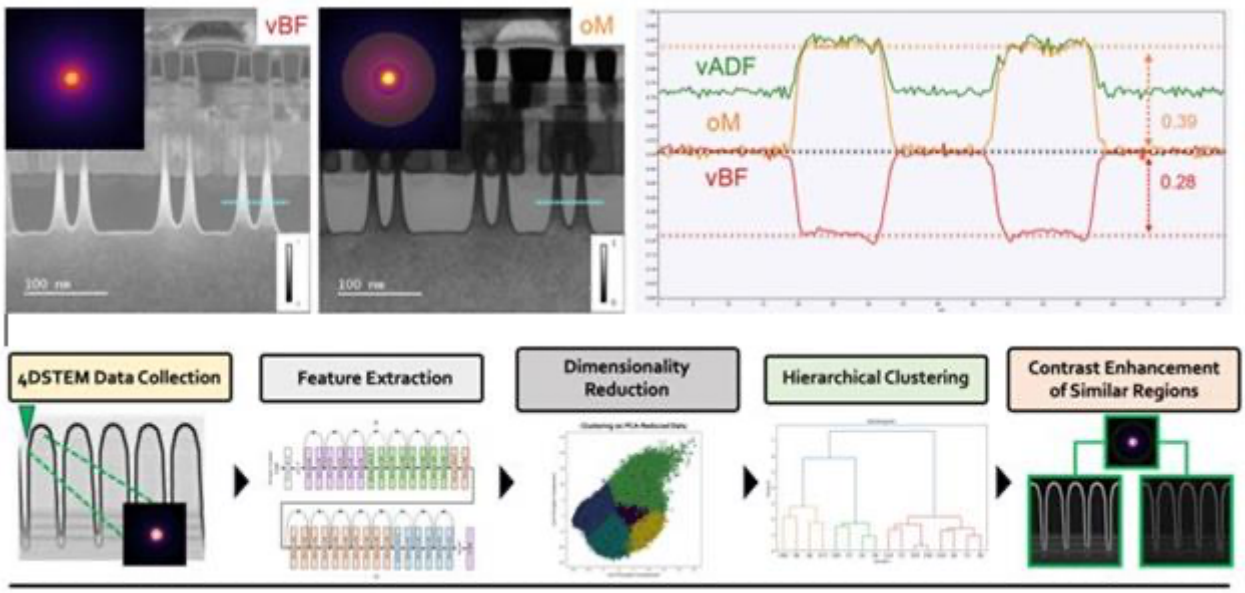

Keywords:

4D STEM, contrast enhancement

Reference:

1. C. Ophus, Microsc. Microanal. 25-3 (2019) 563-582. DOI: 10.1017/S1431927619000497
2. M. Wu et al., J. Phys. Mater. 6 (2023) 045008. DOI: 10.1088/2515-7639/acf524
3.He, K., Zhang, X., Ren, S., & Sun, J. (2015). Deep Residual Learning for Image Recognition. CoRR, abs/1512.03385. Available at: http://arxiv.org/abs/1512.03385

395

A Robust Toolkit to Correlate High Dimensional Multimodal Microscopy

Mr Thomas Selby[1], Mr Cullen Chosy[1,3], Dr Simon Fairclough[2], Mr Taeheon Kang[1], Dr Terry Chien-Jen Yang[1,3], Ms Hayley Gilbert[1,4], Mr Kieran Orr[1,3], Dr Tiarnan Doherty[2], Prof Paul Midgley[2], Prof Samuel Stranks[1,3]
[1]Department of Chemical Engineering and Biotechnology, University of Cambridge, Cambridge, UK, [2]Department of Materials Science and Metallurgy, University of Cambridge, Cambridge, UK, [3]Cavendish Laboratory, University of Cambridge, Cambridge, UK, [4]Diamond Light Source, Harwell Science and Innovation Campus, Didcot, UK

IM-10 (3), Lecture Theater 5, august 30, 2024, 14:00 - 16:00

Background
Spatially correlated multimodal microscopy allows an experimentalist to gain a holistic understanding of their sample by compiling complementary information from separate imaging modalities. This however relies on the robust registration of images between techniques- a difficult task with differences in the contrast mechanism, resolution and presence of artefacts all posing unique challenges. Furthermore, these problems are exacerbated by state-of-the-art instruments which produce high dimensional datasets (often upwards of hundreds of gigabytes), making the nuanced evaluation of scientific hypotheses challenging. Herein we present a general approach to coregister and interpret spatially correlated scanning electron diffraction (SED) and hyperspectral photoluminescence (PL) measurements performed on hybrid perovskites, an emerging class of semiconductor used as active layers in solar cells, LEDs and radiation detectors. SED, a variant of 4D-STEM, allows for information on crystallographic phase, orientation, and defects to be uncovered, whereas hyperspectral PL provides information on optoelectronic characteristics and performance. Given the fact that hybrid perovskites show striking spatial heterogeneity in both structure and performance, the spatial correlation of crystallographic information and PL is motivated by the prospect of unequivocally linking structure-property relationships in these materials.

Methods and Results
To find common areas between separate microscopes, gold fiducial markers are synthesized and deposited onto a thin film similarly to the work of Jones, Osherov and Alsari et al. [1]. Due to the resolution differences between SED (typical probe size ~5 nm) and hyperspectral PL (resolution diffraction limited to ~100s of nm) we record multiple contiguous SED scans before they are stitched together during post processing. To stitch the SED scans together virtual bright or dark field images are formed which act as a proxy for the 4D dataset. A keypoint detection and matching algorithm is then applied between the images; classical choices for this include the scale invariant feature transform (SIFT) or binary robust invariant scalable keypoints (BRISK) algorithms, commonly implemented using OpenCV [2]. Although these are undoubtably valuable tools, it has been empirically found that pretrained neural network-based approaches, such as Key-Net-AdaLAM implemented using Kornia, provide improved mappings [3]. Once the keypoints are detected, the random sample consensus algorithm (RANSAC), or variants thereof, is used to define an affine transform which stitches one image onto the other while capturing differences in rotation, shear, and translation [2,3]. To make these tools accessible a Python based GUI has been developed.

The registration of hyperspectral PL and stitched SED datasets is now considered. Due to the differences in pixel size between the two techniques the hyperspectral PL is upsampled via linear interpolation to match the SED pixel size. To coregister the resultant datasets several options are available. 1) An image transform can be defined by finding where the normalized cross correlation is maximal between the two images. Due to the differences in contrast mechanism a mask can be

applied such that only the Au fiducial marker is considered during this process. 2) The Python package AntsPy, primarily built for the registration of medical images can be utilized [4]. AntsPy uses 'multi-resolution gradient descent' and metrics such as cross correlation or mutual information to define the mapping. Importantly, as all image transforms are known we can then calculate where each 'pixel' from a SED scan corresponds to in the hyperspectral PL data.

Once the two datasets are coregistered the interpretation of any interrelationships between them poses a further separate challenge. Merely considering the SED data the scale of the problem becomes apparent— if 50 SED scans are acquired, each of which contains 512 x 512 diffraction patterns (typical during one experimental session), this amounts to a total of 13,107,200 individual patterns. To rapidly reduce data dimensionality, we have adapted the simple linear iterative clustering (SLIC) algorithm prevalent in the field of remote sensing and applied this to the SED data [5]. This approach allows us to reduce hundreds of thousands of individual diffraction patterns to ~100 single crystal patterns obtained by averaging diffraction patterns over individual grains of the polycrystalline halide perovskite film. SLIC can be thought of as a variant to K-means clustering and provides a general, intuitive, robust, and computationally inexpensive methodology to cluster SED data. Key principles underlying the algorithm are to remove points on your detector which have a low dynamic range or variance prior to clustering such that burdensome computation is only performed on a reduced subsection of the data. Additionally, cluster centroids only consider data in their close vicinity meaning unnecessary computation is further reduced. The spatial and channel Euclidean distances are combined into a single distance measure, with a weighting value being used to define the importance between them. This encodes intuition that 'pixels' close together likely belong to the same cluster. Finally, clusters which are highly correlated are combined before being used to calculate the mean diffraction patterns from the original data. Remarkably this approach proves exceptionally computationally efficient with typical compute times taking approximately a minute using a standard desktop machine (32Gb RAM, 11th Gen Intel(R) Core(TM) i5-11400 CPU). An automated indexing procedure of the clustered SED patterns can then be employed to obtain phase and orientation maps at low computational cost.

Conclusion

The toolkit introduced herein can elucidate structure-property relationships in state-of-the-art optoelectronic materials and provides a robust framework to perform correlative microscopy in related fields.

T.A.S acknowledges funding from EPSRC Cambridge NanoDTC, EP/L015978/1. C.C. acknowledges the support of a Marshall Scholarship, Winton Scholarship, and the Cambridge Trust. T.C.-J.Y acknowledges the support of a Marie Skłodowska-Curie Individual Fellowship from the European Union's Horizon 2020 research and innovation programme (PeTSoC, grant agreement no. 891205). K.W.P.O. acknowledges an EPSRC studentship (project reference: 2275833). T.A.S.D acknowledges Schmidt Science Fellows for a Schmidt Science Fellowship and the Ernest Oppenheimer Fund for an Oppenheimer Research Fellowship. PAM thanks the EPSRC for funding under grant numbers EP/V007785/1, and EP/R008779/1. S.D.S. acknowledges funding from the Royal Society (UF150033) and support from the European Research Council (European Union's Horizon 2020, HYPERION 756962).

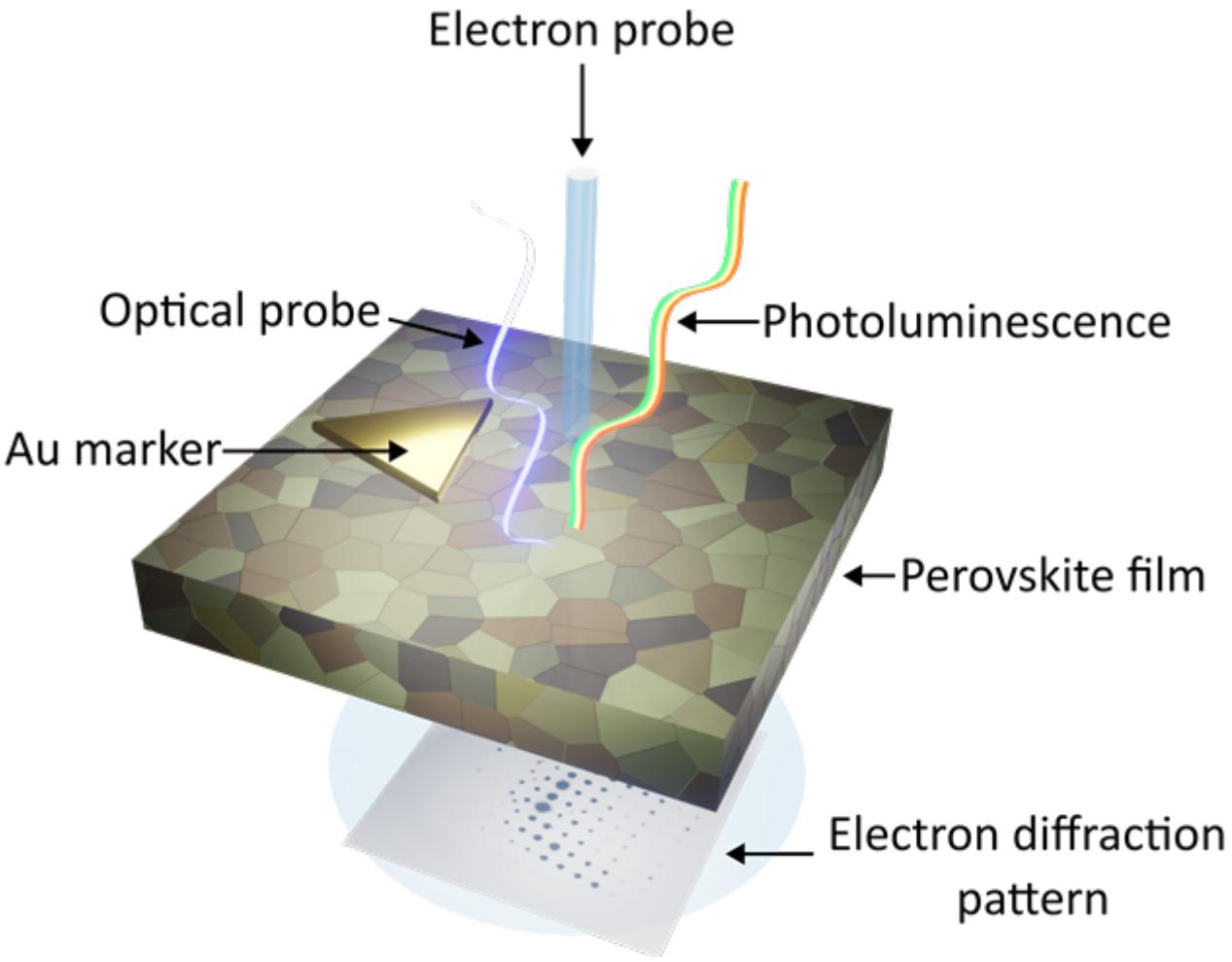

Keywords:

Correlative Microscopy, 4D-STEM, Energy Materials

Reference:

[1] T. W. Jones, A. Osherov, M. Alsari, et al., Energy Environ Sci, 2019, 12, 596–606.
[2] G. Bradski, Dr. Dobb's Journal of Software Tools, 2000, 120, 122-125.
[3] E. Riba, D. Mishkin, J. Shi, D. Ponsa, F. Moreno-Noguer and G. Bradski, A survey on Kornia: an open source differentiable computer vision library for pytorch, 2020.
[4] N. J. Tustison, et al., Sci Rep, 2021, 11, 9068.
[5] R. Achanta, et al., IEEE Trans Pattern Anal Mach Intell, 2012, 34, 2274–2282.

435

Data Augmentation and Innovative Machine Learning Approaches for Classifying EEL Spectra of Transition Metals Oxides

Daniel Del Pozo Bueno[1], Dr. Demie Kepaptsoglou[2], Prof. Quentin M. Ramasse[3], Prof. Francesca Peiró[1], Prof. Sònia Estradé[1]
[1]LENS-MIND, Dept. d'Enginyeria Electrònica i Biomèdica and Institute of Nanoscience and Nanotechnology (IN2UB), Universitat de Barcelona, Barcelona, , [2]School of Physics, Engineering and Technology, University of York & SuperSTEM Laboratory, Heslington - Daresbury, North Yorkshire - Cheshire, [3]Schools of Chemical and Process Engineering & Physics and Astronomy, University of Leeds & SuperSTEM Laboratory, Leeds - Daresbury, West Yorkshire - Cheshire

IM-10 (3), Lecture Theater 5, august 30, 2024, 14:00 - 16:00

Background including Aims:
The field of Scanning Transmission Electron Microscopy (STEM), especially through the application of Electron Energy Loss Spectroscopy (EELS), has experienced significant advancements due to technical innovations such as aberration correctors, direct detectors, and increased computing power. These advancements have facilitated the collection of large and complex datasets, highlighting the need for effective data management and analysis solutions in the STEM community. Machine Learning (ML), with its two main categories of supervised and unsupervised learning, has emerged as a crucial tool for addressing challenges in EELS, including classification, clustering of spectrum images, and denoising tasks [1,2].
However, the effective application of supervised ML is often hindered by the requirement for large, labeled datasets, which are difficult to acquire due to the susceptibility of samples to electron beam damage. Addressing this drawback, this study aims to compare the effectiveness of two supervised ML techniques: soft-margin Support Vector Machines (SVM) and Artificial Neural Networks (ANN) in classifying EEL spectra for the determination of oxidation states in transition metal oxides, particularly focusing on iron and manganese oxides. Additionally, we present a novel unsupervised learning approach that employs Generative Adversarial Networks (GANs) for data augmentation to address the problem of labeled data scarcity and improve the precision and effectiveness of oxidation state detection using EELS.
Methods:
This research presents a comparative analysis of soft-margin SVMs and ANNs, adapted to the specific challenges in EELS data classification [3]. We evaluate these classifiers based on their ability to accurately identify features indicative of oxidation states, such as white lines and the oxygen K edge, and the effect of energy shifts or noisy spectra. To enhance the classifiers' robustness and adaptability, we investigate the impact of incorporating energy-shifted spectra into the training process and explore various normalization methods, including maximum and L2 norms. The latter is analyzed by dimensionality reduction techniques, particularly Uniform Manifold Approximation and Projection. Additionally, we undertake a systematic exploration of ANN architectures through Random Search and Tree-structured Parzen Estimator (TPE) algorithms, aiming to pinpoint the most effective combinations of architecture and parameters for EELS data classification. Finally, we include the innovative use of GANs for data augmentation, which enables the generation of synthetic EEL spectra from a reduced set of experimental data. This approach not only amplifies the diversity and volume of available training data but also reduces the dependency on extensive, experimentally acquired datasets.
Results:
Based on white lines as particularly reliable indicators for oxidation state classification, SVMs are very robust against energy shifts for the EEL features under investigation, and they perform even better when trained on energy-shifted spectra. In comparison, ANNs, especially those employing

convolutional layers, demonstrate a superior ability to adapt to the complexities of EEL spectra, achieving a level of precision comparable to the best SVMs. The analysis of normalization techniques and the strategic use of the cosine kernel in SVMs emerge as effective strategies for avoiding normalization while keeping classification accuracy. Finally, the use of GANs for data augmentation marks a pivotal advancement, since this approach generates synthetic data that closely mirrors the variability and complexity of large experimental data collections, facilitating the training of these classifiers to be both more accurate and more generalized, capable of adapting to the diverse spectra encountered in EELS analysis.

Conclusions:

This work not only elucidates the comparative advantages of SVMs and ANNs in the classification of EEL spectra but also introduces a groundbreaking strategy for overcoming the challenges imposed by the limited availability of labeled datasets. SVMs are particularly recommended for simpler classification tasks where data volume is limited, offering an efficient solution that does not compromise performance. On the other hand, ANNs are more suited to tackling complex classification problems that involve larger datasets, benefiting from their enhanced capacity for learning and adaptation. The successful integration of GANs for data augmentation represents a significant advance, substantially reducing the reliance on extensive labeled datasets and paving the way for more efficient and effective classifier training.

Acknowledgments:

This work has been supported by the Spanish projects PDC2021-121366-I00, PID2019-106165GB-C21 and PID2022-138543NB-C21 financed by MCIN/AEI/ 10.13039/501100011033 and by the European Union NextGenerationEU/PRTR. FP acknowledges the ICREAAcademia 2022 grant from the Government of Catalonia. The authors also acknowledge the support received from the ELECMI - ICTS Electron Microscopy for Materials Science, the funding from Generalitat de Catalunya under project 2021SGR00242, the 2020 FI-SDUR grant from the AGAUR agency, and SuperSTEM acknowledges the Engineering and Physical Sciences Research Council (EP/W021080/1).

Keywords:

ML, EELS, GAN, SVM, ANN

Reference:

[1] del-Pozo-Bueno, D.; Peiró, F.; Estradé, S. Ultramicroscopy 2021, 221, 113190. https://doi.org/10.1016/j.ultramic.2020.113190.

[2] Blanco-Portals, J.; Peiró, F.; Estradé, S. Microscopy and Microanalysis 2022, 28 (1), 109–122. https://doi.org/10.1017/S1431927621013696.

[3] del-Pozo-Bueno, D.; Kepaptsoglou, D.; Peiró, F.; Estradé, S. Ultramicroscopy 2023, 253. https://doi.org/10.1016/j.ultramic.2023.113828.

462

Denoising of 4D-STEM Dataset using Pix2Pix GAN Algorithm and Artifact Reduction Strategy

Junhao Cao[1,2], Dr. Arnaud Demortière[1,2,3,4], Dr. Nicolas Folastre[1,2], Dr. Gozde Oney[5], Dr. Partha Pratim Das[6], Dr. Stavros Nicolopoulos[6]
[1]Centre national de la recherche scientifique (CNRS), Amiens, France, [2]Laboratoire de Réactivité et Chimie des Solides (LRCS, Amiens, France, [3]Réseau sur le Stockage Electrochimique de l'Energie (RS2E) , Amiens, France, [4]ALISTORE-European Research Institute, CNRS , Amiens, France, [5]Institute of Condensed Matter Chemistry of Bordeaux (ICMCB), CNRS , Pessac, France, [6]NanoMEGAS SPRL company, Brussels, Belgium

IM-10 (3), Lecture Theater 5, august 30, 2024, 14:00 - 16:00

Background and Aims
4D Scanning Transmission Electron Microscopy (4D-STEM) has revolutionized the study of nanoscale materials by offering localized structural imaging capabilities through electron diffraction patterns [1]. However, the inherent noise within these patterns often impedes critical structural details, posing challenges to accurate analysis, particularly in orientation-based clustering [2]. In response, this paper presents a comprehensive approach to denoising 4D-STEM datasets, focusing on leveraging Pix2Pix Generative Adversarial Networks (GANs) to reduce noise and the influence of the artefacts [3].
Methods
The methodology is to focus on training a Pix2Pix GAN architecture using paired noisy-clean 4D-STEM image data. Adjusting the conditional GAN framework, the generator network learns to map noise from input images to their corresponding clean counterparts, guided by the discriminator network, which distinguishes between real-clean images and generated ones [3]. This approach effectively captures the intricate relationships between noisy and clean data, facilitating precise denoising. To address artifacts commonly encountered in GAN-generated images [4], we integrate additional regularization techniques and architectural modifications into the generator. Furthermore, architectural adjustments such as skip connections and multi-scale discriminators are implemented to enhance image fidelity and minimize artifact occurrence.
Results
Extensive experimentation was conducted on both synthetic and real-world 4D-STEM datasets to evaluate the effectiveness of our approach. Quantitative metrics, including peak signal-to-noise ratio (PSNR) and structural similarity index (SSIM), were employed to assess denoising performance, complemented by visual comparisons to highlight the clarity and fidelity of denoised images. Results demonstrate significant noise reduction and artifact suppression, enabling clearer visualization of nanoscale structures and more precise analysis. Importantly, our approach offers a substantial time-saving advantage compared to traditional methods, reducing processing time from 15 hours (using e-Pattern processing [5]) to just 0.2 hours.
Conclusion
In conclusion, our methodology provides a robust solution for denoising 4D-STEM datasets, leveraging Pix2Pix GANs while effectively addressing the challenge of artifact reduction. Significantly, this work contributes to advancing the field of materials science by enhancing the utility of 4D-STEM imaging techniques and emphasising the potential of GAN-based approaches in complex image-processing tasks.

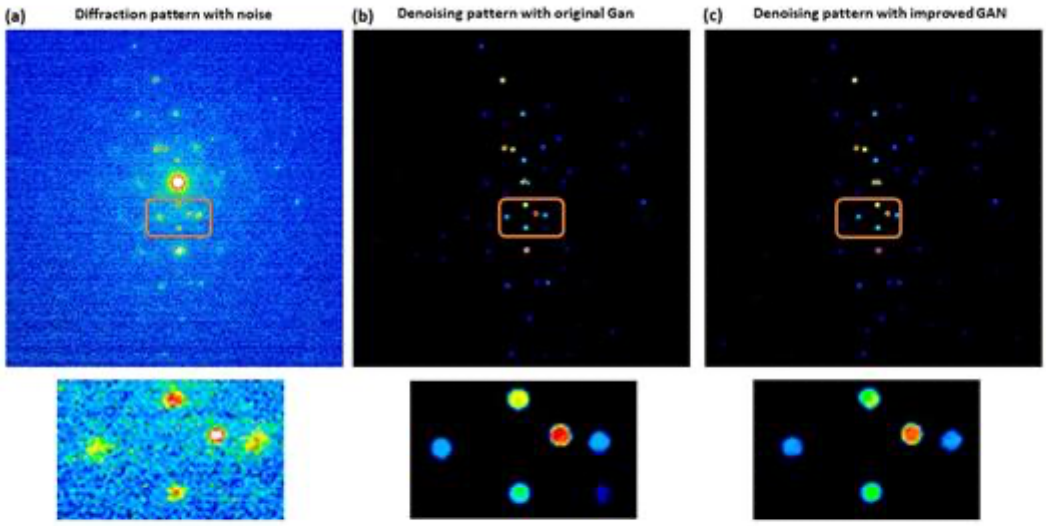

Figure 1. (a) The original dataset. **(b)** Artifacts in the context of GANs refer to unwanted or undesired patterns, distortions, or imperfections that can appear in the generated data. **(c)** The ideal result with the elimination of the artifact.

Keywords:

Deep Learning, Pix2PixGan, Denoising, 4D-STEM

Reference:

[1] S. J. Pennycook and P. D. Nellist, Scanning transmission electron microscopy: imaging and analysis. Springer Science & Business Media, 2011.

[2] R. Tibshirani, G. Walther, and T. Hastie, “Estimating the number of clusters in a data set via the gap statistic,” J R Stat Soc Series B Stat Methodol, vol. 63, no. 2, pp. 411–423, 2001.

[3] P. Isola, J.-Y. Zhu, T. Zhou, and A. A. Efros, “Image-to-image translation with conditional adversarial networks,” in Proceedings of the IEEE conference on computer vision and pattern recognition, 2017, pp. 1125–1134.

[4] X. Zhang, S. Karaman, and S.-F. Chang, “Detecting and simulating artifacts in gan fake images,” in 2019 IEEE international workshop on information forensics and security (WIFS), IEEE, 2019, pp. 1–6.

[5] N. Folastre et al., “Adaptative Diffraction Image Registration for 4D-STEM to optimize ACOM Pattern Matching,” arXiv preprint arXiv:2305.02124, 2023.

1152

Introducing a FAIR RDM infrastructure for electron microscopy and other materials science data

Prof. Christoph Koch[1], Dr. Markus Kühbach[1], Sherjeel Shabih[1], Dr. Sandor Brockhauser[1], Prof. Dr. Erdmann Spiecker[2], Markus Scheidgen[1], Lauri Himanen[1], Ádám Fekete[1], Dr. José A. Márquez[1], Prof. Dr. Heiko Weber[3], Prof. Dr. Claudia Draxl[1]
[1]Department of Physics and CSMB at Humboldt-Universität zu Berlin, Berlin, Germany, [2]Department of Materials Science and Engineering, FAU Friedrich-Alexander-Universität, Erlangen, Germany, [3]Institute of Condensed Matter Physics, FAU Friedrich-Alexander-Universität, Erlangen, Germany

IM-10 (3), Lecture Theater 5, august 30, 2024, 14:00 - 16:00

Digitization and an increase in complexity and price of electron microscopy hardware and characterization techniques, as well as the maturation of machine learning tools to extract patterns from large amounts of very diverse (annotated) data, promise to accelerate materials development by synergistically combining research data from many sources. While some labs have started uploading their (raw) research data to data repositories, this is only a first but insufficient step to realize the above-mentioned potential, as such repositories are typically either specific to a very particular technique or agnostic to much of the domain-specific content of the uploaded data [1,2]. In both cases the research data cannot be easily compared and integrated with experimental data from other sources or numerical predictions, and certainly not without significant human effort,. Therefore, working towards an interoperable knowledge representation for experiments and computer simulations [3-6] is the main motivation for implementing FAIR research data management. This highlights the need for tools for information extraction and semantic mapping. Fundamental to these tools' effectiveness is the creation of thorough and transparent documentation. This needs to be made more complete, shared openly, and should benefit from activities where representatives of the communities agree on defining and using standardized knowledge representations.
We will report on recent progress by the FAIRmat NFDI consortium [7] in extending NOMAD, the world's largest data base for ab-initio computational materials data, to also host experimental research data on the synthesis and characterization of materials in a machine-accessible manner, i.e. annotated with well-defined and interoperable metadata that establish links between related (experimental and computational) quantities [8-10]. We will report on our work on developing a comprehensive data schema for electron microscopy and related techniques, and the corresponding software tools for data converting, visualizing, and online-processing. We have integrated these tools as customizations into NOMAD Oasis to offer a locally-installable version of the NOMAD research data management system to complement its note keeping, file format parsing, cloud-based domain-specific data analyses, and information retrieval capabilities.

Keywords:

FAIR data managament, database

Reference:

[1] https://www.re3data.org
[2] https://explore.openaire.eu
[3] M. D. Wilkinson et al., (2016), https://doi.org/10.1038/sdata.2016.18
[4] A. Jacobsen et al., (2020), https://doi.org/10.1162/dint_r_00024
[5] M. Barker et al., (2022), https://doi.org/10.1038/s41597-022-01710-x
[6] M. Scheffler et al., (2022), https://doi.org/10.1038/s41586-022-04501-x
[7] https://www.fairmat-nfdi.eu/fairmat

[8] M. Scheidgen et al., (2023), https://doi.org/10.21105/joss.05388
[9] https://github.com/FAIRmat-NFDI/
[10] https://gitlab.mpcdf.mpg.de/nomad-lab/nomad-FAIR

18

Miniaturized material testing devices for multimodal in situ microscopic studies

Matthias Weber[1], Dr. Julian Müller[1], Dr. Rainer Steinheimer[2], Prof. Robert Brandt[3], Prof. Axel von Hehl[4], Prof. Benjamin Butz[1]
[1]Micro- and Nanoanalytics Group, University of Siegen, Siegen, Germany, [2]Lehrstuhl für Umformtechnik, University of Siegen, Siegen, Germany, [3]Lehrstuhl für Werkstoffsysteme für den Fahrzeugleichtbau, University of Siegen, Siegen, Germany, [4]Lehrstuhl für Materialkunde und Werkstoffprüfung, University of Siegen, Siegen, Germany

Poster Group 2

To contribute to the understanding of failure and fatigue, we examine the local microstructural strain/stress peaking as well as crack initiation/propagation by in situ methodology. Moreover, systematic errors in load/displacement of the measuring setup may be overcome by highly localized strain measurements, e.g. high-resolution EBSD in conjunction with image correlation. This requires in situ material tests, and we aim at two complementary goals. One is to contribute to alloy development and to optimize microstructure of selected alloys determining the macroscopic mechanical properties.
The second is to validate modern microstructure-based FEM simulations and to develop termination criteria for classical FEM simulations, e.g. for crack initiation. Therefore, the Mechanical Engineering Department develops in situ testing machines for static and dynamic tests. Latest developments are a portable, miniaturized 3-point bending machine for use in FIB/SEM/XRD (Fig. 1 a). Thos enable the direct observation of microstructural changes like crack initiation/propagation, as well as phase transformations, e.g. in steels. As an example, the bending machine (750g, 100x100x50mm) with independent load/displacement sensors allows for massive plastic deformation at loads up to 4kN. Our solution includes a user-friendly interface to lower the entry barriers for beginners (Fig. 1 c). In this contribution, we highlight the possibilities to observe dynamics of crack initiation/propagation, phase transformations, and the local evolution of the microstructure during testing of materials like Al alloys and austenitic steel. Electron backscatter diffraction (EBSD) is employed to in detail understand the crystallographic structure adjacent to the crack (Fig. 1 b). Direct image correlation is used to examine local strain peaking. Future plans involve establishing high-resolution EBSD instrumentation and data analysis for highly localized strain/stress/GND mapping as well as corresponding XRD data during a single experiment.

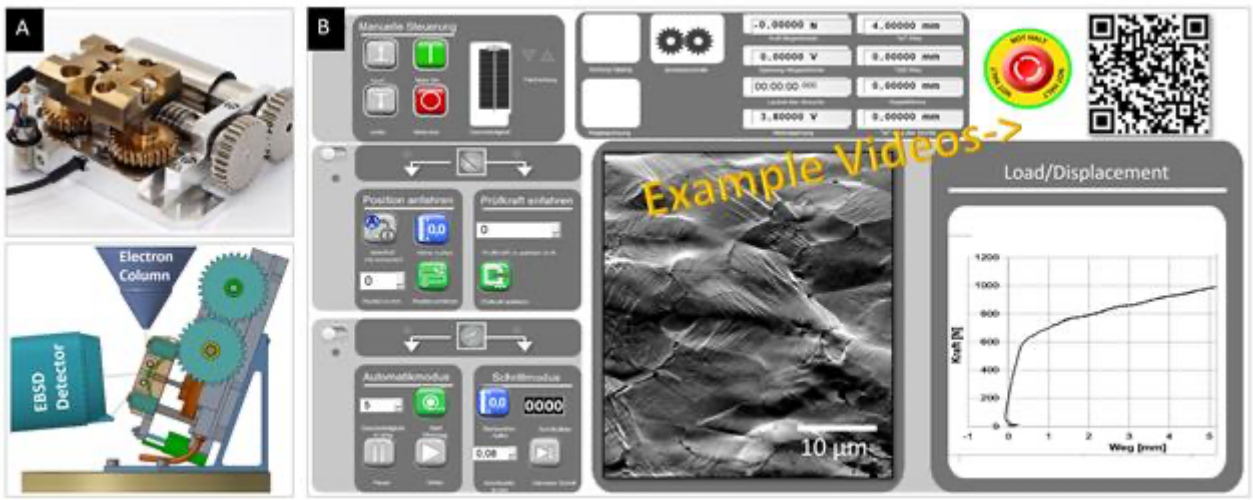

Keywords:

Multimodal, InSitu, Videomicroscopy, Material testing

36

An advanced smart counting mode for pixelated direct electron detectors based on semiconductors

Dr. Björn Eckert[1], Mr. Stefan Aschauer[1], Mr. Martin Huth[1], Mrs. Petra Majewski[1], Mrs. Heike Soltau[1], Mr. Lothar Strüder[2]
[1]PNDetector, München, Germany, [2]PNSensor, München, Germany, [3]University of Siegen, Siegen, Germany

Poster Group 2

Pixelated direct electron detectors identify electrons by their interaction with the sensitive detector volume. The relevant interaction is an energy deposition via electron-electron scattering. However, in applications like 4D-STEM, the user is interested in the spatial-resolved absolute number of incident electrons on the detector surface. Therefore, the goal is to count each electron exactly one time at the position it crosses the detector surface. The following assumptions were made for silicon as detector material but are transferable to other materials as well.
Low-energetic electrons (E ≈ 10 - 30keV), as used in scanning electron microscopes, typically deposit their energy in a small volume very close to the point of entry. This volume is mostly much smaller than the size of the pixel structure (e.g. for the standard pnCCD 48 µm x 48 µm).
High-energy electrons with energies > 100 keV, as usually used for transmission electron microscopes, typically do not deposit their energy locally at one specific point but deposit the energy in many steps along three-dimensional tracks through the detector volume. For electrons with a primary energy of 300 keV, the average length of these tracks is 450 µm. The shape of these tracks is caused by multiple scattering of the electrons in the detector volume and, therefore, is stochastic.
The energy deposition in the three-dimensional detector volume locally generates charge carriers that form a charge cloud. Direct electron detectors like the pnCCD collect the charge cloud at the opposite side of the entrance window. Therefore, the charge cloud drifts due to an applied electric field to the opposite side of the detector. During the drift time, the size of the charge cloud increases due to repulsion of the charge carriers themselves and due to diffusion. In comparison to the statistical behavior of the energy deposition, the drift process behaves deterministically. The collected charge carriers in each pixel of the pixel structure correspond to the binned two-dimensional projection of energy deposition, widened by the drift process. The total number of charge carriers is directly related to the amount of deposited energy.
For low primary energy, the structure of the charge cloud is mostly just influenced by the primary energy of the electron itself, and its point of entry relative to the pixel structure. Therefore, for electrons that enter the detector at the same point with the same primary energy the pixel-wise collected charge clouds look similar. For higher energetic electrons, the size and the shape of the pixelated charge cloud are mostly influenced by multiple scattering. Therefore, the distribution of the pixel-wise collected charge carriers is different for each individual electron. During the detector readout, the pixel-wise collected charge carriers are transferred into a detector response. If the measuring process of the number of individual charge carriers in each pixel is sufficiently precise, the detector response is a good approximation of the two-dimensional projection of the charge cloud. The structure of the 2D projection can be used to calculate the point of entry for individual electrons for higher energetic electrons on pixel level and for lower primary energies even on sub-pixel level. However, for some applications in TEMs and SEMs require a higher electron flux on the detector such that the measured two-dimensional projection of the charge clouds of two or multiple primary electrons overlap. This leads to three different regimes depending on the flux. The first regime is where the detector response of individual electrons is separable. The second regime has contributions where multiple electron traces overlap but the contributions of the individual primary electrons are still visible. The third regime is dominated by a very high flux that leads to intensity

images. In the third regime, the contributions of individual primary electrons are not visible anymore. Different regions in the same diffraction pattern can hold different regimes.
Our algorithm can handle the different regimes in flux on pixel level and reconstructs the number of contributing primary electrons and their points of entry. The point of entry reconstruction happens depending on the energy of the primary electrons and the flux on physical pixel level or subpixel level in real-time. In this contribution, we will show that the proposed Smart Counting algorithm significantly increases the precision in counting the number of primary electrons and their spatial position compared to a simple counting mechanism by individual discriminators on pixel level.

Keywords:

pixelated direct electron detector
pnCCD

Reference:

Ryll, H., et al, Journal of Instrumentation 11 (2016)

58

Fractal: An open-source framework for reproducible bioimage analysis at scale using OME-Zarrs

Dr. Joel Lüthi[1]
[1]BioVisionCenter, University of Zurich, Zurich, Switzerland

Poster Group 2

Background incl. aims
Analyzing large amounts of microscopy images in a FAIR manner is an ongoing challenge, turbocharged by the large diversity of image file formats and processing approaches. Recent community work on an OME next-generation file format [1] offers the chance to create more shareable bioimage analysis workflows. Building up on this and to address issues related to the scalability & accessibility of bioimage analysis pipelines, the BioVisionCenter, a newly-created structure of the University of Zurich & the Friedrich Miescher Institute for Biomedical Research, is developing Fractal [2], an open-source framework for processing images in the OME-Zarr format.

Methods
The Fractal framework consists of a server backend & web-frontend that handle modular image processing tasks. It facilitates the design and execution of reproducible workflows to convert images into OME-Zarrs and apply advanced processing operations to them at scale, without the need for advanced expertise in programming or large image file handling.

Results
Fractal allows users to orchestrate the analysis of terabytes of high content microscopy images on high performance clusters. It comes with pre-built tasks to perform instance segmentation with state-of-the-art machine learning tools, to apply registration, and to extract high-dimensional measurements from multiplexed, 3D image data. We are providing a web front-end to facilitate user interactions with Fractal and streamline the submission of image analysis jobs to a slurm cluster. Finally, by relying on OME-Zarr-compatible viewers like napari [3], MoBIE [4] and ViZarr [5], Fractal enables researchers to interactively visualize terabytes of image data stored on their institution's remote server, as well as the results of their image processing workflows.

Conclusions
We present the open-source framework Fractal for FAIR image analysis at scale in the OME-Zarr format.

Keywords:

OME-Zarr, bioimage-analysis, workflows, processing, FAIR

Reference:

[1] Moore et al., 2023, https://doi.org/10.1007/s00418-023-02209-1
[2] Fractal: https://fractal-analytics-platform.github.io
[3] napari contributors, 2019, https://zenodo.org/record/3555620
[4] Pape et al., 2023, https://doi.org/10.1038/s41592-023-01776-4
[5] Manz et al., 2022, Nature Methods. https://doi.org/10.1038/s41592-022-01482-7

61

Comprehensive 3D Characterization Workflow for Solid Oxide Cells

Dr Bartlomiej Winiarski[1], Patrick Barthelemy[2], Chengge Jiao[3], Dirk Laeveren[3], Dalton Cox[4], SA Barnett[4]
[1]Thermo Fisher Scientific, Brno, Czech Republic, [2]Thermo Fisher Scientific, Waltham, USA, [3]Thermo Fisher Scientific, Eindhoven, The Netherlands, [4]Northwestern University, Evanston, USA

Poster Group 2

Background
Performance and durability of solid oxide cell (SOC) electrodes depend heavily on their porous microstructure properties and evolution over time. Ga+ FIB-SEM tomography has been pivotal for reconstructing SOC microscopic structures with nanometric precision [1], albeit limited to small volumes. With the emergence of Plasma FIB-SEM (PFIB-SEM), offering access to significantly larger material volumes [2], SOC microstructure investigation has taken a leap forward.
The porous nature of SOC microstructures poses challenges during both data collection and processing, resulting in artifacts like FIB curtaining and back-pore issues. Though techniques such as pressure-filling pores with resin [3] and rocking polish [2] mitigate these, electron charging effects persist. Deep Learning (DL) methods have shown promise in addressing back-pore issues [4], but challenges remain in electron charging compensation.
Post-segmentation, serial-sectioned SEM images undergo further processing to create 3D digital representations. This involves numerical simulations incorporating morphological parameters like tortuosity and constrictivity, crucial for understanding transport properties. Various software packages aid in this 3D characterization process [5].
This contribution presents a complete workflow for SOC microstructure characterization, from 3D reconstruction to comprehensive quantification. Using a Plasma FIB-SEM platform and automated serial sectioning software, a large 3D volume of SOC electrode is obtained, enabling detailed analysis. Advanced SEM imaging techniques coupled with DL-based segmentation streamline data processing, significantly reducing workflow time.

Methods
To demonstrate the workflow (Figure 1), we characterize a fresh solid oxide fuel cell (NYDC-55-3-0). Using the Plasma FIB-SEM platform and automated serial sectioning software (Auto Slice and View 5 - ASV5), we collect a large 3D volume (180 × 150 × 30 µm³) with a voxel size of 32 × 32 × 50 nm³. The Xe+ plasma beam current of 60 nA @ 30keV serial sections the specimens with a ±3° beam rocking motion and a 25 nm cut advancement. After each odd PFIB cut, SEM images are simultaneously acquired perpendicular to the cut face using a through-lens detector (TLD) for secondary electrons (SE) and a retractable concentric backscattered electron detector (CBS) for backscattered electron images. We utilize an SEM current of 200pA @ 2keV high tension and a 5 µs pixel dwell time to exploit the charge contrast phenomenon captured by the TLD-SE detector, enabling the separation of percolated and non-percolated Ni. The backscattered electron images from the CBS detector highlight voids and YSZ grains. The activated ASV5 auto functions for SEM, including source tilt, lens alignments, stigmatisms, focus, and image matching for drift correction, ensure consistent imaging conditions throughout the ASV run. By employing auto image matching for drift correction and SEM imaging at the normal angle to the cut face, we maintain volume-lossless conditions in the 3D image stack before data post-processing.

Results
We developed automated Avizo recipes to streamline data processing, analysis, and enable consistent and reliable data quantification and 3D visualization. The image stack doublets are

subjected to denoising and segmentation into Ni, YSZ, and Voids using DL models [6], which also distinguish between percolated and non-percolated phases. The recipes calculate various spatial parameters (Figure 2) such as tortuosity [7], TPBs (total length, length/volume), phase volume fractions, percentage of non-percolating for each phase, and surface area/volume for Void|YSZ, Void|Ni, and YSZ|Ni. Notably, recent advancements in SEM image post-processing and denoising using DL algorithms in Avizo software have reduced SEM imaging time by 50%, resulting in a 25-30% reduction in the total acquisition time for the entire dataset.

Conclusion

This study shows comprehensive workflow that harnesses deep-learning predictions, encompassing the entire process from PFIB-SEM-based 3D microstructure analysis to meticulous quantification, illustrated through the examination of a freshly prepared solid oxide fuel cell. Our innovations have led to a thousandfold increase in image data acquisition volume compared to previous studies, all while maintaining a consistent voxel size. To ensure robust identification of material constituents, we simultaneously acquired CBS BSE and TLD SE images, ensuring 99.99% confidence. Key focuses include precise specimen preparation, optimizing PFIB-SEM setup for serial-sectioning, SEM image acquisition, DL-based post-processing and segmentation, recipe-oriented 3D quantification of morphological parameters, and report generation. Advanced SEM imaging techniques, coupled with automation and recent advancements in SEM image post-processing and segmentation using ML algorithms, streamline the characterization process, significantly reducing workflow execution time.

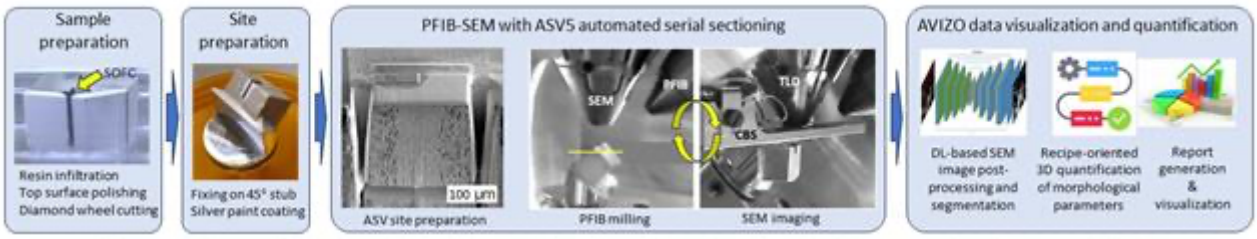

Figure 1. A complete characterization workflow from 3D microstructure to comprehensive quantification

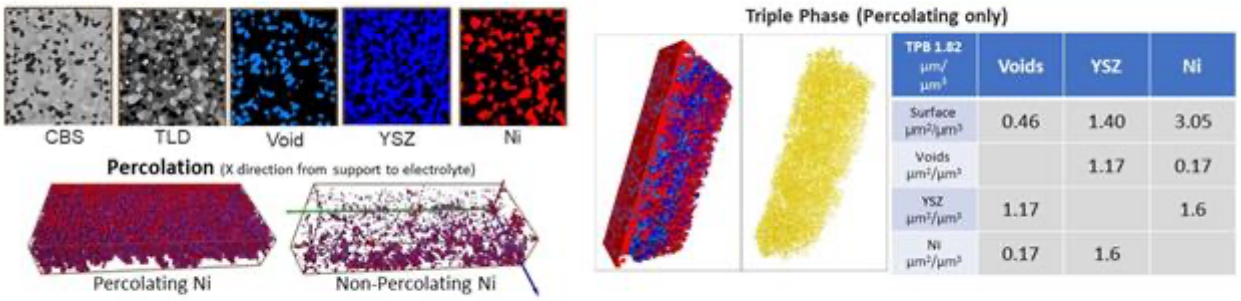

Figure 2. Shows results of Avizo post-processing, segmentation, and quantification of SEM image doublets. Triple-phase boundary for percolating Ni, (c) visualization of percolating and non-percolating Ni.

Keywords:

PFIB-SEM, Deep-Learning, Serial-Sectioning Tomography, SOFC

Reference:

1. JR Wilson-et-al., Nature Materials 5 (2006), p. 541.
2. TL Burnett-et-al., Ultramicroscopy 161 (2016), p. 119.
3. CS Kuroda- Y Yamazaki, ECS Trans. 11 (2007), p. 509.
4. SJ Cooper-et-al., J. Electroch. Soc. 169 (2022), p. 070512.
5. L Holzer-et-al., in “Tortuosity-and-Microstructure...”, ed. R Hull, (Springer, Cham, 2023), p.114.

71

FFT denoising methodology through CNN for the study of WS2 vacancies

Ivan Pinto[1], Mr. Marc Botifoll[1], Mr. Yuki Wang[3], Pf. Chen Wang[3], Pf. Jordi Arbiol[1,2]
[1]Catalan Institute of Nanoscience and Nanotechnology (ICN2), CSIC and BIST, Barcelona, Spain, [2]ICREA, Pg. Lluis Companys 23, Barcelona, Spain, [3]MSE, Tsinghua University, Beijing, China

Poster Group 2

2D materials as WS2 have become increasingly relevant and widely studied in recent years due to their electronic and optical applications [1]. One of the most effective techniques for characterizing these materials and studying their physical properties is High-Angle Annular Dark-Field (HAADF) imaging in a Scanning Transmission Electron Microscope (STEM). On the other hand, to study lighter atoms it is common to use Integrated Differential Phase Contrast (iDPC) STEM. These techniques allow researchers to study the crystallography of the material to determine the presence of defects. These images often contain noise that poses a challenge when studying vacancies. Consequently, we developed an FFT denoising technique employing a Convolutional Neural Network (CNN) with a U-NET architecture [2, 3]. The CNN was trained using more than 5000 simulated spectra from diverse materials and various orientations. After FFT denoising, we could perform an inverse FFT (IFFT) to return to real space. This results in a significantly cleaner image, rendering crystallographic analysis more accessible, as atomic positions become much more discernible. Conversely, the FFT denoising method leads to the emergence of ‘fake atoms' in locations where vacancies should exist. While this outcome may initially appear counterproductive, it was, in fact, the crucial element that enabled the execution of this study. In this way, by subtracting the original experimental HAADF-STEM image from the filtered one, we obtain a new images where the bright spots correspond to the atomic vacancies
(Figure 1).
In conclusion, the methodology employed in this study has enabled a statistically significant analysis of vacancies across multiple images. Each image has been subjected to a detailed examination of more than 3000 atomic positions, yielding robust and reliable results. This approach not only provides a profound understanding of vacancy distribution but also gives the way for automating the statistical analysis of vast amounts of images within short timeframes. This potential for automation not only enhances process efficiency but also holds promise for accelerating the pace of discovery and understanding in research fields reliant on atomic-scale image analysis.

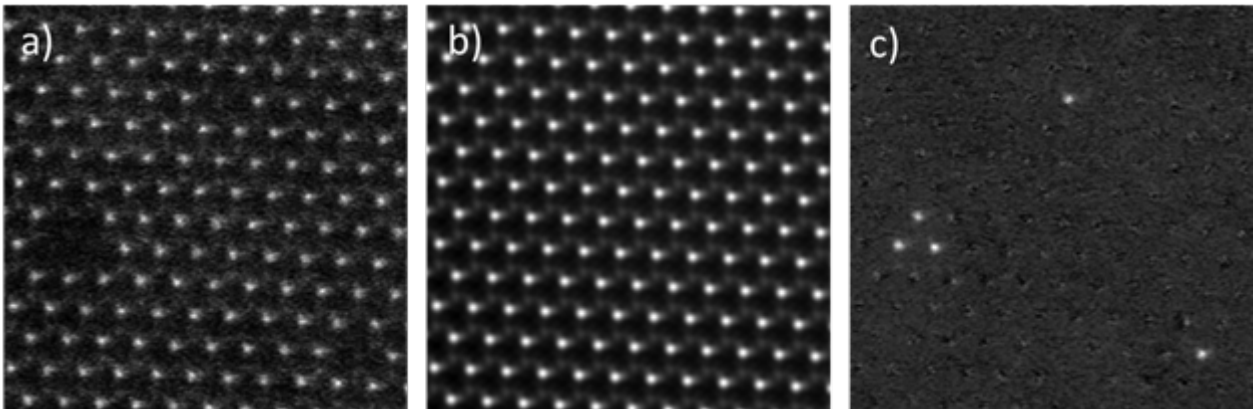

Keywords:

CNN, FFT, iDPC, HAADF-STEM, vacancies

Reference:

[1] Kumbhakar P. Chowde G., Tiwary C., Frontiers in Materials, 8 (2021) 721514

[2] Ziatdinov M., Dyck O., Maksov A. et al., ACS Nano, 11, 12 (2017) 12742–12752
[3] Botifoll M., Pinto-Huguet I., Arbiol J., Nanoscale Horiz., 7 (2022) 1427-1477

108

MIPAR Spotlight: Shedding Light on Next-Generation Detection for Microscopists

CEO Sammy Nordqvist[1], Mr Sammy Nordqvist[2], Dr John Sosa[1], Mr Michael Kudlinski[1]
[1]MIPAR Image Analysis Software, Columbus, United States, [2]SciSpot, Stenungsund, Sweden

Poster Group 2

Background
For scientists and engineers across various disciplines, image analysis serves as a vital tool for gaining deeper insights into complex phenomena. Whether studying biological structures, geological formations, engineering components or materials microstructures, the ability to extract quantitative data from images is invaluable. Image analysis enables engineers and researchers to replace manual analysis and increase productivity, to gain additional data insights and improve statistics, and to advance their work by solving complex problems. By harnessing the power of image analysis, scientists and engineers can accelerate research, optimize manufacturing processes, and improve performance of products across a wide range of fields, ultimately advancing our understanding of the natural world and improving technology.

Method and results
Using deep learning and powerful image analysis engines, MIPAR (www.mipar.us) allows users to perform a fast, accurate and automated analysis of images. Through a user-friendly interface, engineers and researchers can personalize analysis to their samples as well as visualize and extract measurements - all without programming. Through five integrated applications, MIPAR offers flexibility and efficiency for 2D and 3D analysis applications. The key ingredients are in the Recipes, which include a series of analysis steps that are tailored to each application. As a result, researchers and engineers can now easily solve problems such as grain size analysis excluding the twins, particle analysis of clusters, defect identification and many more.

Seamlessly integrated within the MIPAR ecosystem, the Snap tool, powered by Spotlight, offers accelerated creation of training datasets for an efficient and streamlined model training workflow. The accurate segmentations provided by Spotlight allow for less time spent creating models and algorithms, leading to faster data collection. MIPAR Spotlight simplifies image analysis even further by limiting the need for custom model configurations and amplifying a model’s ability.

Conclusion
This presentation will overview the advantages of using MIPAR Spotlight, the new cutting edge of detection, to analyse grains, particles, droplets, and defects with real industrial applications.

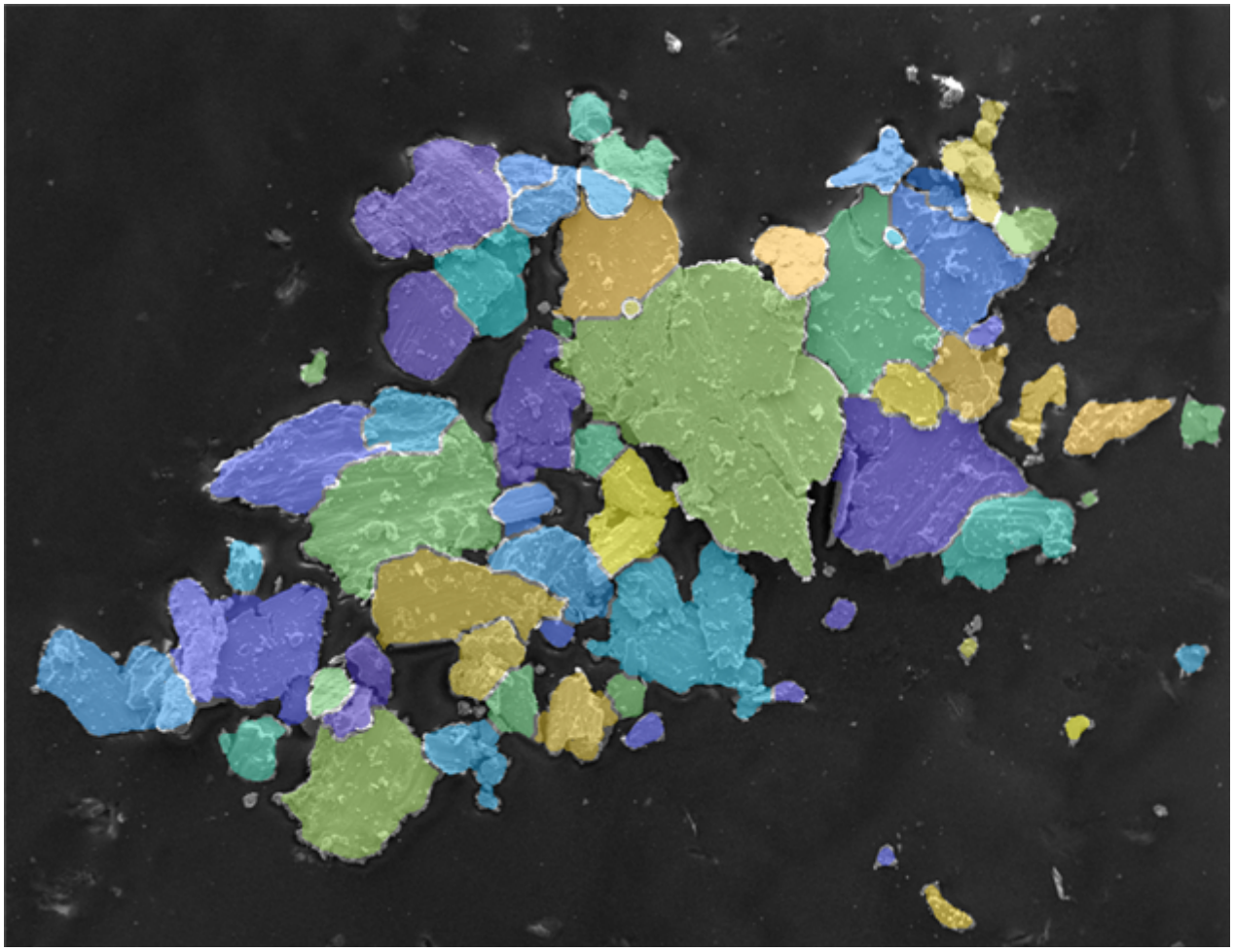

Keywords:

image analysis, deep learning, microscopy

226

Unlocking 3D nanoparticle shapes from 2D HRTEM images: a Deep Learning breakthrough

Romain Moreau[1], Dr. Hakim Amara[1], Dr. Maxime Moreaud[2], Dr. Jaysen Nelayah[3], Mr. Adrien Moncomble[3], Dr. Damien Alloyeau[3], Pr. Christian Ricolleau[3], Dr. Riccardo Gatti[1]
[1]Université Paris-Saclay, ONERA, CNRS, Laboratoire d'Études des Microstructures, Châtillon, France, [2]IFP Énergies Nouvelles, Solaize, France, [3]Université Paris Cité, CNRS, Laboratoire Matériaux et Phénomènes Quantiques (MPQ), Paris, France

Poster Group 2

Background incl. aims
Nanoparticles (NPs) are typically observed and analysed using High Resolution Transmission Electron Microscopy (HRTEM) for highly precise structural studies at the atomic scale. However, determining their 3D shapes from 2D HRTEM images is a tedious process. Indeed, this type of analysis is based on manual post-processing which suffers, among other issues, from experimental noise or human bias performed at post-experimental stage. In this context, the integration of artificial intelligence (AI) methodologies into data acquisition and analysis protocols is a very promising approach [1]. To tackle the problem of identifying the 3D shape of NPs, we developed a Deep Learning (DL) model to automate this task ensuring reliable statistical analysis of a large number of NPs many of which cannot be identified by conventional methods.
Methods
For this purpose, we extend an approach we had developed to identify the structure of carbon nanotubes from their Moiré patterns obtained from HRTEM images [2]. More precisely, the DL model, leveraging Convolutional Neural Networks (CNNs), is trained on datasets of simulated HRTEM images of NPs, labelled according to their shapes, ranging from 4 to 8 nm. A critical point of this study was generating a representative and optimised dataset. To accomplish this, we constructed atomistic 3D models of NPs deposited on an amorphous carbon substrate, subjecting NPs to random rotations to encompass all potential observed orientations. Furthermore, we simulated the amorphous substrate using realistic carbon membrane derived from a tight-binding framework and noise models, to mimic experimental conditions [3]. Finally, HRTEM images were simulated using the Dr Probe code [4] based on the multi-slice method with parameters consistent with aberration-corrected transmission electron microscopes.
Results
The objective of generating an optimal training dataset was attained through comprehensive studies evaluating the impact of various parameters, including amorphous carbon, resolution, focusing conditions, NPs' size, and NPs' orientations, on DL model predictive accuracy.
Conclusion
This approach has resulted in the development of an efficient and accurate DL framework for predicting 3D NP shapes from 2D HRTEM images, validated across both simulated and experimental datasets (see figure).

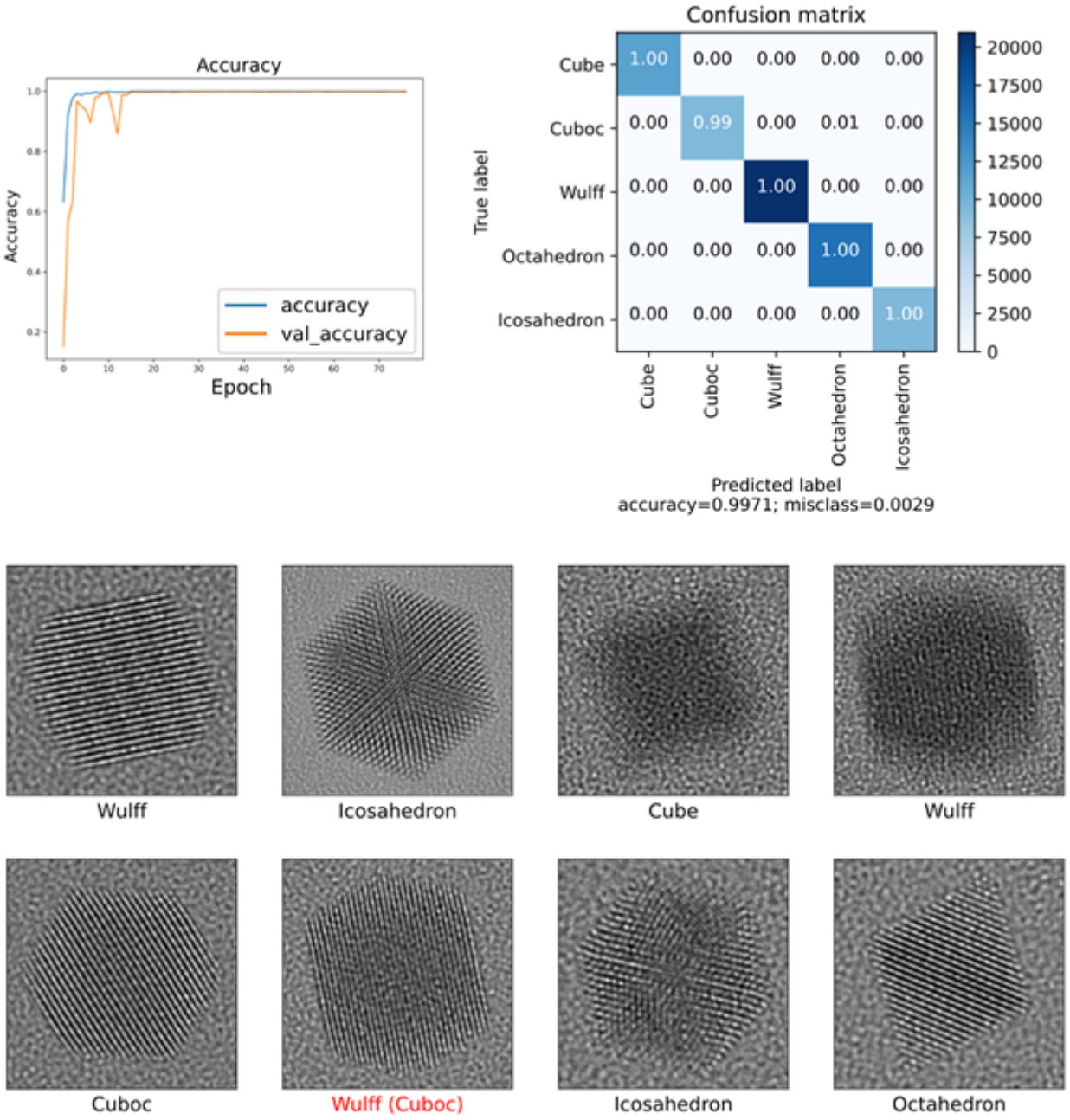

Figure. (Top) Performance of the model (confusion matrix) trained with around 45 000 images for classifying five different shapes of NP. (Bottom) Examples of 3D shape predictions on simulated TEM images with one error (in red).

Keywords:

DL; nanoparticle; TEM; atomistic simulation

Reference:

[1] S. R. Spurgeon et al., Nat. Mater. 20, 274 (2021)
[2] G. D. Förster et al., Carbon 169, 465 (2020)
[3] C. Ricolleau et al., J. Appl. Phys. 114, 213504 (2013)
[4] J. Barthel, Ultramicroscopy 193, 1 (2018)

237

Application of reinforcement learning to aid the alignment of an electron microscope

Richard Konstantin Jinschek[1], Dr. Mounib Bahri[2], Dr. Mario Gianni[3], Dr. Yao-Chun Shen[4], Dr. Nigel D. Browning[2,5]
[1]Distributed Algorithms Centre for Doctoral Training, University of Liverpool, Liverpool, UK, [2]Department of Mechanical, Materials and Aerospace Engineering, University of Liverpool, Liverpool, UK, [3]Department of Computer Science, University of Liverpool, Liverpool, UK, [4]Department of Electrical Engineering and Electronics, University of Liverpool, Liverpool, UK, [5]SenseAI Innovations Ltd., Brodie Tower, University of Liverpool, Liverpool, UK

Poster Group 2

Background incl. aims
In both SEM and TEM, the alignment process for each experiment is unique and not replicable. If not done well this also has major implications on the stability of the experiments and the quality of the obtained data regardless of the specimen or sampling technique. It requires days of diligent practice on a variety of electron microscopes in order to become an expert and be able to collect data with the highest possible resolution consistently across experiments.
A proposed solution to this skill barrier is a digital twin for an electron microscope, with the purpose being to make experiments more reproducible, efficient and improving the overall reliability and resilience of experiments [1]. The initial steps in this is to automate the alignment process, starting with the eucentric height using machine learning (ML) techniques.
Methods
The proposed method for finding the optimal eucentric height is reinforcement learning (RL), a subset of ML where an agent learns how to interact with an environment in order to make decisions. Using a q-learning function and a reward function the agent is able to determine the optimal action in order to achieve the correct z-height. For training an agent on images at different z-heights learning a q-table is sufficient due to the small and finite action space. However, for applications on a microscope, a deep-q-network (DQN) is required, which instead of knowing the possible rewards from a trained q-table estimates the rewards and works for larger action spaces [2].
Results
Initial tests on a small state space where the environment is defined as images taken at different z-heights with intervals of 2µm ranging from 0µm to 50µm (including the eucentric height), show that the agent is able to learn a q-table within 10000 iterations. With this initialized q-table the agent is able to find the image that was taken at the eucentric height instantaneously.
Conclusion
Preliminary tests indicate that reinforcement learning holds promise as a viable solution for automating the alignment process of an EM, potentially reducing the expertise needed to conduct experiments effectively and accurately.

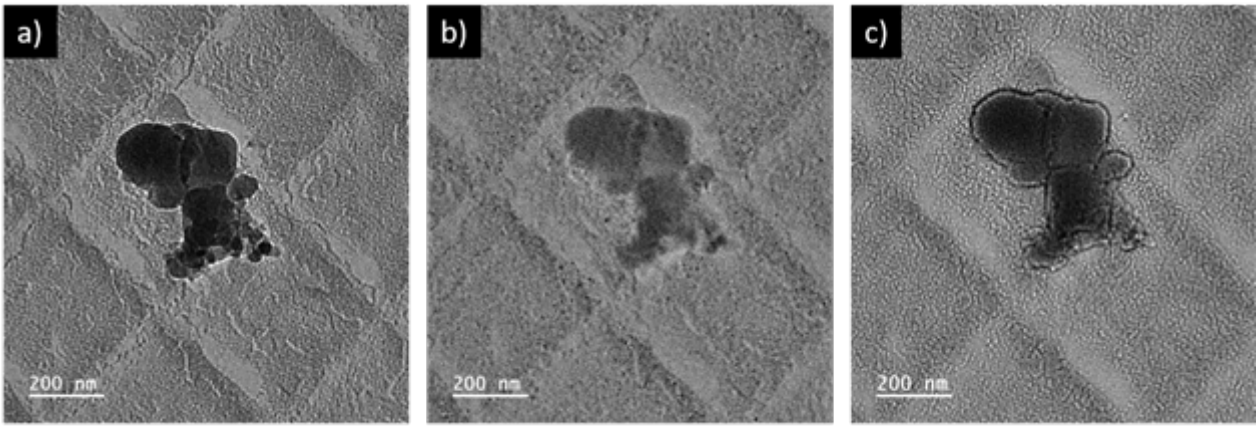

Figure 1. Images taken at different z-heights in order to facilitate the training of a RL agent. (a) 0µm, (b) 26µm and (c) 50µm.

Keywords:

Digital Twin, Reinforcement Learning, Deep-Q-Network

Reference:

1. VanDerHorn, Eric, and Sankaran Mahadevan. "Digital Twin: Generalization, characterization and implementation." Decision support systems 145 (2021): 113524.
2. Mnih, Volodymyr, et al. "Playing atari with deep reinforcement learning." arXiv preprint arXiv:1312.5602 (2013).

371

Mapping of interstitial atoms using super-resolution and optimized machine-learning techniques

Dr. Cyril Guedj[1]
[1]Univ. Grenoble Alpes, CEA, LETI, Grenoble, France

Poster Group 2

Abstract- Dedicated machine-learning techniques applied to superresolved HRSTEM images are used to map interstitial atoms with decananometric spatial resolution and picometric precision. This methodology is illustrated with the technologically-relevant case of etched GaN, used for power devices. In general, an average chemical concentration evolution close to a typical erf implantation profile is obtained, in agreement with atomistic simulations.

Keywords: imaging, super-resolution, superresolution, machine-learning, mapping, interstitials, TEM, STEM, HRSTEM

I. BACKGROUND AND GOALS

The interstitial atoms have a potential impact on the performance and reliability of microelectronic or electro-optic or quantum devices, but the precise mapping of their distribution is a very difficult task. In the field of MOSc-HEMT power devices, the etching steps may induce a detrimental ion implantation at critical interfaces in the case of recessed hybrid processes. These defects might potentially induce parasitic leakages currents and a detrimental reduction of breakdown voltages. The local defectivity increase due to such technological steps usually occurs in an ultrashallow range (nanometric or below), which is very difficult to precisely estimate. To tackle this major characterization challenge, novel methodologies have been developed, patented [1], and will be detailed here.

To map the chemical concentration profiles, many state-of the art techniques are currently used, such as secondary ion mass spectrometry (SIMS), electron energy loss spectrometry (EELS) or Energy dispersive X-ray analysis (EDX) among others, but all the techniques have their intrinsic limitations. For instance, it is usually very difficult to distinguish between substitutional and interstitial atoms with these characterization methods. Interstitial atoms are so small that they are generally very difficult to detect by conventional transmission electron microscopy [2]. Hence, it is often preferable to use aberration-corrected scanning transmission electron microscopy (HRSTEM or 4D-STEM) in HAADF mode (Z-contrast imaging) for heavy atoms and annular bright filed (ABF) or customized imaging modes for lighter elements [3],[1]. Light atoms such as H, Li or O play an important role in energy devices, and their mapping at the picometer level is useful to assess their potential electrical activity. In this presentation, we use our patented tools to extract the precise positions of interstitial atoms from superresolved HRSTEM images and optimized machine-learning algorithms.

II. METHODOLOGY

The original HRSTEM-HAADF images are obtained by aberration-corrected electron microscopy using the FEI Titan Themis microscope operated at 200 keV.

All the details of the methods are provided in the following patents. The patent EP4020378B1 is used to denoise the image by convolution.

The patent EP 4020379A1 provides the superresolved image, with a resolution typically increased by a factor of 5 compared to the original image.

Then the patent EP3671190B1 is used to obtain the positions of the interstitials using machine-learning based methodology with 3 binary classes: interstitial atoms, substitutional atoms and elsewhere. Only 3 areas are sufficient for an efficient supervised training with the Fast Random Forest algorithm [4], based on tree bagging and feature sampling.

III. RESULTS AND DISCUSSION

A typical result of atomic mapping is displayed on Fig. 1, in the case of etched GaN. The substitutional atoms are represented in grey, whereas the interstitial atoms are colorized. The spatial Abbe resolution is estimated from the superresolved diffractogram. The pic (-6,12,0) provides an horizontal resolution of 27 pm while the presence of the (0,0,13) reflection implies a vertical resolution of 38 pm, which is close to the record obtained by ptychography [5].

The vertically-averaged profiles are typical of implantation profiles, in agreement with atomistic simulations (Fig. 1 bottom). These results are consistent with the energetics of the plasma etch, when ion bombardment is expected. The possible vertical alignment of interstitials is attributed to possible channeling effects inside the implantation tracks.

This approach, validated by simulations and atomistic modeling, provides a universal methodology to map the interstitial atoms at the atomic scale, with a spatial resolution around 30 pm or even better in the case of ultrathin (about 20 nm thick) TEM lamellae with sample preparations close to perfection.

IV. CONCLUSIONS

Using super-resolution and machine-learning, it is possible to obtain accurate maps of interstitial atoms from high-resolution electron microscopy images, to analyze and optimize the technological processes involving ion implantation or surface damage. This method is universal, and the spatial resolution achieved by these combined techniques is close to the best currently achievable.

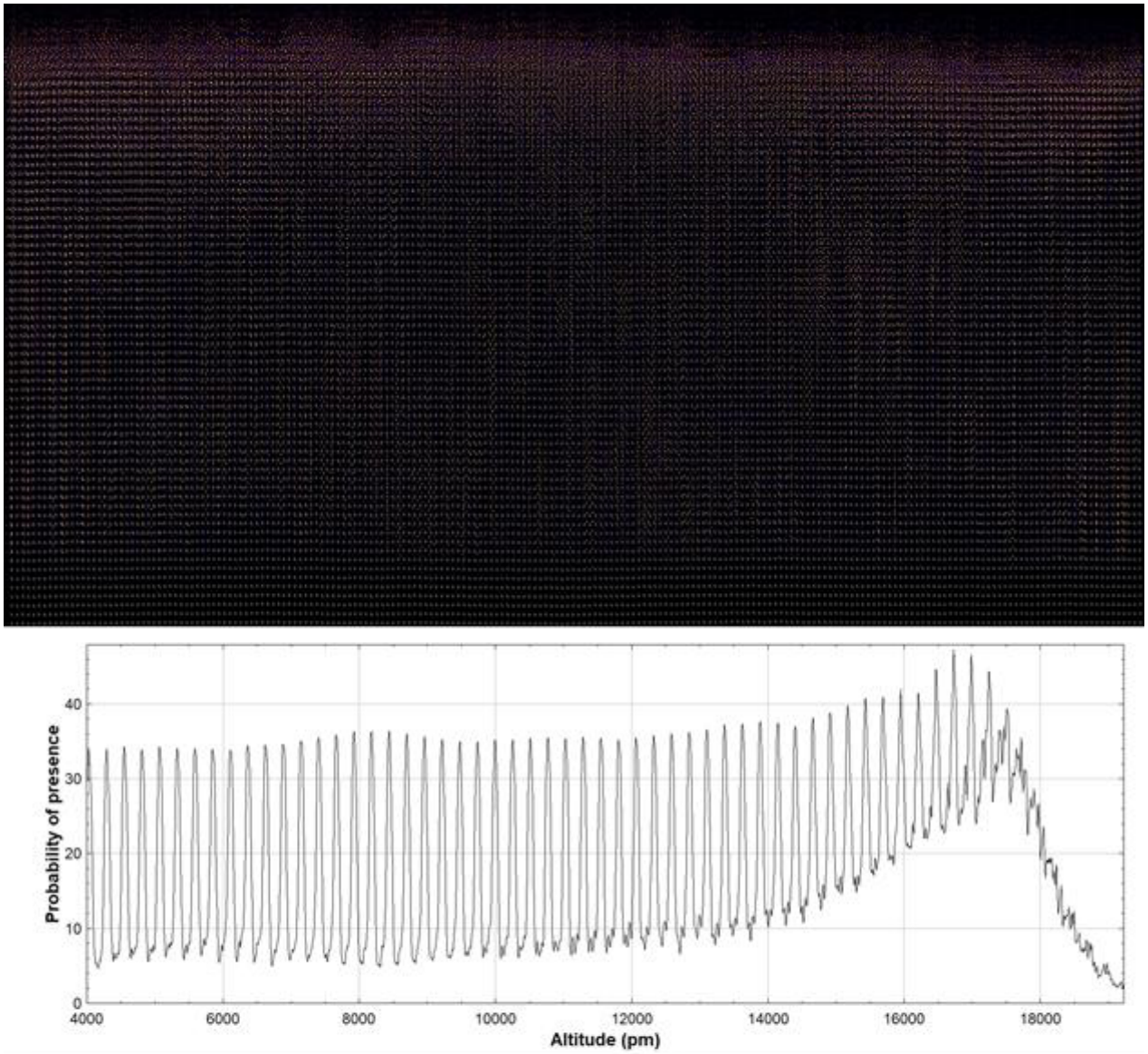

Fig. 1: Superresolved distribution of atoms after an etching process of GaN involving implantation.

Top: distribution of Ga atoms (grey) and interstitial atoms (color) extracted from a HRSTEM-HAADF image of GaN P63mc (186) oriented [210]. The scale bar is calibrated from the theoretical interreticular distances of the (001) horizontal planes. The image size is 62858 * 19229 pm^2.
Bottom: vertically averaged probability of atomic presence. The main periodic oscillations are attributed to the Ga (002) planes of GaN. The implantation profile is visible in the bottom part of the curve, and the fraction of interstitials increases towards the etched surface, with a typical erf profile function.

Keywords:

super-resolution, superresolution, machine-learning, TEM, interstitial

Reference:

[1] C. Guedj, patents EP4276750A1, FR3135554A1, EP4020379A1, FR3118254B1, FR3118256A1, EP4020378B1, EP3671190B1, FR3090876B1
[2] Meyer, J., Girit, C., Crommie, M. et al. Imaging and dynamics of light atoms and molecules on graphene. Nature 454, 319–322 (2008). https://doi.org/10.1038/nature07094
[3] Yoon-Jun Kim, Runzhe Tao, Robert F. Klie, and David N. Seidman, "Direct Atomic-Scale Imaging of Hydrogen and Oxygen Interstitials in Pure Niobium Using Atom-Probe Tomography and Aberration-Corrected Scanning Transmission Electron Microscopy", ACS Nano 2013 7 (1), 732-739, https://doi.org/10.1021/nn305029b
[4] L. Breiman, "Random Forests", Machine Learning, 45, 5-32 (2001)
[5] Zhen Chen, Yi Jiang, Yu-Tsun Shao, Megan E. Holtz, Michal Odstrcil, Manuel Guizar-Sicairos, Isabelle Hanke, Steffen Ganschow, Darrell G. Schlom, David A. Muller, Science 372, 826–831 (2021)

448

Multi-scale cements and concrete characterization using X-ray Microscopy, automated phase classification, and machine learning

Ria Mitchell[1], Prof John Provis[2], Dr Giacomo Torelli[3], Mr Kajanan Selvaranjan[3], Dr Antonia Yorkshire[3], Dr Sarah Kearney[3], My Andy Holwell[1]
[1]ZEISS Microscopy, Cambridge, UK, [2]Paul Scherrer Institut, Villigen, Switzerland, [3]University of Sheffield, Sheffield, UK

Poster Group 2

Background incl. aims
There is a growing need to quantify and characterize the varying components within cements and concretes in multiple dimensions and at the multi-scale. This is particularly true for cements and concretes developed for the nuclear industry, whether as vessels for nuclear reactors or for nuclear waste containment, and to understand their constituents more holistically in three dimensions. However, cements and concretes are generally challenging to image in 3D, particularly at high resolution; this is because of typically large core sizes and consequential limited X-ray penetration, as well as varying chemistries of the components, and differing grain sizes. Further, because most of the components are calcium based, it can be difficult to differentiate them using density-based greyscale data alone when using traditional reconstruction (FDK) techniques. Because of these difficulties, scans usually need to contain many projections and long exposure times, therefore leading to long scan times and limited throughput. Here, we apply a variety of machine learning and AI approaches in a new XRM > machine learning reconstruction > AI quantified phase classification workflow. This workflow vastly improves the resulting scan data and enhances the component quantification process.

Methods
Here, we use non-destructive 3D imaging via X-ray Microscopy (XRM), combined with a novel 3D automated quantitative phase classification technique to spatially characterize the mineralogical phases in a variety of cements and concretes. We collected multi-scale 3D scans on a ZEISS Xradia Versa 620 X-ray Microscope (XRM), the data being subsequently run through numerous reconstruction options belonging to the Advanced Reconstruction Toolbox (ART): this includes DeepRecon Pro, a machine learning based approach for advanced denoising, enhanced contrast, and faster scans, and DeepScout, which allows users to upscale higher resolution interior tomographies to larger fields of view without sacrificing resolution. Finally, we use Mineralogic 3D to spatially characterize and quantify the mineralogy/phases within the concretes and cements in 3D (Mitchell et al., 2024).

Results
We find that DeepRecon Pro is effective at reducing noise in the resulting scan data (Figure 1). We also find that by using DeepRecon Pro, we can collect fewer projections (801 rather than 2401), resulting in better quality data, and we are able to collect scans three times quicker (29 minutes instead of 1 hour 35), leading to greater throughput of samples. We also find that we can improve the size of the field of view for high resolution scans; we are able to upscale 5.8 um voxel size scans from 5.9 mm3 field of view to 23 mm3, resulting in a field of view increase, and resolution recovery, of roughly 4x. This consequently leads to more representative segmentations over larger sample areas and better-quality data. In the final step we have applied Mineralogic 3D to achieve quantitative phase classification of the concrete components; we are able to distinguish components of similar chemical composition and contrast (in particular, those that are Ca-rich), segment, and quantify them, which is an improvement on standard thresholding which does not take into account

the scan conditions and relative density of the material. The results presented here show how new software options (DeepRecon Pro, DeepScout, Mineralogic 3D) are valuable to improve the image quality, characterization, and quantification of cements and concretes in 3D.

Keywords
Cements/concretes; automated phase classification; Tomography; Image processing

References:
Mitchell, R. L., Holwell, A., Torelli, G., Provis, J., Selvaranjan, K., Geddes, D., Yorkshire, A., & Kearney, S. (2024). Cements and concretes materials characterisation using machine-learning-based reconstruction and 3D quantitative mineralogy via X-ray microscopy. Journal of Microscopy, 1–9. https://doi.org/10.1111/jmi.13278

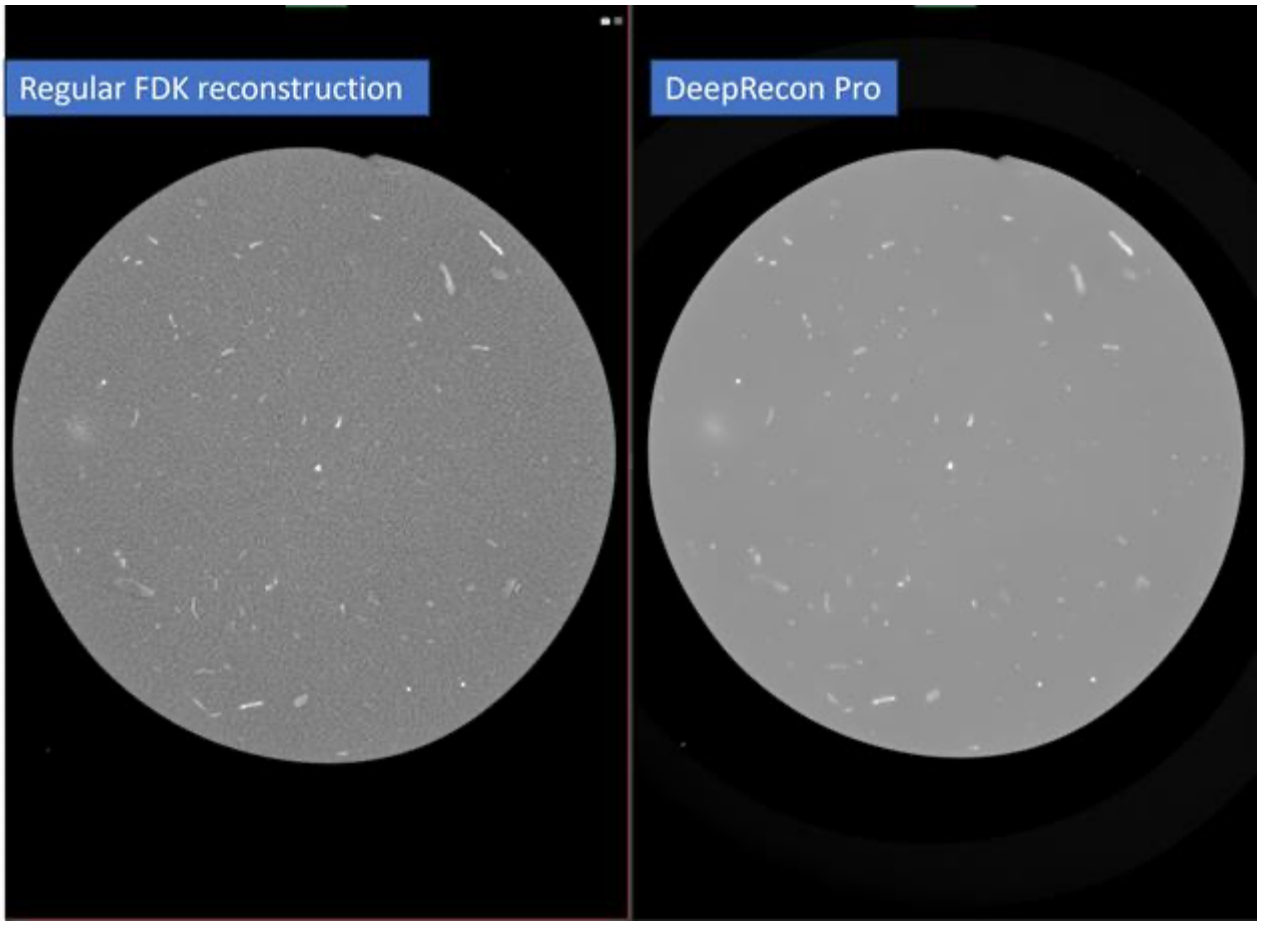

Keywords:

concrete; phase classification; tomography

Reference:

Mitchell, R. L., Holwell, A., Torelli, G., Provis, J., Selvaranjan, K., Geddes, D., Yorkshire, A., & Kearney, S. (2024). Cements and concretes materials characterisation using machine-learning-based reconstruction and 3D quantitative mineralogy via X-ray microscopy. Journal of Microscopy, 1–9. https://doi.org/10.1111/jmi.13278

494

Event-responsive Beam-modulated STEM with Multi-frame and Sparse Scanning

Dr Jonathan Peters[1,2,3], Matthew Mosse[1,2], Bryan Reed[4], Daniel Masiel[4], Michele Conroy[5], Lewys Jones[1,2,3]

[1]Advanced Microscopy Laboratory (CRANN), Trinity College Dublin, Dublin, Ireland, [2]School of Physics, Trinity College Dublin, Dublin, Ireland, [3]turboTEM Ltd., , Ireland, [4]Integrated Dynamic Electron Solutions, Inc., Pleasanton, USA, [5]Department of Materials, London Centre of Nanotechnology, Imperial Henry Royce Institute, Imperial College London, London, UK

Poster Group 2

Recent advances in high-speed signal processing electronics allow any analog STEM detector to operate in an event-counting mode, measuring individual electron detection events in real time. This technology delivers images with zero dark-noise, improved linearity, and SNR limited only by ideal Poisson counting statistics [1]. By combining such event-counting hardware with fast electrostatic dose-modulators (EDM) [2], a real-time 'event responsive' imaging mode can be realised [3]. We call this Trigger Event Modulated Probability Observation STEM, or TempoSTEM for short.

TempoSTEM operates in a fundamentally different way from classical STEM imaging. In classical STEM, we observe fixed periods (dwell times) and record the varying numbers of transmitted/scattered events that arrive at a detector. In TempoSTEM, we specify a fixed number of events and measure the varying time needed for the image signal to reach that number of events in each pixel location. In both pulse counted STEM and TempoSTEM the operator sees images expressed in quantitative units of events-per-microsecond. However, there is one key difference; in TempoSTEM the beam is blanked for the remainder of the pixel once the threshold is met, significantly reducing dose and sample damage. The beam is un-blanked at the start of the next pixel and a fresh measurement begins.

Information theory predicts that for every successive electron detected within each pixel time, there is a diminishing return on information content; this has also been confirmed experimentally [3]. This creates a balance where a lower Tempo trigger exit condition ensures the most efficient detection per-electron, but it does not ensure the most readily analysable SNR overall. Here we present a mode to iteratively update noisy high-variance pixels to achieve improved resolution and SNR.

Another common approach to increase the SNR of an image is through the stacking of multiple frames. Where a hardware EDM is present [2], a further option is to only revisit a subset of pixels in subsequent frames in the series. After the first noisy scan-frame of a TempoSTEM acquisition, such as with a trigger of n=1 electron, we can calculate the local variance of image pixels. On the second scan frame, we can revisit only pixels that are outliers by, say, more than one standard deviation of their neighbours. This might be around 25-30% of the pixels for example. For these pixels, an additional TempoSTEM observation can be made and the beam blanked elsewhere to minimise dose. The rescanned pixels have now received the dose equivalent to an n=2 TempoSTEM exit condition, and the scattering rate estimate is updated. On a third scan for example, the number of outlier pixels reduces and even fewer are rescanned to an effective n=3 exit condition. After some number of rescans the variance is converged, and the image acquisition can be considered complete. For an equivalent target resolution a dose saving of around 2x is achieved even relative to the already low-dose TempoSTEM approach. This method pushes below one event per-pixel-per-frame, maximising the information from each electron, increasing the best achievable combination of resolution and beam damage.

Keywords:

Low-dose, event-responsive, STEM, intelligent-scanning

Reference:

1. JJP Peters et al., Nature Communications 14 (2023) 5184
2. BW Reed et al., Mic. & Microanalysis 28 (2022) 2230.
3. JJP Peters et al., Mic.& Microanalysis 29 (2023) 1754.

569

Coupling Clustering and Channeling Contrast in the Scanning Electron Microscope

Dr. Sudeep Kumar Sahoo[1,2], M. Thierry Douillard[1], Dr. Bianca Frincu[2], Mme Christine Nardin[2], Dr. Hdr Cyril Langlois[1]
[1]INSA Lyon, MATEIS Laboratory, Lyon, France, [2]Constellium Technology Center (C-TEC), , France

Poster Group 2

Background incl. aims
Channeling contrast in the Scanning Electron Microscope (SEM) facilitates the imaging of crystals and their defects. A name for this approach has been coined as ECCI for “Electron Channeling Contrast Imaging”. This contrast arises from the diffraction of the electron beam as it traverses through the crystalline sample, and is intricately linked to the crystalline orientation of the underlying crystal. Within a grain, the channeling contrast hence aids in the recognition of crystalline defect. In a polycrystalline sample, neighbouring grains can be differentiated by the channeling contrast due to their difference in orientation. However, obtaining multiple ECCI images with different angles of electron beam incidence on the crystal is necessary: (i) to identify the defect character (such as screw or edge dislocations) and (ii) to ensure that all grains are detected within a polycrystalline region of interest. Eventually, the acquired ECCI image series have to be treated quantitatively to extract valuable information about the microstructure. In this context, machine learning, particularly clustering algorithms, is extremely beneficial for analyzing ECCI data. As an example, defects like dislocations and stacking faults can be detected in an ECCI image series by clustering [1-2]. In the present work, the idea is to process ECCI image series by clustering: (i) to extract the grain size distribution rapidly in an automatic and reproducible manner, (ii) to extract meaningful information about the microstructure, i.e., recrystallized fraction in an aluminum alloy [3], and (iii) to reduce dramatically the computation time of orientation maps using the eCHORD approach [4].

Methods
The raw dataset consists of a series of ECCI images acquired by rotating the region of interest (ROI) in the SEM, with the sample being tilted to~10-15°. Such an image series constitutes a datacube from which intensity profiles can be extracted at each ROI position, reflecting the variation of the backscattered electron (BSE) signal due to the sample rotation. To demonstrate the effectiveness of clustering algorithms for estimating grain size distributions, a copper thin film of 3 µm thickness exhibiting submicronic twins as thin as 80 nm in thickness is employed as a test sample. For determining the recrystallisation fraction, a 6XXX aluminum sample is considered and subjected to heat treatment to achieve a ~75% recrystallised microstructure. Finally, to explore the possibilities for fast-indexing within the framework of the eCHORD approach, duplex steel with coexisting austenite and ferrite phases is adopted.

Results
The intensity profiles defined at each place in the ROI will be used to cluster the data for grain size distribution calculations. The HDBSCAN algorithm [5] was selected for clustering, as it does not require the number of clusters (i.e., of grains) as an input. Furthermore, the algorithm automatically determines a reasonable criterion for defining a cluster. The influence of the intensity profiles pre-treatments is discussed, as well as the minimal number of images required for the clustering is explored, which is found to be between 10 to 20 ECCI images only.
For the recrystallisation fraction, it appears that the non-recrystallised area in the ROI corresponds to pixels that are left apart within the “noisy” class during the clustering using HDBSCAN. The results show good agreement with the recrystallised fractions as determined by EBSD on the same ROI.

Concerning eCHORD orientation mapping, the approach involves grouping similar intensity profiles into clusters, computing the mean profile for each cluster, and subsequently indexing it by comparing it to an eCHORD database. In this case, over-clustering is not a problem, and the KMEANS algorithm has been used with a significantly higher number of clusters than the apparent grain count, ensuring a reasonable spatial resolution is maintained. If some clusters belong to the same grain, the indexing operation will yield the same crystallographic orientation in the final map. This approach has been applied to the image series of duplex steel, allowing it to discriminate between the austenite and ferrite phases. Due to the tremendous GPU-computed indexing speed, it is possible to compare all the cluster profiles to both austenite and ferrite databases in order to perform phase mapping and retrieve the correct orientations.

Conclusion

This work demonstrates that clustering the ECCI image series using several types of clustering algorithms (HDBSCAN, KMEANS) can be extremely beneficial for several applications such as grain size distribution calculation, recrystallization fraction determination, phase discrimination, and orientation map computation.

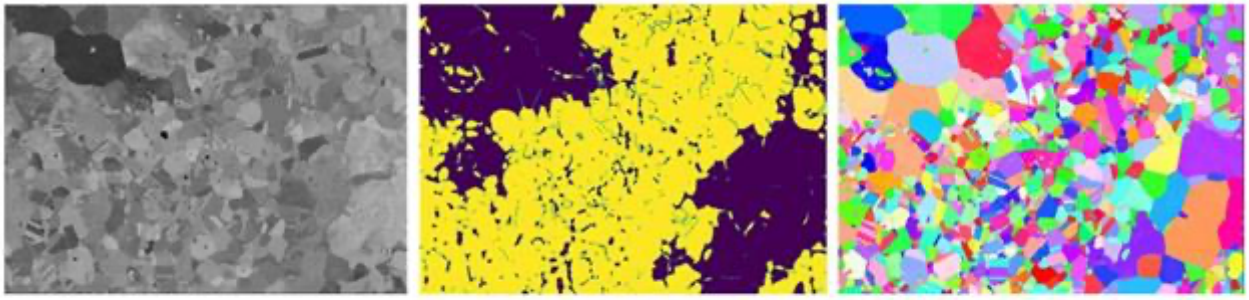

Figure 1: Duplex steel microstructure characterization a) ECCI image at rotation 0°, b)phase map with austenite (yellow) and ferrite (blue), c) IPF Z.

Keywords:

HDBSCAN, KMEANS, eCHORD, orientation mapping

Reference:

[1] S. Cazottes, A. Bechis, C. Lafond, G. L'Hôte, C. Roth, T. Dreyfus, P. Steyer, T. Douillard, C. Langlois (2019) Toward an automated tool for dislocation density characterization in a scanning electron microscope. Materials Characterization 158 109954

[2] J. Gallet, M. Perez, S. Dubail, T. Chaise, T. Douillard, C. Langlois, S. Cazottes (2022) About the automatic measurement of the dislocation density obtained by R-ECCI. Materials Characterization 194 112358

[3] R.Facchinetti, C. Langlois, S. Cazottes, C. Maurice, B. Frincu, C. Nardin, T. Douillard (2023) Quantitative analysis of partially recrystallised microstructures from BSE-SEM imaging, Materialia, 32, 101969.

[4] C. Lafond, T. Douillard, H. Saad, S. Deville, S. Meille, Ph. Steyer, S. Cazottes, C. Langlois (2021), eCHORD orientation mapping of bio-inspired alumina down to 1 kV, Materialia 20

[5] L. McInnes, J. Healy, S. Astels (2017), hdbscan: Hierarchical density based clustering In: Journal of Open Source Software, Open Journal, volume 2, number 11.

650

Image Restoration from Subsampled STEM Measurements using Deep Learning

Amirafshar Moshtaghpour[1], Dr. Matthieu Terris[2], Prof. Mike Davies[3], Prof. Angus Kirkland[1,4], Abner Velazco Torrejón
[1]Rosalind Franklin Institute, Didcot, United Kingdom, [2]Université Paris-Saclay, Palaiseau, France, [3]University of Edinburgh, , United Kingdom, [4]University of Oxford, Oxford, United Kingdom

Poster Group 2

Background
Scanning Transmission Electron Microscopy (STEM) has been shown to be a powerful tool for observing the atomic structure of complex materials. However, the radiation damage induced by the electron beam limits imaging beam-sensitive materials with acceptable signal-to-noise ratio. Subsampled STEM [1] has recently been investigated as an approach for reducing the radiation damage without compromising the level of signal per each measurement (or probe position). It is achieved by subsampling the grid of probe positions, which results in an incomplete set of measurements. A complete STEM image is then recovered from those subsampled measurements through an inpainting process.
A myriad of inpainting methods have been introduced based on, e.g., variational [2], Plug-and-Play (PnP), and deep learning frameworks [3]. In this work, we focus on PnP methods, which have been widely used for solving various imaging problems by using an off-the-shelf denoiser as an image prior.
Methods
We propose a deep learning-based inpainting method. Inspired by the work on Deep Denoiser Prior (DDP) for image restoration [4], we utilize a pre-trained deep neural network as an implicit image prior and then integrate that pre-trained network into an iterative inpainting algorithm. We discuss how the training of a DDP can be improved using synthetic and experimental STEM images corrupted by different sources, such as detector noise, scan distortion, sample movement, and aberrations. Therefore, we also introduce a new tool for the fast generation of synthetic STEM images.
Additionally, inspired by recent work on invariant priors [5], we demonstrate that enforcing equivariance to certain transformations, such as rotations, reflections, and translations, during the denoising step, improves the quality of inpainting.
Results
The results of our inpainting method are shown in Figure 1. The images tested in Figure 1 were not used for the training of the denoiser neural network. Ground truth synthetic images of SrTiO3 and Si were generated using our image generation tool. These images were then randomly subsampled with respect to 25% of probe positions. Despite slight imperfections around the boundary of the images, marked by a yellow arrow, the reconstructed images are of very high quality, with Signal-to-Reconstruction Error Ratios (SREs) greater than 43 dB.
Conclusion
This work presents an inpainting method for subsampled STEM data that leverages the power of both variational and deep learning methods. Given the flexibility of PnP methods, any neural network architecture can be used as a DDP. In the future, we plan to extend this work to inpainting subsampled data in different modes of electron microscopy, such as scanning electron microscopy and 4-dimensional STEM.

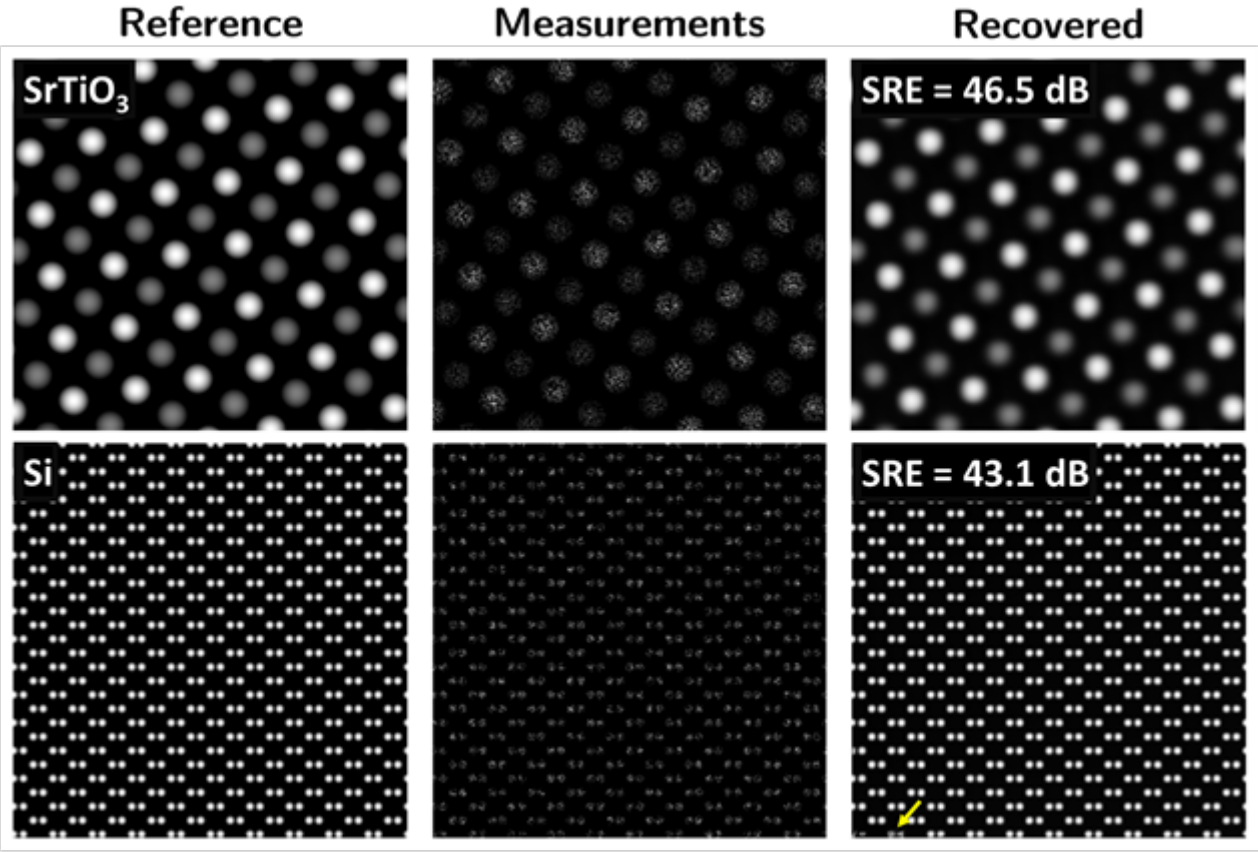

Figure 1. Examples of reference, measurements, and recovered images. Reference images are synthetically generated and were not used for training of the neural network. Measurements are generated by 25% subsampling of the probe positions at random. Signal-to-Reconstruction error Ratio (SRE) is shown in dB.

Keywords:

Deep Learning, STEM, Inpainting, Low-Dose

Reference:

[1] D. Nicholls, A. W. Robinson, J. Wells, A. Moshtaghpour, M. Bahri, A. Kirkland, and N. D. Browning, "Compressive Scanning Transmission Electron Microscopy," in proceedings of the International Conference on Acoustics, Speech, and Signal Processing, Singapore, 2022.
[2] P. L. Combettes, L. Condat, J-C Pesquet, and B.C Vu, "A forward-backward view of some primal-dual optimization methods in image recovery," in proceedings of the International Conference on Image Processing, 2014.
[3] W. Shi, F. Jiang, S. Liu, and D. Zhao, "Scalable convolutional neural network for image compressed sensing," In Proceedings of the IEEE/CVF Conference on CVPR, pp. 12290-12299, 2019.
[4] K. Zhang, Y. Li, W. Zuo, L. Zhang, L. Van Gool, and R. Timofte, "Plug-and-play image restoration with deep denoiser prior," IEEE Transactions on Pattern Analysis and Machine Intelligence, 44(10), pp. 6360-6376, 2021.
[5] M. Terris, T. Moreau, N. Pustelnik, and J. Tachella, "Equivariant plug-and-play image reconstruction," arXiv preprint arXiv:2312.01831, 2023.

652

pyEELSMODEL: python library for model-based EELS quantification

Daen Jannis[1,2], Mr. Jo Verbeeck[1,2]
[1]EMAT, Universiteit Antwerpen, Antwerpen, Belgium, [2]NANOlab, Universiteit Antwerpen, Antwerpen, Belgium

Poster Group 2

Electron energy loss spectroscopy is a powerful method used to investigate the elemental abundance and electronic structure of a material. Extracting this information from the experimental data is a complex process and multiple methods exist to get the results where each of them have their own advantages and disadvantages. Moreover, each method has free input parameters which influences the final results and can lead to experiments bias and reproducibility issues, especially in the common case where all parameters and the exact workflow is not shared.

In this work, an open-source python package (pyEELSMODEL) is presented which offers multiple alternative EELS quantification methodologies[1] . The library allows a transparent way to share a specific data processing workflow from raw data to a resulting plot that can appear in a paper. pyEELSMODEL expands upon the former EELSMODEL (c++) software which introduced the model-based philosophy in the EELS community [2]. This method attempts to describe the experimental data with a physical model and optimizes the parameters of this model via a minimization scheme such as least squares or maximum likelihood. The values of these optimized parameters can be used to estimate information on the material such as eg. elemental abundance. The new pyEELSMODEL package is written in python making it, in general, easier to integrate and extend as compared to the former c++ code. Multiple robust quantification workflows are available and can be easily used by the novice EELS user via eg. Jupyter notebooks.
This package is also particularly useful for testing and validating novel data processing methodologies since its results can easily be benchmarked against more common methodologies and could act as a test standard against which to make performance claims.

In this presentation, we will demonstrate the use of pyEELSMODEL on several experimental STEM-EELS maps showcasing the robustness and speed of the model-based quantification methodology for modern large size datasets. In Fig. 1, EELS quantification is used to get elemental maps on a mix of copper and silver nanoparticles on top of a carbon substrate. The lower plots show the resulting fitted model on silver (a) and copper (b).

Fig 1. Elemental maps of copper and silver nanoparticles on top of a carbon substrate. (a) Shows the fitted model on a silver nanoparticle whereas (b) shows a fit on the copper nanoparticle.

Keywords:

EELS, Quantification, Model-based

Reference:

[1] pyEELSMODEL repository: https://github.com/joverbee/pyEELSMODEL
[2] Verbeeck J. et al; Model based quantification of EELS spectra; Ultramicroscopy; 2004; doi:10.1016/j.ultramic.2006.05.006

654

Cellular in-situ Assessment of Complex Tissue Environments in 3D

Dr. Ralph Palmisano[1], MSc Vasco F Fontes[1,2,3], Prof. Stefan Uderhardt[1,2,3]
[1]Optical Imaging Competence Centre Erlangen (OICE), Friedrich-Alexander University Erlangen-Nürnberg (FAU) , Erlangen, Germany, [2]Department of Internal Medicine 3, Friedrich-Alexander University Erlangen-Nürnberg (FAU) and Universitätsklinikum Erlangen, Erlangen, Germany, [3]Deutsches Zentrum für Immuntherapie (DZI), Friedrich-Alexander University Erlangen-Nürnberg (FAU) and Universitätsklinikum Erlangen, Erlangen, Germany

Poster Group 2

The tissue microenvironment has emerged as a critical determinant of immune cell function and inflammatory disease outcome. However, assessing complex multicellular niches within the intact anatomy of a tissue and linking them to cellular in-situ function with the necessary volumetric dimension and spatial resolution remains a challenge. Our goal is to develop workflows that enable quantitative and functional volumetric imaging of intact tissue compartments during the course of inflammation. We use computational reconstruction to correlate the 3D positioning of immune and non-immune cells with microanatomical patterns of tissue architecture. In this way, we seek to define functional niches and establish comprehensive phenotyping of local environments during the onset, progression and resolution of inflammatory disease.

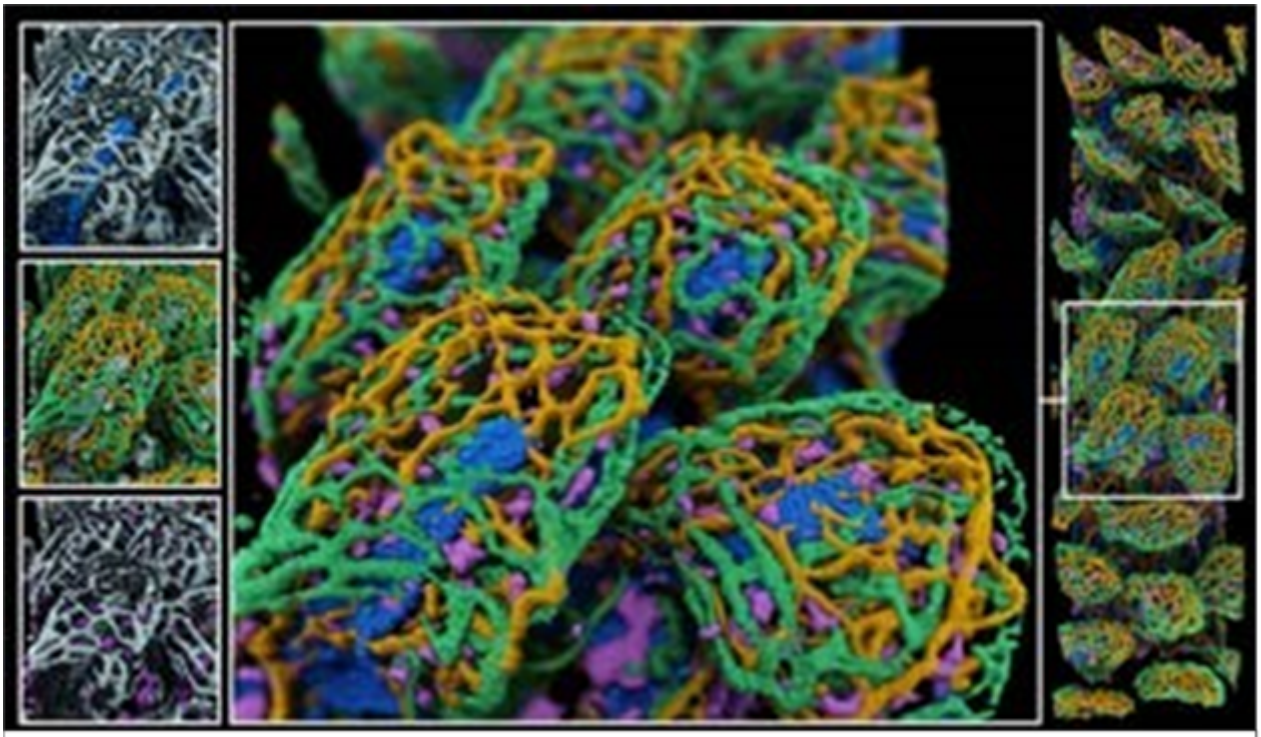

Ray-trace rendering of intestinal vasculature, nerves, lymphatics and mucosal macrophages after machine learning-assisted semantic classification.

Keywords:

Quantitative and functional volumetric imaging

666

Comparative Analysis of Self-Supervised Learning Techniques for Electron Microscopy Images

Dr.-ing. Bashir Kazimi[1], Prof. Dr. Stefan Sandfeld[1,2]
[1]Forschungszentrum Jülich, Institute for Advanced Simulation – Materials Data Science and Informatics (IAS-9), Aachen, Germany, [2]RWTH Aachen University, Chair of Materials Data Science and Informatics, Aachen, Germany

Poster Group 2

Background incl. aims
Deep learning has revolutionized a wide array of tasks across different domains, including electron microscopy (EM) image analysis, by leveraging large labeled datasets for training. However, the scarcity of such labeled datasets in EM necessitates the exploration of alternative methods. Self-supervised learning (SSL) emerges as a promising approach to leverage unlabeled data, featuring techniques such as, e.g., masked image modeling (MIM) — which predicts missing parts of the input data, as well as contrastive learning — which learns by distinguishing between similar and dissimilar pairs of data. This study aims to investigate the impact of these SSL techniques on EM images, providing a case study on the effectiveness of leveraging unlabeled data in a domain where labeled datasets are limited and expensive to create.
Methods
Utilizing the “NFFA dataset”, which comprises 21,169 Scanning EM images across 10 categories, we established a baseline by training models from scratch with random weight initialization. We then pre-trained models using two SSL approaches: Masked Autoencoders (MAE) for MIM and Momentum Contrast V3 (MoCoV3) for contrastive learning, followed by fine-tuning on the NFFA dataset. Another pixel-based MIM technique, Multi-level Feature Fusion (MFF), was also tested. The performance of each SSL technique was evaluated based on accuracy improvements and convergence speeds relative to the baseline. Our analysis highlights the distinctions between MIM and contrastive learning approaches in handling EM images.
Results
The baseline model yielded an accuracy of 77.42%. Upon employing SSL techniques, significant improvements were observed: finetuning with MAE weights achieved an accuracy of 92.84%, MFF led to 93.86%, and MoCoV3 led to an accuracy of 92.56%. MFF, in particular, demonstrated a superior ability to enhance feature learning from unlabeled data, indicating its impact in the task of EM image classification. Furthermore, all SSL-pretrained models showcased accelerated convergence rates compared to the baseline.
Conclusion
This study confirms the viability and potential of SSL techniques in EM images. MIM, exemplified by MFF, outperformed contrastive learning in this domain, suggesting that methods focusing on reconstructing or predicting unseen parts of the image are particularly beneficial for EM tasks. The results advocate for a targeted selection of SSL strategies based on specific dataset characteristics and task requirements, highlighting a path forward for efficient model training in EM image analysis and beyond. The influence of SSL pretraining was studied in this research and experiments were conducted on SEM image classification. Further research in this direction includes investigating the influence of SSL pretraining on dense, pixel-wise classification (i.e., semantic segmentation) tasks in EM.

Keywords:

Self-Supervised-Learning, Electron-Microscopy, Image-Classification, Masked-Image-Modeling, Contrastive-Learning

Reference:

1. He, K., Chen, X., Xie, S., Li, Y., Dollár, P. and Girshick, R., 2022. Masked autoencoders are scalable vision learners. In Proceedings of the IEEE/CVF conference on computer vision and pattern recognition (pp. 16000-16009).
2. Liu, Y., Zhang, S., Chen, J., Yu, Z., Chen, K. and Lin, D., 2023. Improving pixel-based mim by reducing wasted modeling capability. In Proceedings of the IEEE/CVF International Conference on Computer Vision (pp. 5361-5372).
3. Chen, X., Xie, S. and He, K., 2021. An empirical study of training self-supervised vision transformers. In Proceedings of the IEEE/CVF international conference on computer vision (pp. 9640-9649).
4. Aversa, R., Modarres, M. H., Cozzini, S., & Ciancio, R., 2018. NFFA-EUROPE - 100% SEM Dataset
5. Conrad, R. and Narayan, K., 2021. CEM500K, a large-scale heterogeneous unlabeled cellular electron microscopy image dataset for deep learning. Elife, 10, p.e65894.

667

EDX-based annotation of biological features in large-scale EM

Peter Duinkerken[1], Dr. Ahmad Alsahaf[1], Dr. Jacob Hoogenboom[2], Dr. Ben Giepmans[1]
[1]Department of Biomedical Sciences, University Groningen, University Medical Center Groningen, Groningen, the Netherlands, [2]Department of Imaging Physics, Delft University of Technology, Delft, the Netherlands

Poster Group 2

Background
Advances in electron microscopy (EM) of bio-samples now enable ultrastructure to be inspected at biologically relevant scales. Capabilities in data analysis have however not kept pace with the throughput increase offered by novel acquisition approaches and automation. Moreover, the greyscale nature of the electron micrographs complicates a comprehensive analysis of all that is hidden within. The analysis of EM datasets is typically based on manual annotations, allowing in-depth analysis by segmenting the data into biologically meaningful features. However, such annotations are laborious and subject to the annotator's interpretation of the data. Furthermore, deep learning can used to automate segmentation but the need for manually annotated ground 'truth' remains. Energy-dispersive X-ray (EDX) imaging, or ColorEM, provides elemental context to the recorded ultrastructure, allowing variations in elemental concentrations to be reflected in color [1]. In this study we further tailored acquisitions to ColorEM and explored its potential to highlight biological features in a data-driven manner.

Methods
Pancreatic tissue composed of hormone-containing endocrine cells and zymogen-containing exocrine cells was epoxy-embedded and subjected to ultramicrotomy. A Thermo Fisher Scientific Talos S/TEM equipped with two Bruker XFlash 6-100 EDX detectors was used to interrogate the sectioned sample. The spectral richness was promoted by improving the acquisition parameters necessary for heterogenous cellular material. Greater context was provided through a mosaic acquisition of a full islet of Langerhans.

Results
ColorEM has been further improved and successfully implemented on pancreatic tissue. The high-resolution and energy-dispersed recordings allow the ultrastructure of biological tissue to be visualized in its elemental context. Various biological features such as heterochromatin, hormone- and zymogen-containing granules and lysosomes, can be readily discerned in the elemental images. The final large stitched image not only provides elemental context to the ultrastructure, but also places this in the larger context of the tissue.

Conclusions
Here we implement large-scale ColorEM, supplementing the spatial EM data with spectral EDX data. We leverage the addition of the spectral dimension to provided elemental context to the recorded biological ultrastructure, with the tiled acquisition providing the context of the tissue. Selection of which elements to visualize is based on a data-driven approach where the dissimilarity in terms of elements, and combinations thereof, amongst the biological features are identified.

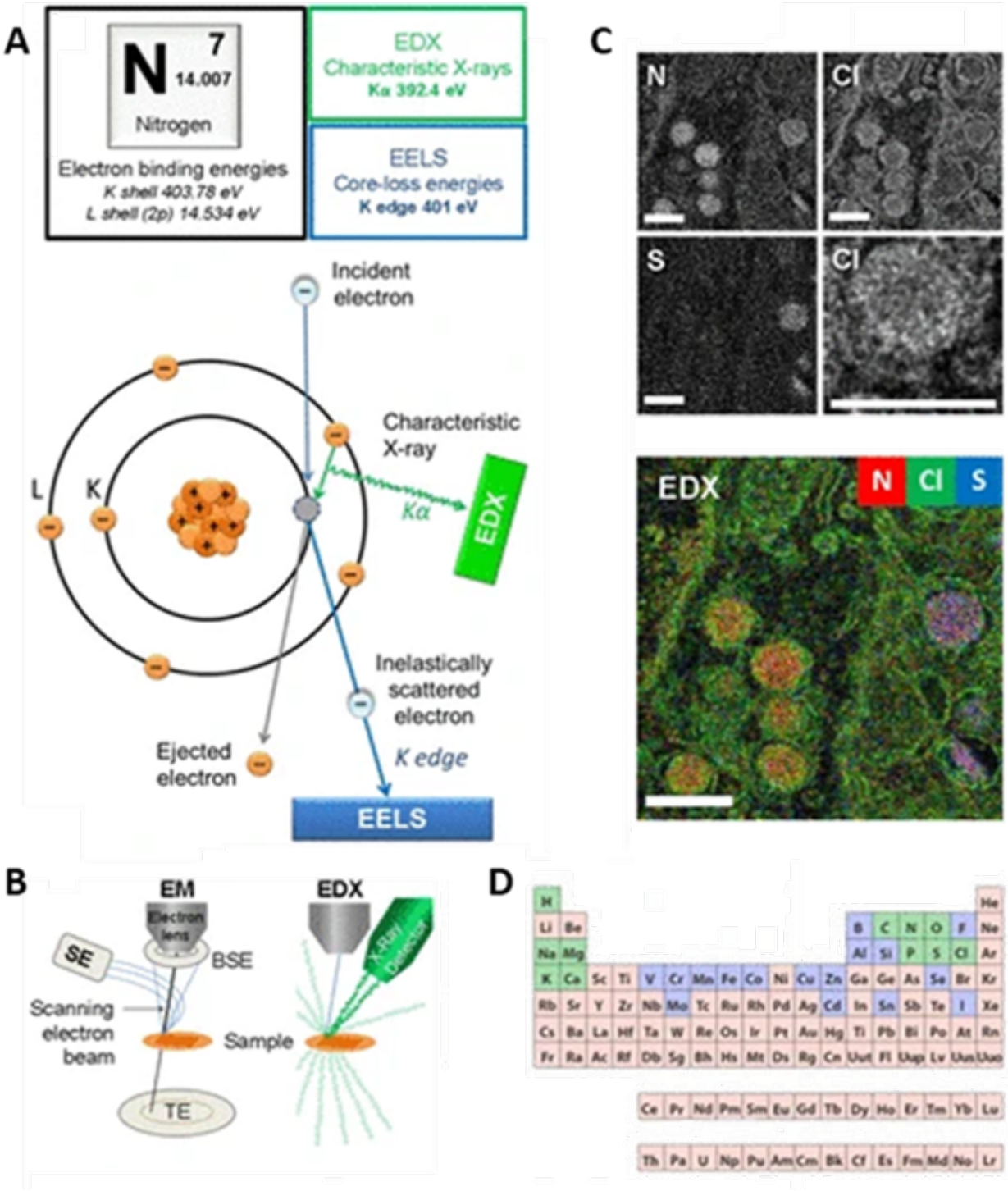

Implementation of ColorEM on biological tissue through EDX. (A) Interactions of the electron beam with the elements in the sample, illustrated here for a nitrogen atom (N), yields element-specific signals. **(B)** EDX imaging can be achieved by complementing a scanning-based EM system with an EDX detector. **(C)** Elemental abundance maps of nitrogen, sulphur (S), chlorine (Cl) and a colored composite thereof shows the elemental differences between cellular features such as the granules containing glucagon (left) and insulin (right) and the heterochromatin (top left). **(D)** Periodic table of elements with elements commonly found in the human body in green and trace elements in purple. Modified from [2], in which details are provided; (D) reproduced from https://askabiologist.asu.edu/content/atoms-life. Bars 0.5 µm

Keywords:

STEM, EDX, ColorEM, Label-free, Hyperspectral

Reference:

1: Scotuzzi M, Kuipers J, Wensveen DI, de Boer P, Hagen KC, Hoogenboom JP, Giepmans BN (2017) Multi-color electron microscopy by element-guided identification of cells, organelles and molecules. Sci Rep.7:45970

2: Pirozzi NM, Hoogenboom JP, Giepmans BNG. ColorEM: analytical electron microscopy for element-guided identification and imaging of the building blocks of life (2018) Histochem Cell Biol.150:509

668

Improving segmentation of FIB tomography data

Dr.-Ing. Martin Ritter[1], M.sc. Trushal Sardhara[2], Prof. Dr. med. Roland Aydin[2], Prof. Dr.-Ing. Christian Cyron[2]
[1]Electron Microscopy Unit, Hamburg University of Technology, Hamburg, Germany, [2]Institute for Continuum and Material Mechanics, Hamburg University of Technology, Hamburg, Germany

Poster Group 2

Background incl. aims
Accurate reconstruction of nanostructures using focused ion beam (FIB) tomography data is challenging due to slicing and imaging artefacts, as well as intensity ambiguities in the scanning electron microscope backscattered electron (BSE) images. We propose a multimodal machine learning approach that combines intensity information obtained at multiple electron beam accelerating voltages (multiV) to improve the three-dimensional (3D) reconstruction of hierarchical nanoporous gold (HNPG) structures. The proposed method significantly improves segmentation accuracy and leads to more precise 3D reconstructions for real FIB tomography data.
Methods
MultiV FIB tomography of epoxy infiltrated HNPG with ligament sizes of 15 nm and 110 nm was performed using a Dual Beam FEI Helios NanoLab G3 system and its ASV4 control software for automated tomography. During multiV tomography, each slice was imaged using a BSE detector three times with accelerating voltages of 1, 2, and 4 kV and a beam current of 50 pA. To compensate for drift during the process, 2 fiducial markers were prepared and positioned on the cross-section and on top of it. A ruler system was implemented also on top of the cross-section to monitor and measure the thickness of each slice. We developed 3 multimodal architectures for 3D nanostructure reconstruction with machine learning, employing different data fusion techniques: early fusion, intermediate fusion and late fusion.
Results
Our results indicate that the late fusion architecture excelled among the three options. Remarkably, the intermediate fusion architecture exhibited significantly poorer metrics than the late fusion architecture. This drop in performance can be attributed to the large size of the ML model, which posed challenges for optimization given a limited amount of training data. However, the effectivity of training data may be improved using domain adaptation. In a comparative study, confronting our ML-multiV method with a cluster-based k-means clustering algorithm and also ML models trained using individual single kV datasets, the multiV model outperformed all other segmentation techniques.
Conclusion
FIB-SEM tomography data are affected by artifacts and ambiguities in image intensities. These effects make it difficult to use cluster-based segmentation methods. More advanced ML-based methods can efficiently suppress the effects, even when trained only on a single set of synthetic FIB tomography images. The multimodal ML method with a late fusion architecture using multiV imaging data will further improve segmentation accuracy.

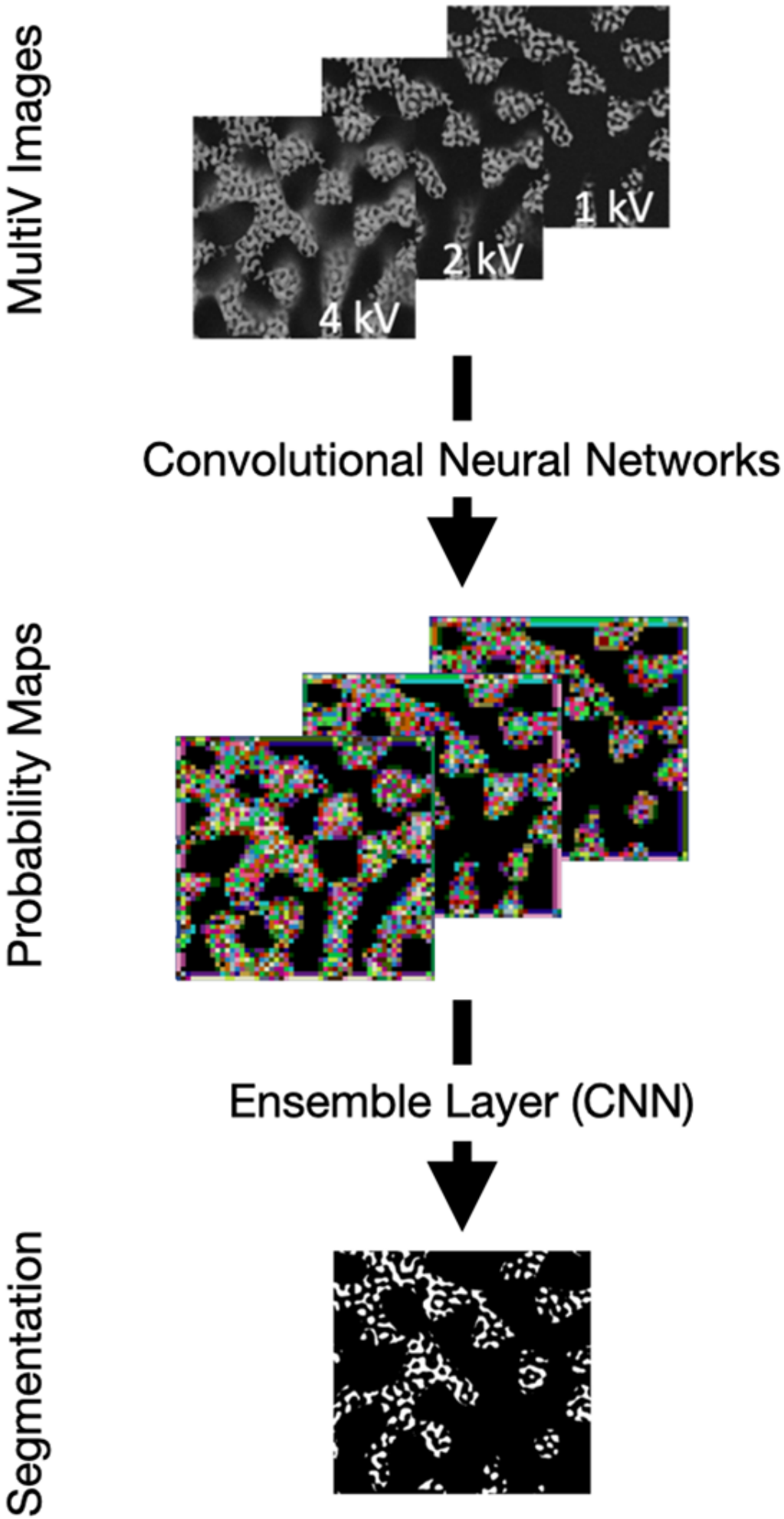
MultiV Images
4 kV
2 kV
1 kV
Convolutional Neural Networks
Probability Maps
Ensemble Layer (CNN)
Segmentation

Keywords:

FIB tomography, multimodal ML, segmentation

Reference:

The authors acknowledge funding from the Deutsche Forschungsgemeinschaft (DFG, German Research Foundation) – SFB 986 – Project number 192 346 071

688

Deep Learning assisted denoising of in situ liquid STEM-movies of nanoparticle nucleation and growth

Adrien Moncomble[1], Damien Alloyeau[1], Guillaume Wang[1], Hakim Amara[1,2], Riccardo Gatti[2], Maxime Moreaud[3], Christian Ricolleau[1], Jaysen Nelayah[1]
[1]Université Paris Cité, CNRS, Paris, France, [2]Université Paris-Saclay, ONERA-CNRS, Chatillon, France, [3]IFP Energies Nouvelles, Solaize, France

Poster Group 2

Over the recent years, the comprehension of the formation mechanism of metallic nanoparticles (NPs) has greatly benefited from in situ liquid TEM that enables imaging of the nucleation and growth of individual NPs in liquid media. However, these experiments pose challenges regarding both data acquisition and analysis. In particular, substantial scattering from the liquid around the NPs and the electron transparent SiN membranes significantly diminish the signal quality [1]. One solution would be to increase the electron dose rate, but this can lead to undesirable effects due to radiolysis. The other one is to use post-experiment techniques to remove the noise while keeping the signal of interest. Herein, we present an innovative approach that combines deep-learning (DL) and scanning transmission electron microscopy kinematic simulations [2] to denoise in situ liquid STEM-movies of NPs during their nucleation and growth in liquid media, a complex task where multiple information is intertwined.
Within a commercial liquid cell, we can visualize the formation of gold NPs, induced by the interactions between the electron probe and the precursor. We acquired a video of these events using a double corrected JEOL ARM 2100. To analyze and understand the growth mechanism, each frame was denoised by a homemade convolutional neural network similar to U-Net [3]. However, the quality of the results obtained is correlated to the quality of the training data. Hence, numerical simulations are a solution in the case of liquid electron microscopy where we cannot acquire data experimentally.
Our work consists of the development and optimization of the dataset and the CNN architecture. Besides considering the size and shape dispersions of nanoparticles, kinematic simulations account for a significant obstacle in studying NP growth by liquid cell TEM which is the formation of NPs on the opposite membrane of the cell. The latter contributes to the random background fluctuations because they are imaged way out-focus. Once we considered these challenges, our method effectively denoises low and high magnification videos, thus elevating the signal-to-noise ratio from 1 to 8 [Figure 1], above the threshold value of 5 set by the Rose criterion [4]. Consequently, our analysis pipeline facilitates the study of NP growth mechanisms with improved statistics and fewer acquisition constraints. We will show the application of this methodology to investigate surface site attractiveness on both gold nanocubes and nanorods within the context of NP synthesis.
In this work, we demonstrate the application of deep learning to the specific case of the denoising of in situ liquid microscopy. Thanks to this, we were able to get a better visualization and, thus, a better understanding of the mechanisms of the formation of nanoparticles.

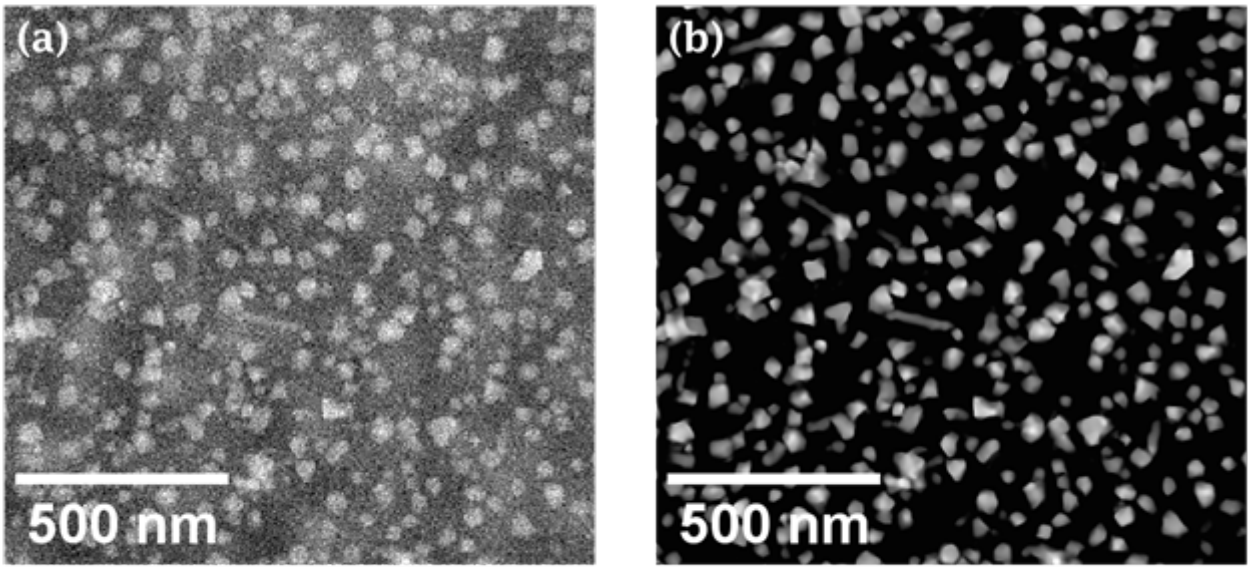

Figure 1 – Example of the denoising of the frame of a video of the growth of gold nanoparticles. (a) is the original image and (b) is the denoising of (a) using deep learning denoising.

Keywords:

Liquid TEM, AI, denoising

Reference:

[1] de Jonge, N., Ultramicroscopy 187, 113–125 (2018).
[2] He, D. S., Li, Z. Y. & Yuan, J., Micron 74, 47–53 (2015).
[3] Ronneberger, O., Fischer, P. & Brox, T., MICCAI 9351, 234-241 (2015).
[4] Rose, A., Adv. Electron. Electron Phys. 1, 131–166 (1948).

847

TEMsuite – A Matlab-based software platform for TEM data analysis

Simon Hettler[1,2]
[1]Instituto de Nanociencia y Materiales de Aragón (INMA), CSIC-Universidad de Zaragoza, Zaragoza, Spain, Zaragoza, Spain, [2]Laboratorio de Microscopías Avanzadas (LMA), Universidad de Zaragoza. Zaragoza, Spain, Zaragoza, Spain

Poster Group 2

Background incl. aims

Transmission electron microscopy (TEM) can provide a wealth of information on structure and composition at the atomic level for many different kinds of samples. To obtain this information, numerous different imaging, diffraction or spectroscopic techniques are available, e.g., high-angle annular dark-field (HAADF) scanning (S)TEM, selected-area electron diffraction (SAED), electron energy-loss spectroscopy (EELS) or energy-dispersive X-ray spectroscopy (EDX) to name some of the more common ones. To perform an advanced data analysis, again a multitude of dedicated software exists, many of them being freely available, such as HyperSpy for multidimensional spectroscopic analysis [1] or PETS for analysis of diffraction data [2]. Despite the availability of these specialized software, most users, especially those that only occasionally perform TEM analysis, still use commercial, proprietary software to perform basic data treatment and the threshold to learn yet another, even more specialized software is high. With the aim to speed up my own data processing tasks, I have written a software platform based on Matlab that facilitates several basic and advanced data analysis processes and which I have made freely available [3].

Methods

The software is written in Matlab with a graphical user interface (GUI) made up of a main window, a figure window for display and several windows to control the data analysis (Figure A). The software follows a session-based approach that allows to load and process different TEM data types at the same time. The sessions can be stored and reloaded at a later point to continue the data analysis. The following list describes several of the tasks that TEMsuite allows to perform: Basic image processing (contrast settings, line scans, export images as .jpg or .tif, add a scale bar, …), alignment of images series and export to movie, FFT filtering and analysis of reflection spots in the FFT. The software possesses a comprehensive set of tools for diffraction analysis including an automatic peak detection, fitting and correlation as well as the calculation of radial or azimuthal profiles. EELS multidimensional data can be visualized and analyzed statistically (principal-component analysis (PCA), non-negative matrix factorization (NNMF)). Core-loss EELS data can be quantified using theoretical scattering cross sections and the background-subtracted spectra can be fitted to obtain chemical information of the studied specimens.

Results

Several publications contain results from data analyses conducted with TEMsuite, for example the study on quasi-van der Waals epitaxial growth of WS_2 on sapphire [4] or the investigation of iron/cobalt-oxide core-shell nanoparticles for catalytic applications [5]. Figure (B) shows the NNMF analysis of an EELS spectrum image obtained from the interface between sapphire substrate (left), WO_3 interface and WS2 and carbon protection layers. The analysis yielded the clear separation between the four contributions and the plasmon peak energies of the associated spectra correspond with expected values [4]. The chemical map (Fe: green, Co: blue, O: red) obtained by a spatially-resolved EELS analysis of an iron/cobalt-oxide core-shell nanoparticle shows the clear formation of a Co-rich shell (top left in Figure C) [5]. The Co presence manifests itself as well in the intensity ratio of

the O-K pre-peak and the following valley, as visualized in the spectrum and the corresponding map (top right) in Figure C.

Conclusion

I developed the TEMsuite software initially to speed up my own TEM data processing but improved its design and setup with the aim to obtain a version that can be used by other users. The software is thought as platform for basic and advanced TEM data analysis currently focusing on image, FFT, diffraction and mainly EELS analysis and it is planned to be further expanded to include more techniques throughout the following years. The software is freely available as source code [3].

Figure caption: (A) TEMsuite GUI with main window (top left) including the list of loaded image and spectroscopy data, figure window (right) with an example EELS-spectrum image quantification and the EELS window (bottom left) to control the EELS data analysis. (b) Example analysis of a quasi-van der Waals epitaxially grown monolayer of WS_2 by NNMF yielding four contributions of carbon protection layer, sapphire substrate, interface (WO_3) and WS_2 monolater. (C) Example analysis of an EELS spectrum image of a Fe/Co-oxide core-shell nanoparticle with chemical map (top left), comparison of O-K spectra from shell and core (bottom) and map of the intensity ratio between the O-K pre-peak at 532 eV and the following valley (top right).

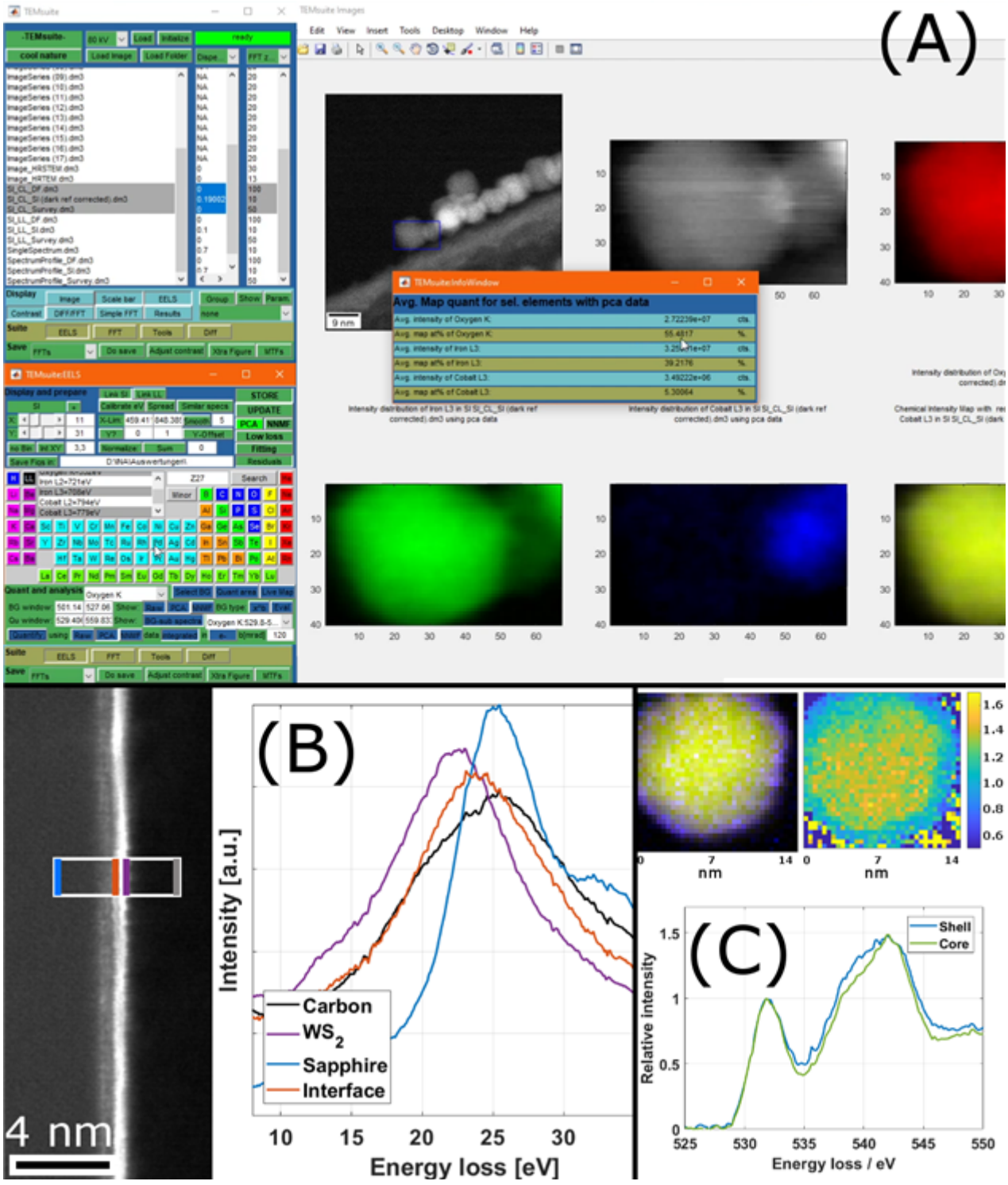

Keywords:

Data analysis, software, TEM, EELS

Reference:

[1] F. de la Peña et al, HyperSpy, https://doi.org/10.5281/zenodo.592838.
[2] L. Palatinus, PETS, http://pets.fzu.cz/.
[3] TEMsuite source code available on https://www.hettlers.eu/matlab/.
[4] A. Cohen et al, ACS Nano 17, 6, 5399–5411 (2023).
[5] L. Royer et al, ACS Catal. 13, 280-286 (2023).

874

Leveraging AutoScript for Cross-Platform Deep Learning Solutions in Electron Microscopy

Remco Geurts[1], Pavel Potocek[1], Noopur Jain[1], Ricardo Egoavil[1], Bert Freitag[1], Maurice Peemen[1], Yuri Rikers[1]
[1]ThermoFisher Scientific, Eindhoven, Netherlands

Poster Group 2

Python's widespread adoption is supported by a wide community that has developed an extensive toolkit of open-source libraries. Electron microscopy vendors have introduced Application Programming Interfaces (APIs) enabling users to design sequences for comprehensive control over electron optics, detectors, sample positioning, and data acquisition. [1,2,3]
These Python-accessible libraries facilitate classical image processing tasks, including object detection, drift correction, and feature tracking, which have been pillars of electron microscopy scripting for over twenty years. Applications range from Focused Ion Beam (FIB)/Scanning Electron Microscopy (SEM) defect analysis and Transmission Electron Microscopy (TEM) lamella preparation to semiconductor metrology, with TEM image processing and data analysis being particularly prominent.
The adoption of closed-loop image processing in electron microscopy is driven by the increasing volume of multimodal data generated by these instruments. Direct data offloading is inefficient and risks post-processing error identification, leading to valuable time losses.
Recent advancements in machine learning and deep learning have significantly enhanced their performance and integration speed, facilitating their inclusion in closed-loop automation sequences for complex tasks such as object detection, classification, and feature extraction.
ThermoFisher Scientific's AutoScript, a cross-platform Python-based API, streamlines and refines electron microscopy workflows by harnessing deep learning techniques. This paper highlights two applications:
1. SEM Feature Analysis: Utilizing a Thermo Scientific Helios microscope, this experiment automates the creation of binary masks for feature analysis on aluminum powder samples. Instance segmentation enables feature separation, counting, and property analysis (e.g., size and shape), allowing real-time experimental optimization based on material properties identified by deep learning algorithms.
2. TEM Atom Detection: Demonstrated with a Thermo Scientific Talos F200, this application automates the detection of atom positions and diameters in HR-STEM images of SrTiO3. Neural networks facilitate rapid atomic structure predictions and interface identification, optimizing imaging parameters on-the-fly.
These cases exemplify the transformative impact of cross-platform, Python-based APIs in electron microscopy, showcasing their potential to enhance efficiency, accuracy, and the scope of achievable experiments through automation and advanced data analysis.

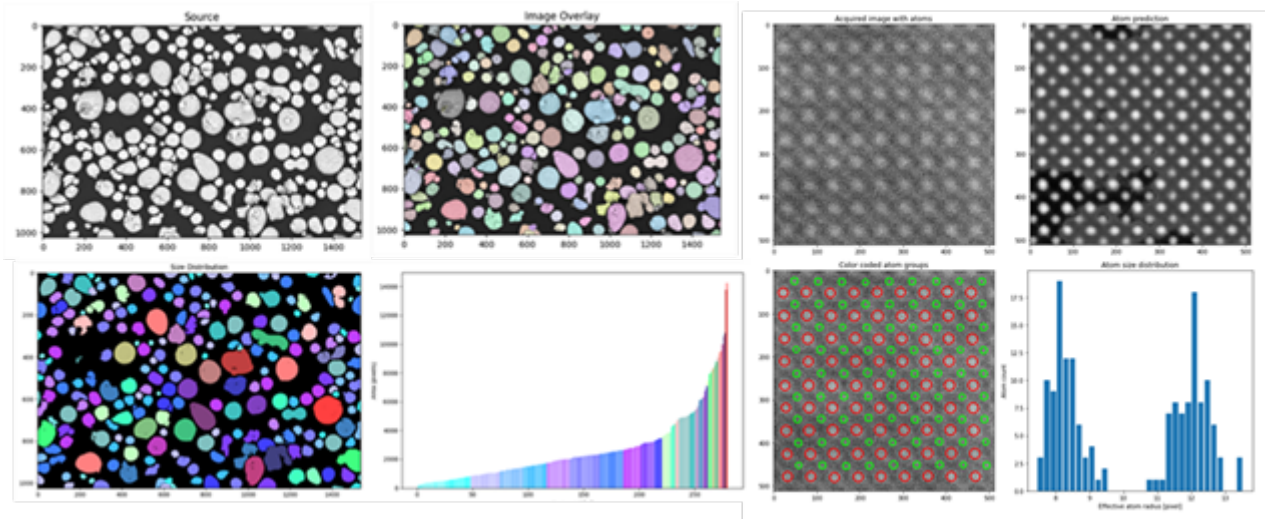

Keywords:

EM Automation, Deep Learning, AI

Reference:

[1] Wagner, A., Blauner, P., Longo, P. et al. Focused Ion Beam Metrology. MRS Online Proceedings Library 396, 675 (1995). https://doi.org/10.1557/PROC-396-675
[2] R Young and PD Carleson and X Da and T Hunt et al. High-yield and high-throughput TEM sample preparation using focused ion beam automation, ISTFA98 Proceedings
[3] DRG Mitchell, Applications of custom scripting in digital micrograph: general image manipulation and utilities. https://inis.iaea.org/search/search.aspx?orig_q=RN:34030866 The 17th Australian Conference on Electron Microscopy2002

893

A high-throughput compositional study of nanocrystals using a machine learning-assisted algorithm for STEM hyperspectral datasets

Mr. Basem Qahtan[1,3], Dr. Yurii P. Ivanov[1], Mr. Nikolaos Livakas[2,3], Mr. Francesco Di Donato[2], Prof. Liberato Manna[2], Dr. Giorgio Divitini[1]
[1]Electron Spectroscopy and Nanoscopy, Istituto Italiano di Tecnologia, Genoa, Italy, [2]Nanochemistry, Istituto Italiano di Tecnologia, Genoa, Italy, [3]Dipartimento di Chimica e Chimica Industriale, Università degli Studi di Genova, Genoa, Italy

Poster Group 2

Background incl. aims

In nanomaterials research, the analysis of heterogeneous ensembles of nanocrystals presents a significant challenge, often requiring the extraction of information from diverse classes of particles or phases, in a process that is often prone to operator bias and poor statistics. Lead Halide Perovskite (LHP) nanocrystals (NCs) are a promising class of materials for optoelectronic applications that feature a broad compositional flexibility and are often the subject of extensive studies that cover a broad parameter space for the synthesis or modification of the basic structures. Here we focus on CsPbCl3 NCs where the halide is replaced through exposure to increasing amounts of iodine and using STEM-EDX to track ex situ the change in halide [1]. Our primary objective is to extract compositional information at the single-particle scale while minimising the electron dose onto the sample, a critical consideration to preserve sample integrity and minimise carbon contamination. The analysis of nanocrystals poses unique challenges due to their heterogeneous nature and varying chemical compositions. To address this gap, our research seeks to leverage the capabilities of TEM hyperspectral imaging coupled with machine learning algorithms. The primary objective is twofold: first, to develop a robust framework capable of extracting detailed compositional information from individual nanocrystals within a large ensemble, and second, to enable high-throughput analysis.

Methods
The proposed methodology entails the integration of a machine learning-assisted algorithm (Segment every grain – SEG [2]) within HyperSpy [3] , a versatile environment designed for the analysis of hyperspectral datasets. SEG can reliably identify features in STEM micrographs, and the algorithm is designed to process datasets with a low signal-to-noise ratio (SNR), mitigating the risk of sample damage or alteration.
The algorithm is designed around modular Python scripts to construct adaptable analysis pipelines. These scripts facilitate seamless integration with existing workflows, allowing researchers to tailor the analysis to specific datasets or scientific inquiries. The modular nature of the scripts enhances flexibility and scalability for samples that produce a very low signal due to their limited thickness or beam sensitivity.

Results
Preliminary results demonstrate the efficacy of the proposed approach in extracting detailed compositional information from a population of nanocrystals in sets of STEM hyperspectral datasets. A halide replacement effect through a jump-the-gap mechanism is observable as the nanocrystal population generally splits into the two populations, with some outlier values that can be studied in detail in further work. A study of the lateral size distribution is carried out across all the nanocrystals of different chemical compositions of multiple samples, tracking the morphology through chemical conversion. Furthermore, a frame-by-frame analysis is employed to study the effect of the electron

dose damage on the chemical composition of the nanocrystals, finding similar behaviour for different halide species.

Conclusion

The integration of machine learning with STEM hyperspectral datasets represents a significant advancement in nanocrystal analysis. By combining state-of-the-art algorithms with open-source platforms and modular scripting, researchers can unlock new insights into the complex world of nanomaterials through high-throughput data processing algorithms. This flexible algorithm can be customised and developed towards automated in-line analysis in the future.

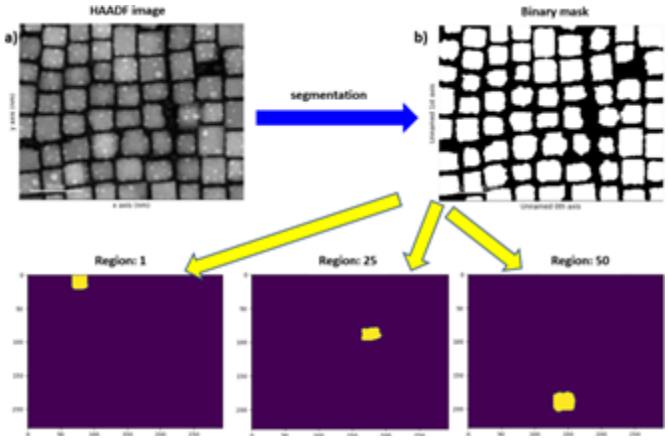

Keywords:

electron microscopy, STEM-EDX, machine learning

Reference:

[1] N. Livakas et al., “CsPbCl3 → CsPbI3 Exchange in Perovskite Nanocrystals Proceeds through a Jump-the-Gap Reaction Mechanism,” J. Am. Chem. Soc., Sep. 2023, doi: 10.1021/jacs.3c06214.
[2] zsylvester, “Segment Every Grain (SEG) algorithm.” Accessed: Sep. 07, 2023. [Online]. Available: https://github.com/zsylvester/segmenteverygrain.
[3] F. de la Peña et al., “hyperspy/hyperspy: Release v1.7.3.” Zenodo, Oct. 2022. doi: 10.5281/zenodo.7263263.

934

Automatic signal clasification of the Low-Loss Region in Electron Energy Loss Spectroscopy

Vanessa Costa-Ledesma[1], Daniel del-Pozo-Bueno[1], Catalina Coll Benejam[2], Josep Nogués[2], Borja Sepulveda[3], Laura Bocher, Mathieu Kociak[4], Javier Blanco-Portals[1], Sònia Estradé Albiol[1], Francesca Peiró[1]
[1]LENS-MIND, Dept. d'Enginyeria Electrònica i Biomèdica and Institute of Nanoscience and Nanotechnology (IN2UB), Universitat de Barcelona, Barcelona, Spain, [2]2Catalan Institution for Research and Advanced studies, ICREA Academia, Bellaterra, Spain, [3]3Instituto de Microelectrónica de Barcelona (IMB-CNM, CSIC)Campus UAB, Bellaterra, Spain, [4]4Laboratoire de Physique des Solides (LSP), Microscopie électronique STEM, Orsay, France

Poster Group 2

Localised Surface Plasmon Resonance (LSPR) is a non-propagating electron-density wave that is confined at the surface of a metallic nanoparticle. They can enhance the electromagnetic radiation, concentrating it into sub-wavelength volumes. Its resonance can be tuned by changing the surrounding medium and its geometry. This unique property opens a wide range of applications across various fields of applied research.
Electron Energy Loss Spectroscopy (EELS) within a Scanning Transmission Electron Microscope (STEM) has revealed remarkable capabilities in the analysis of plasmons at nanometric scale, as this technique achieves sub-angstrom spatial resolution and can excite the complete range of LSPR modes supported by the nanostructure. By employing EELS, the plasmonic properties can be correlated with geometric or structural characteristics, enabling a more comprehensive understanding of the plasmonic response.
In this study, based on the analysis of Silicon/Gold nanopillars samples, we demonstrate that clustering techniques can be used for detecting LSPRs in EELS. We propose a novel combination of unsupervised machine learning strategies that detect LSPRs in EELS spectrum images. To demonstrate the effectivity of this methodology, we studied Si/Au nanopillars. The detection of LSPRs is done by reducing the dimensionality of the data, clustering this low-dimensional space, and recuperate the spatial space. We demonstrate that using this methodology, it is possible to recover the LSPRs, among distinct spectra in a large EELS dataset, and easily make a plasmonic spatial map without the need for prior knowledge or labelling of the data.

Keywords:

EELS, Plasmons, Nanowires

973

Interpretable evaluation of STEM images of nanostructures via homology analysis

Mr. Ryuto Eguchi[1,2], Dr. Yu Wen[1,2], Dr. Ayako Hashimoto[1,2]
[1]National Institute for Materials Science, Tsukuba, Japan, [2]University of Tsukuba, Tsukuba, Japan

Poster Group 2

Background incl. aims
Recently, a mathematical framework called persistent homology (PH) has made it possible to quantify materials structural information at a wide range of scales, from the atomic to the nanoscale. PH quantitatively expresses the hole structures of data in terms of their number and scale. Particularly, it is highly suited for discerning the subtle order within inhomogeneous structures, such as amorphous [1] and glass materials [2]. Until now, PH analysis has predominantly focused on three-dimensional atomic arrangements; however, it is also feasible on two-dimensional image data. Here, we applied PH analysis for two-dimensional TEM images, representing a highly useful approach in structural analysis.
In our previous works [3,4], the homological feature known as 'Betti number' was applied for structures of self-assembled Pt/CeO_2 nanocomposites, which were captured by scanning TEM (STEM). The N-th Betti number corresponds to the number of N-dimensional holes, such as connected components, rings (0- and 1-dimensional holes, respectively), and so forth. This homological feature could successfully quantify CeO_2 phase connectivity and further, relationship with the oxygen ion conductivity.
To explore more effective descriptor for the nanostructures, we apply one of the most used PH methods, Persistent Diagram (PD). The key concept in PD lies in tracking the scale required for the appearance (birth, b) and disappearance (death, d) of the N-dimensional holes by continuous deformation of object which called ‘filtration’. Consequently, it includes information on the shapes of the N-dimensional holes, unlike the Betti number. We aim to demonstrate its effectiveness for nano-structural analysis and extract important homological feature for classifying the Pt/CeO_2 nanostructures. To ensure both quantitativity and interpretability, we employed a consistent approach that directly extract interpretable features from PDs.

Method
Firstly, Pt/CeO_2 nanocomposites were synthesized by the annealing of the Pt_5Ce alloy. The 12 nanocomposites with various nanostructures were prepared by changing annealing temperature (500, 600, and 700℃) and syngas ratio (CO:O2 = 0:1, 1:1, 2:1, and 3:1). The nanostructures were characterized through STEM (JEM-2100F, JEOL, Japan) operating at an acceleration voltage of 200 kV. Then, the obtained images were binarized and noise-removed with the OpenCV library in Python. The sequential procedures related to PD acquisition, vectorization for Principal Component Analysis (PCA) were conducted by using data analysis software “Homcloud” [5]. Finally, we used random forest method to find the most important descriptor for classifying Pt/CeO_2 nanostructures.

Result
The binarized STEM images clearly show the self-assembled Pt/CeO_2 nanocomposites that consist of Pt (white) and CeO_2 (black) phases. We focused on the CeO_2 phase for PH analysis to examine its relationship with oxygen ion conductivity. The nanostructures changed from a maze-like to a striped appearance as the annealing temperature increased. Their 0th and 1st PDs also changed depending on the structural changes.
To clarify the relationship between the structural changes and distribution changes of b-d points in PDs, we extracted five interpretable features, each based on the understanding of individual

quadrants in the 0th and 1st PD. The three features, the average width and total length of the striped CeO_2 phases, and the number of CeO_2 phases can be obtained from the 0th PDs. Their trends toward annealing temperature coincide with those from the actual STEM images. The number of ring and gulf-like structures can be obtained from the 1st PDs, focusing on negative and positive b region, respectively. These quantification with PDs could capture trends more clearly compared with conventional observation.
Furthermore, we conducted PCA with vectorized PDs to extract their critical information, which emphasizes the difference between homological features in structures. By the first and second principal components in the 0th and 1st PDs, the 12 nanostructures were relatively well categorized. Through PD reconstruction using the first principal components in the 0th and 1st PDs, we identified a critical region in the PDs: the region in the 1st PDs with d value smaller than characteristic size. In this critical region, d value corresponds to the size of the CeO_2 gulf-like phases. This result suggests that the number of small gulf-like phases is effective as a simple interpretable feature to differentiate Pt/CeO_2 nanostructures. Finally, we applied all interpretable features extracted from PDs thus far to a random forest classification and evaluated their importance. As a result, two key descriptors emerged: the width of the CeO_2 phase and the number of small gulfs. Remarkably, in the scatter plot of the two descriptors, the 12 nanostructures could be classified effectively. In this manner, using a few simple interpretable descriptors, we can more easily discuss and quantitatively evaluate the structural differences arising from variation in synthesis conditions, compared to PCA.

Conclusion

This study investigated the effectiveness of PH analysis in analyzing the STEM images of the nanostructures. Firstly, five interpretable features could be extracted directly from the 0th (the average width and total length of the striped CeO_2 phases, and the number of CeO_2 phases) and 1st (the number of ring and gulf-like structures of CeO_2 phase) PDs. Regarding the gulf-like structure, the PCA results suggest that the number of smaller structures than the characteristic size could particularly differentiate the 12 nanostructures. Finally, we showed that key descriptors can classify nanostructures through the random forest classification, enabling us to interpret their differences easily.

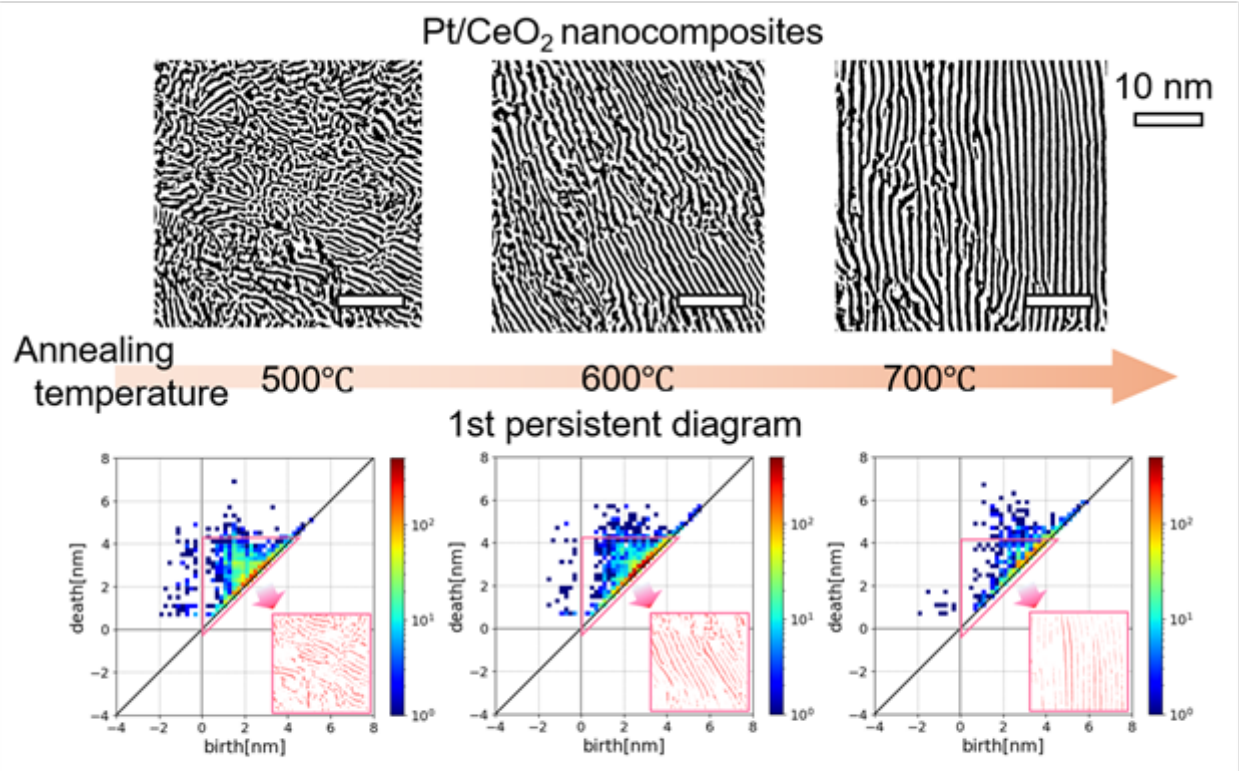

Binarized HAADF-STEM images of Pt/CeO_2 nanostructures synthesized at different temperature (top), and 1st PDs of their CeO_2 phases (bottom). The triangle regions in the 1st PDs indicate critical regions for classifying the nanostructures. Images insets show the result of inverse analysis on each Pt/CeO_2 nanostructures obtained from their triangle regions in the1st PDs.

Keywords:

persistent homology, interpretable machine learning

Reference:

[1] Y. Hiraoka, T. Nakamura, A. Hirata, E.G. Escolor, K. Matsue and Y. Nishiura, PNAS 113, 7035 (2016).
[2] T. Nakamura, Y. Hiraoka, A. Hirata, E.G. Escolar and Y. Nishiura, Nanotechnol. 26, 304001 (2015).
[3] Y. Wen, A. Hashimoto, A.S.B.M. Najib, A. Hirata and H. Abe, Appl. Phys. Lett. 118, 054102 (2021).
[4] Y. Wen, H. Abe, A. Hirata and A. Hashimoto, ACS Appl. Nano Mater. 4, 13602 (2021).
[5] Homcloud : https://homcloud.dev/

990

From volume electron microscopy datasets to segmentation models, feature quantification, and data reuse

Dr. Ilya Belevich[1], Kirk Czymmek[2], Johanna Bischof[3], Aastha Mathur[3], Lucy Collinson[4], Eija Jokitalo[1]
[1]University of Helsinki, Helsinki, Finland, [2]Donald Danforth Plant Science Center, Saint Louis, USA, [3]Euro-BioImaging ERIC Bio-Hub, EMBL, Heidelberg, Germany, [4]Francis Crick Institute, London, UK

Poster Group 2

Advancements in microscopy techniques have led to the generation of ever-increasing amount of data, demanding efficient analysis methods. Image segmentation tools, particularly those powered by Artificial Intelligence (AI), have become critical components for processing this data. However, segmentation is just the first step in unlocking the wealth of information hidden within these complex datasets. Quantitative analysis methodologies are essential for extracting meaningful biological insights.

Here delves into the power of AI-driven segmentation for quantitative analysis in electron microscopy. We demonstrate the segmentation of a U2OS cell FIB-SEM dataset [1] using a newly developed tools within Microscopy Image Browser (MIB) [2]. Our approach leverages the "segment-anything" model [3] for ground truth generation of training labels alongside a newly developed 2.5D deep learning workflow for image segmentation in DeepMIB tool [4] of MIB. This powerful combination allows for efficient generation of accurate models for various cellular organelles, including mitochondria, endoplasmic reticulum (ER), Golgi apparatus, nuclear envelope, lysosomes, and peroxisomes [5]. These models serve as the foundation for in-depth quantitative analysis.

Moving beyond segmentation, we explore potential analysis pathways. A typical pipeline might begin with volumetric analysis of organelles, providing valuable information about their size and distribution. This analysis can be further extended by developing custom methods to quantify specific features relevant to cell biology research. Examples include measuring the density of nuclear pores, quantifying the sheet-to-tubule ratio of the ER, or analyzing the contact points between ER and mitochondria.

In addition, we showcase the immense potential of large-volume electron microscopy data, extending its utility beyond the scope of the original research project. Sharing these datasets responsibly is crucial for unlocking their full potential and enabling broader scientific exploration. By fostering responsible data sharing practices [5], we can collectively extract even deeper insights from these rich datasets, leading to significant advancements in our understanding of cellular biology.

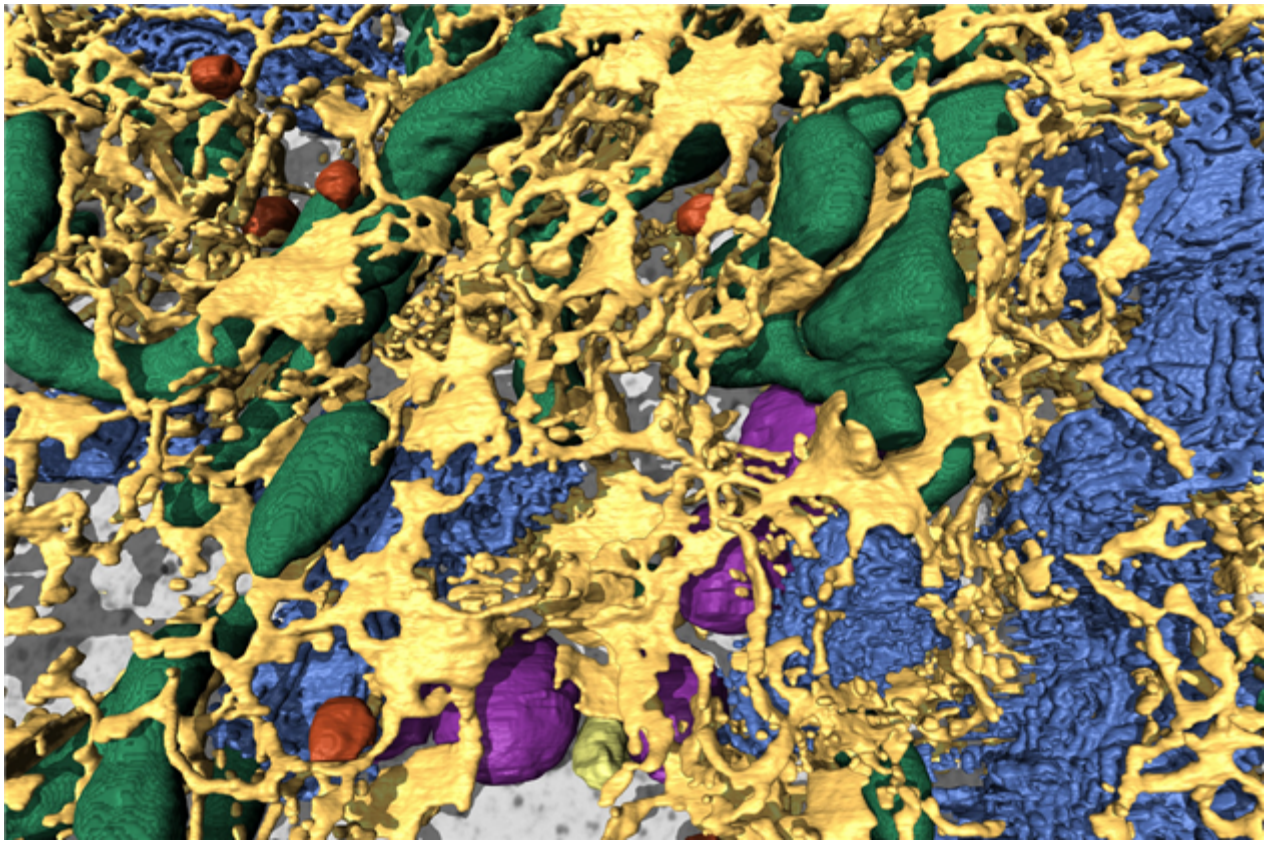

Keywords:

volume microscopy deep learning FIB-SEM

Reference:

1. Belevich I, Schertel A, Zaversek T, Szyrynska N, Saarnio S, Jokitalo E, Human bone osteosarcoma epithelial cell (U2-OS), EMPIAR, doi: 10.6019/EMPIAR-11746
2. Belevich I, Joensuu M, Kumar D, Vihinen H, Jokitalo E. Microscopy Image Browser: A Platform for Segmentation and Analysis of Multidimensional Datasets. PLoS Biol. 2016 Jan 4;14(1):e1002340. doi: 10.1371/journal.pbio.1002340
3. Kirillov A, Mintun E, Ravi N, Mao H, Rolland C, Gustafson L, Xiao T, Whitehead S, Berg AC, Lo W-Y, Dollár P, Girshick R, Segment Anything, arXiv:2304.02643, doi: 10.48550/arXiv.2304.02643
4. Belevich I, Jokitalo E. DeepMIB: User-friendly and open-source software for training of deep learning network for biological image segmentation. PLoS Comput Biol. 2021 Mar 2;17(3):e1008374. doi: 10.1371/journal.pcbi.1008374
5. Czymmek KJ, Belevich I, Bischof J, Mathur A, Collinson L, Jokitalo E., Accelerating data sharing and reuse in volume electron microscopy. Nat Cell Biol. 2024 Apr 12. doi: 10.1038/s41556-024-01381-3

1019

Quantitative Elemental Mapping Of Bimetallic Nanoparticles From Atomic Scale STEM-HAADF Images

Adrien Moncomble[1], Damien Alloyeau[1], Guillaume Wang[1], Nathaly Ortiz-Peña[1], Hakim Amara[1,2], Riccardo Gatti[2], Maxime Moreaud[3], Christian Ricolleau[1], Jaysen Nelayah[1]
[1]Université Paris Cité / CNRS, Paris, France, [2]Université Paris-Saclay / CNRS, Chatillon, France, [3]IFP Énergies Nouvelles, Solaize, France

Poster Group 2

Background incl. aims
Alloying of metal at the nanoscale is often used to enhance nanoparticles' physical/chemical properties and engineer new ones leading to multimetallic nanoparticles (NPs) with different chemical structures [1]. Access to composition is paramount for a fundamental understanding of nanoalloys' chemical and physical properties. In transmission electron microscopy (TEM), particle composition can be accessed by spectroscopic techniques such as energy-dispersive X-ray spectroscopy (EDX). However, EDX requires a set-up with a high-brightness electron source and wide-angle detection to collect as much signal as possible. Even then, if we work at atomic resolution, the quantification of the composition of atomic columns is possible but limited as there is a lot of noise as compared to signal [2]. A promising alternative for quantitative composition determination is atomic-resolution high-angle annular dark field scanning TEM (HAADF-STEM) with strong compositional sensitivity [3]. In this contribution, we propose an innovative method to quantify the composition of individual atomic columns in bimetallic NPs from their intensities in 2D HAADF-STEM images using deep learning.

Methods
In this work, we studied CuAu NPs between 5 and 10 nm synthesized via pulsed laser deposition (PLD). The HAADF STEM images were acquired on a double-corrected cold FEG JEOL ARM 200F. Elemental composition from individual columns was retrieved from the corresponding HAADF signal with regression-based deep learning, U-Net [4]. The network was trained on simulated images, obtained with a multislice algorithm, and their corresponding elemental maps. The predicted elemental maps were compared to the ground truth STEM EDX profiles to assess the accuracy of our methods.

Results
Multislice simulations show that the aberration-corrected HAADF-STEM intensity of atomic columns is influenced by their composition, atomic configuration, and thickness. As these parameters are intertwined, a simple regression-based statistical analysis of the local variations of intensity is not enough to access the full underlying information. Therefore, we developed a deep learning approach with U-Net to be able to disentangle the complex relation of these parameters and predict the composition of atomic columns of the whole particle [Figure 1]. We show that for robust prediction the training dataset is of paramount importance and it needs to span across all possible configurations from the size, and shape, up to the composition and ordering of the atoms. Here, we will present the implementation of this method for the study of chemically disordered and ordered CuAu NPs.

Conclusion

We have developed a deep-learning approach to predict the composition of bimetallic NPs at the atomic columns scale from a single HAADF-STEM image. Our method is adapted to high throughput and on-the-fly prediction which is suitable for in situ experiments. One other advantage of this method in comparison to EDX is the quantification of the composition without contaminating and damaging the NPs.

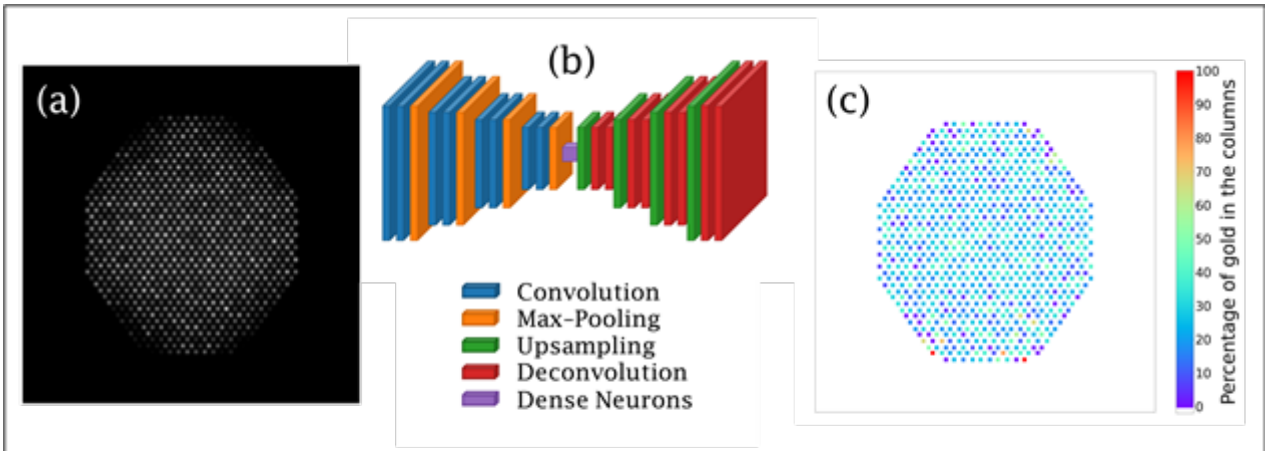

Figure 1 – Example of the prediction of the composition map using a U-Net. (a) Simulated HAADF STEM of a chemically disordered Cu3Au NPs. (b) U-Net CNN architecture. (c) Predicted map of the repartition of the Au in the image (a).

Keywords:

HAADF-STEM, Deep Learning, Bimetallic Nanoparticles

Reference:

[1] Ferrando, R., Jellinek, J. & Johnston, R. L., Chem. Rev. 108, 845–910 (2008).

[2] Breyton, G. et al., Phys. Rev. Lett. 130, 236201 (2023).

[3] Crewe, A. V., Wall, J. & Lanomore, J.,Science 168, 1338–1340 (1970).

[4] Ronneberger, O., Fischer, P. & Brox, T., MICCAI 9351, 234-241 (2015).

1031

U-NET Enhanced 4D-STEM/PNBD: Advancing Microscopy Image Reconstruction

Pavlina Sikorova[1], Miroslav Slouf[2], Radim Skoupy[1], Ewa Pavlova[2], Vladislav Krzyzanek[1]
[1]Institute of Scientific Instruments, Czech Academy of Sciences, Brno, Czech Republic, [2]Institute of Macromolecular Chemistry, Czech Academy of Sciences, Prague, Czech Republic

Poster Group 2

Background
This work is focused on our recent improvements of 4D-STEM/PNBD method (Four-Dimensional Scanning Transmission Electron Microscopy/Powder NanoBeam Diffraction) [1-3], which provides a user-friendly way to use a modern SEM as a fast powder electron diffractometer. SEM must be equipped with a 2D-array detector of transmitted electrons (pixelated STEM detector). The pixelated detector yields standard STEM/BF images in the form of a standard scanning matrix. Moreover, each position within the scanning matrix is a 2D nanobeam diffraction pattern, which is captured thanks to the 2D-array of pixels within the pixelated detector. In 4D-STEM/PNBD method, the sum of the post-processed individual diffraction patterns is then used to obtain powder diffractogram.
The reduction of the 4D-STEM dataset to 2D-powder diffractogram and eventually to its 1D-radially averaged profile can be automated by means of our open-source Python packages STEMDIFF and EDIFF. The latest available versions support fast parallel processing on multiple cores, user-friendly Jupyter notebook interface and independence from any third-party software.
The current development aims to improve individual diffraction patterns so that even samples usually very challenging to study (such as specimens with high amorphous background and low diffraction power) can be processed satisfactorily. The 4D-STEM-in-SEM datasets of these difficult samples can be quite challenging to process and get the diffraction patterns that could compete with the quality of standard TEM/SAED diffractograms. Conventional image enhancement methods have failed because they cannot remove the background and noise without affecting the diffraction intensities. Therefore, deep learning methods were used to develop a model that would sufficiently suppress unwanted image deterioration. In this contribution, we introduce a U-Net Autoencoder (U-NAE) for noise and background removal in 4D-STEM-in-SEM complex datasets.
Methods
As the ideal target 4D-STEM-in-SEM data (clean, noise- and background-free diffractograms) were not available, an artificial dataset must have been simulated. The synthetic target data were derived from actual datasets of several different crystals (network input data) using multi-scale filtering, image transformations, thresholding, and manual corrections (a lengthy and inefficient procedure). After collecting the paired dataset (input/target data), each was split into 3 sub-datasets – 60% for training, 30% for validation and 10% for testing. Then finally, an architecture of a denoising neural network could have been designed. Given the limited dataset, the convolutional U-Net architecture was a suitable choice because it can find key features in the data from which it reconstructs the desired output. It consists of three parts – encoder (contracting path which captures contextual information), bottleneck (low-dimensional representation of the input), and encoder (extending path generating a clean image from the bottleneck representation).
The U-NAE encoding part consists of 3 blocks of convolutional layers that reduce the input image of size 256x256x1 to a feature map of size 32x32x64. This bottleneck-representation is then passed through the decoding part (3 blocks of convolutional layers which also work with the information from the encoder transferred by skip connections and reconstruct the data to its original resolution). At the end, there are 3 fully-connected convolutional layers that fine-tune the output.
The model was trained using ADAM optimizer with mean squared error (MSE) as the criterial function. Additional metric to monitor for model performance assessment was mean absolute error

(MAE). The validation loss after each epoch was the key score when assessing the network's learning state, as it is indicative of its generalization capabilities and how well it performs on newly introduced data. Training data was fed to the network in batches of 32 images, and the learning rate was adapting during training as it was designed to gradually decrease when approaching the global optimum.

Results

During training, the model's validation MSE dropped from 8135.73 to 25.31, and the MAE from 23.58 to 2.47. The model with the lowest validation loss was saved to avoid possible overfitting in the final training epochs. It was then tested on a test dataset that had not yet been introduced to the network and has shown to improve the quality of datasets acquired by our 4D-STEM-in-SEM technique, even for the challenging samples. Clear evidence of the functionality of U-NAE is shown in Fig. 1, where even for the most primitive method of obtaining a diffractogram (simple summation) the improvement in the quality of the output image is clearly visible, as well as the noticeable improvement of the radial distributions of the diffractograms.

Conclusion

The U-NAE has been proven effective on various challenging datasets, yet limitations arise in handling heavy noise levels, potentially leading to unsatisfactory results. Future efforts will prioritize optimizing the U-NAE architecture to address these challenges and explore alternative training strategies to enhance its performance. Incorporating domain-specific knowledge may further broaden its applicability in material science research. In addition, further work to refine the simulation of the target data could also improve model performance.

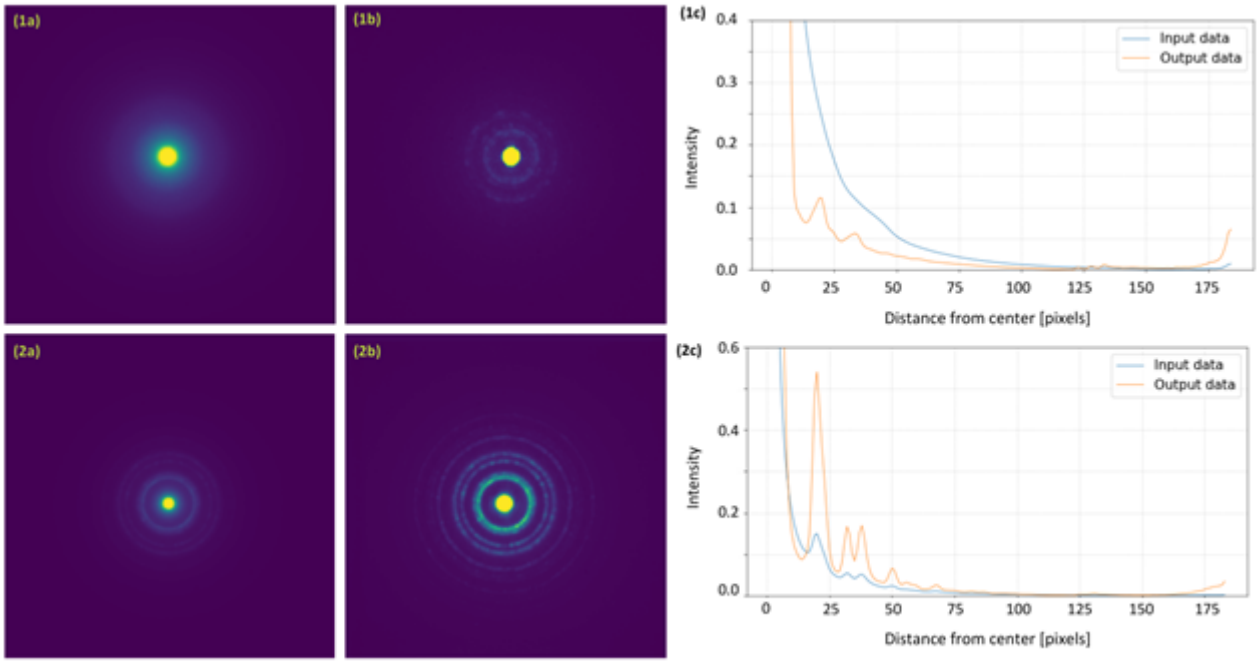

Figure 1: Comparison of diffraction patterns for FeO (1) and Au (2): summation of original diffractograms (a), summation of U-NEA denoised diffractograms (b), comparison of radially averaged diffraction patterns (c)

Keywords:

4D-STEM-in-SEM, U-NET, 4D-STEM/PNBD, diffraction, denoising

Reference:

[1] Slouf M et al.: Nanomaterials 11 (2021) 962, doi: 10.3390/nano11040962
[2] Slouf M et al.: Materials 14 (2021) 7550, doi: 10.3390/ma14247550
[3] Skoupy R et al.: Small Methods 7 (2023) 2300258, doi: 10.1002/smtd.202300258

Acknowledgement: This work was supported by the Technology Agency of the Czech Republic (project TN02000020), the Czech Science Foundation (project 21-13541S) and the Czech-BioImaging large RI project (LM2023050 funded by MEYS CR).

1074

Label-free biological composition predictions in EM images

Msc Stijn Karaçoban[1], PhD Ryan Lane[1], MSc Daniel Spengler[2], BSc Anouk Wolters[3], Associate Professor Carlas, S. Smith[2], Associate Professor Jacob, P. Hoogenboom[1]
[1]Imaging Physics, Delft University of Technology, Delft, The Netherlands, [2]Delft Center for Systems and Control, Delft University of Technology, Delft, The Netherlands, [3]Cell Biology, University Medical Center Groningen, Groningen, The Netherlands

Poster Group 2

Background incl. aims
Large-scale and volume electron microscopy (EM) allow biologists to understand structural relations in biological systems from the nanometer up to the millimeter scale and beyond. However, EM data can be difficult and time-consuming to interpret and process due to a lack of biological specificity. Fluorescence microscopy (FM) can be used together with EM in correlative light and electron microscopy (CLEM) to add biologically relevant data to the EM images. CLEM does come at the cost of increased complexity and restrictions in sample preparation and measurement workflow. Furthermore, high-throughput EM methods like multi-beam scanning electron microscopy (MB-SEM) can be hard to combine with CLEM. We aim to develop a machine-learning model that can extract biologically relevant information from EM images, which is generalisable to different methods of EM.
Methods
Convolutional neural networks (CNNs) have been shown to perform well on various image-translation tasks in biomedical contexts. We explored the use of a CNN to extract biological information from EM images by imitating real fluorescence. We used a network architecture inspired by U-net, only with a truncated up-sampling arm to account for the resolution mismatch between EM and FM data. The network, named CLEMnet, was trained on CLEM datasets obtained using an integrated array tomography workflow. The dataset consists of rat pancreas tissue samples. The islet of Langerhans was stained with Hoechst, which binds DNA and RNA and immunolabeled for insulin using Alexa 594.
In regular EM, it can take a long time to acquire large volumes of EM data. To solve this, high-throughput EM methods have been developed. One of these methods is multi-beam optical scanning transmission electron microscopy (MB-OSTEM). In MB-OSTEM, contrast is generated by the number of transmitted electrons. As CLEMnet is only trained on data from one microscope, using only backscatter electrons as a detection method, it is not directly applicable to datasets imaged under different conditions like with OSTEM. To still be able to use CLEMnet with MB-OSTEM data, we propose to transform the MB-OSTEM data such that it appears as backscatter electron (BSE) SEM using another CNN. Imaging biological samples using EM introduces beam damage into the sample. This makes generating training data for a CNN by sequential imaging in both an SEM and MB-OSTEM unviable, as the damage would appear during the second acquisition. Using generative adversarial networks (GANs), a network structure called Cycle-GAN can perform image-to-image translation tasks without the need for paired training data. We thus trained a Cycle-GAN network to be able to transform MB-OSTEM data such that it becomes similar to BSE SEM images, like the ones CLEMnet is trained on. This could thus allow for the automatic extraction of biologically relevant data from high-throughput EM techniques.
Results
Network predictions of CLEMnet show a good qualitative agreement with the recorded fluorescence signal. By superimposing the recorded and predicted signals, we can see overlap between the recorded and predicted signals. The Hoechst signal is localised to nuclei and the endoplasmic reticulum. The network trained on the immunolabeled insulin is capable of distinguishing between the different types of granules in the sample. Quantitative network performance was evaluated using

the Pearson correlation coefficient (PCC). The Hoechst-based network achieved a PCC of 0.51, and the Insulin-based network achieved a PCC of 0.765. The PCC serves as an indication of network performance. Still, inaccuracies in the recorded dataset, like inaccuracies in the EM-FM registration and bleed-through from the different fluorescent stains, can result in a spurious reduction of the PCC.

The OSTEM training data for the Cycle-GAN contains numerous staining artefacts. Despite this, we can qualitatively see that Cycle-GAN is able to translate OSTEM data into BSE SEM-like data. Furthermore, when CLEMnet trained on the Hoechst dataset is applied to this translated data, we can see that the resulting signal is localised to the nuclei and ER as expected.

Conclusion

Preliminary results demonstrate our ability to use a CNN trained on BSE SEM data to extract biologically relevant data from OSTEM images. Future work will look into extending this to MB-OSTEM data. In this future work, we will acquire a CLEM dataset using MB-OSTEM to be able to quantitatively compare the predicted signal from CLEMnet to real fluorescence data when applied to translated MB-OSTEM data. This work could help to make the interpretation and analysis of large-scale EM data more approachable, as CLEMnet is able to provide biological context to EM datasets.

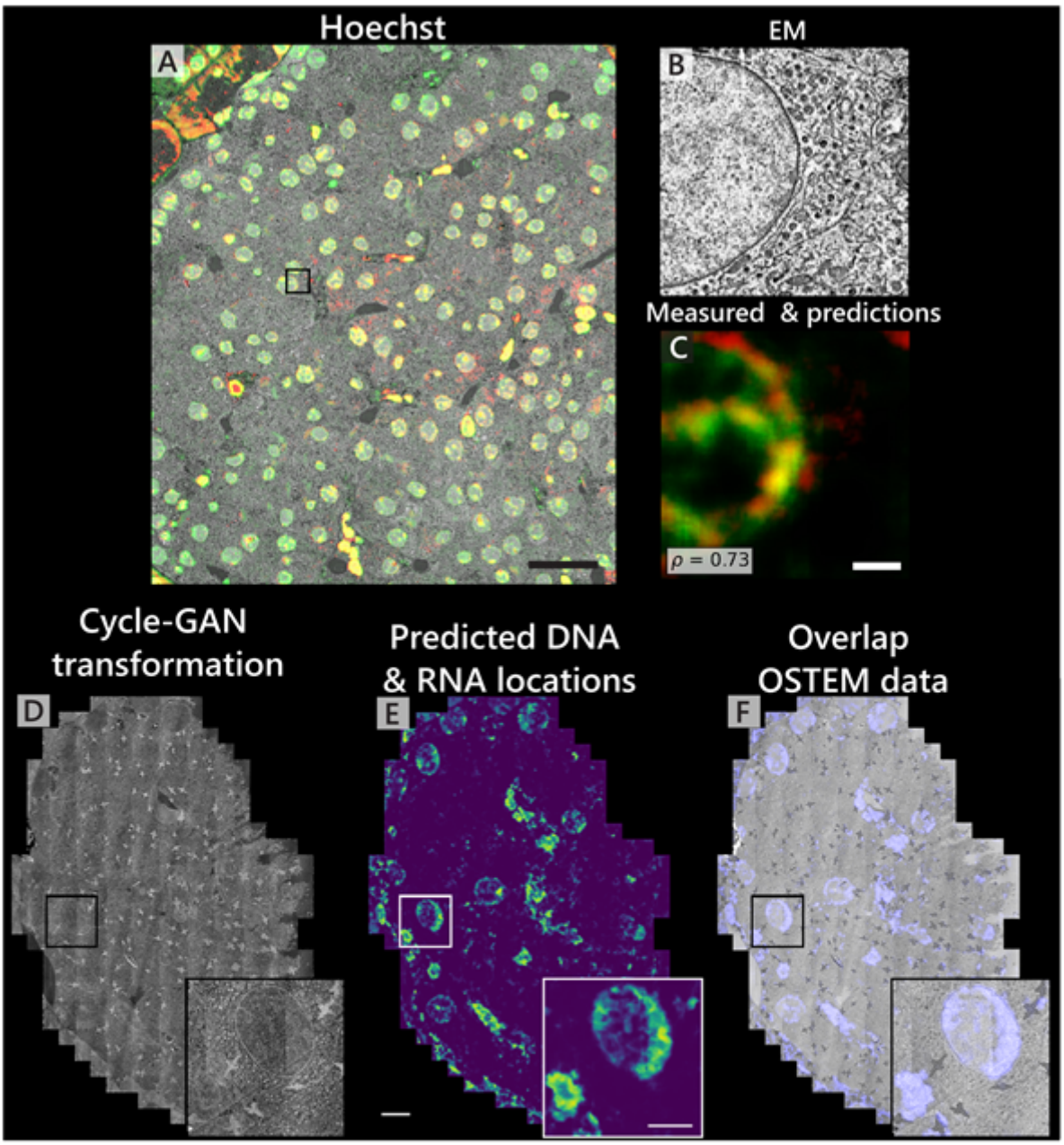

Figure 1. CLEMnet prediction for the localization of DNA & RNA. **A)** Overlap of measured Hoechst signal (red), network prediction (green) and EM data (gray). **B)** zoom inset showing the EM data. **C)** Inset overlapping prediction (green) and measured (red). **D)** OSTEM image transformed by a Cycle-GAN to imitate BSE SEM images. **E)** CLEMnet predictions on D. **F)** Overlap between the original OSTEM data and the CLEMnet preditions on the transformed data. **scale bars: A)** 20µm **B-C)** 1µm **D-F)** 10µm.

Keywords:

CLEM, Machine learning, transfer learning

Reference:

Kievits, A. J., Lane, R., Carroll, E. C., & Hoogenboom, J. P. (2022). How innovations in methodology offer new prospects for volume electron microscopy. Journal of microscopy, 287(3), 114–137. https://doi.org/10.1111/jmi.13134

Ronneberger, O., Fischer, P., & Brox, T. (2015). U-net: Convolutional networks for biomedical image segmentation. In Medical image computing and computer-assisted intervention–MICCAI 2015: 18th international conference, Munich, Germany, October 5-9, 2015, proceedings, part III 18 (pp. 234-241). Springer International Publishing.

Lane, R., Wolters, A. H., Giepmans, B. N., & Hoogenboom, J. P. (2022). Integrated array tomography for 3D correlative light and electron microscopy. Frontiers in Molecular Biosciences, 8, 822232.

Lane, R. (2022). Integrated Array Tomography: Development and Applications of a Workflow for 3D Correlative Light and Electron Microscopy. https://doi.org/10.4233/UUID:951AFAEB-1F03-45CB-8A86-CACBF9CA0F64

Zhu, J. Y., Park, T., Isola, P., & Efros, A. A. (2017). Unpaired image-to-image translation using cycle-consistent adversarial networks. In Proceedings of the IEEE international conference on computer vision (pp. 2223-2232).

1099

Deep learning-based single cell volume segmentation for soft X-ray microscopy data

Valentina Alberini[1,2], Aurélie Dehlinger[1,2], Dr. Christian Seim[1,2], Dr. Holger Stiel[2,3], Dr. Antje Ludwig[4], Prof. Dr. Birgit Kanngießer[1,2]
[1]Technische Universität Berlin, Berlin, Germany, [2]Berlin Laboratory for innovative X-ray technologies (BLiX), Berlin, Germany, [3]Max-Born-Institute (MBI), Berlin, Germany, [4]Charité Universitätsmedizin Berlin, Berlin, Germany

Poster Group 2

Background and Aims:
Soft X-ray microscopy within the water window spectral range offers non-destructive imaging capabilities with nanometer resolution and a penetration depth of up to 10 µm. This enables the investigation of biological samples in a near native state in three dimensions. The interpretation of X-ray microscopy images of biological cells can be challenging due to the similar absorption characteristics of carbon-based structures within these samples. To address this challenge, we have developed a contrast enhancement protocol, to improve the interpretability of the acquired images. Subsequently, an efficient segmentation technique based on deep learning is deployed for the extraction of biologically relevant information from the large amount of data generated by fast tomogram acquisition.
Methods:
We employed a laboratory-based soft X-ray microscope operating within the water window (500 eV photon energy). To enhance the contrast in acquired images, we developed a contrast enhancement protocol incorporating an adaptation of the Paganin filter as well as an unsharp masking filter. Additionally, we deployed a neural network model utilizing a U-Net architecture for the segmentation of THP-1 cell tomograms. This approach leverages the natural higher contrast of lipid membranes to facilitate segmentation.
Results:
The implementation of the contrast enhancement protocol resulted in improved contrast-to-noise ratios, thereby enhancing the interpretability of acquired images. Moreover, the neural network-based segmentation technique efficiently extracted biologically relevant information from tomograms, as confirmed by organelle volume calculations that align with tabular data. This segmentation can enable quantitative insights at the subcellular level, including the location and distances between different organelles, as well as their concentrations.
Conclusions:
Our study offers a comprehensive approach to soft X-ray microscopy analysis, addressing challenges in image interpretation and data segmentation. The developed contrast enhancement protocol and segmentation techniques facilitate efficient and accurate investigation of biological samples at the sub-cellular level. For the generalization of the segmentation process, increasing both the volume and quality of the data, as well as refining sample preparation, is necessary. Nevertheless, our advances contribute to analyse soft X-ray microscopy data more efficiently.

Keywords:

Soft X-ray microscopy; Tomography; Segmentation;

Reference:

[1] Dehlinger, A. et al., (2020). Microscopy and Microanalysis, 26, 1124
[2] Dyhr, M. C. A. et al., (2023). Proceedings of the National Academy of Sciences, 120, e2209938120
[3] Paganin, D. et al., (2002). Journal of Microscopy, 206, 33

1173

Development of an automated pipeline for segmenting and analyzing organelle contacts in Volume Electron Microscopy.

Miss Analle Abuammar[1], Miss Odara Medagedara[1], Mr Aaran Vijayakumaran[1], Mr Vito Mennella[1], Mr Kedar Narayan[2]
[1]University of Cambridge, Cambridge, United Kingdom, [2]National Cancer Institute at NIH center for cancer research, Bethesda , United States

Poster Group 1

Background incl. aims
Volume electron microscopy (vEM) is recognized as a powerful imaging tool capable of providing detailed insights into the 3D structure of cells, tissues, and model organisms at the nanometer scale. However, the manual segmentation process required for analyzing vEM datasets is time-consuming and limits the application and throughput of this technique. In response, this study aims to address these limitations by implementing deep learning approaches for automated segmentation based on a Panoptic-DeepLab (PDL) architecture. Specifically, the researchers aim to develop an automated segmentation workflow using Empanada-Napari plugins for reconstructing airway cells and efferent ductules of the male reproductive system in 3D. Furthermore, the study seeks to demonstrate the adaptability of these tools for generating tissue and organelle-specific segmentation models trained on relatively few 2D images, with the goal of improving efficiency and accuracy.
Methods
The researchers employed a deep learning-based approach utilizing the PDL architecture for automated segmentation of vEM datasets. Empanada-Napari plugins were developed to facilitate the 3D reconstruction of airway cells and efferent ductules, originally designed for segmenting mitochondria. The segmentation models were trained on a limited number of 2D images, highlighting a strategy for achieving robust results with minimal training data. Additionally, custom Python scripts were developed to extract cells of interest from the automatically segmented volumes, enabling single-cell quantitative analysis. Adapted image analysis methods were utilized to quantify spatial relationships between distinct organelles within the cell volume, including identifying points of contact on both semantic and instance segmented objects.
Results
The study demonstrates the effectiveness of the automated segmentation workflow in accurately segmenting airway cells and efferent ductules from vEM datasets. The segmentation models, trained on a relatively small number of 2D images, yield exceptional results when compared to human-validated data. The developed tools enable precise quantitative analyses of cellular metrics such as volume, surface area, and number of organelles, enhancing understanding of cellular processes and functions. Furthermore, the adapted image analysis methods successfully quantify spatial relationships between organelles, providing insights into organelle topology within cells.
Conclusion
The automated segmentation workflow and accompanying tools presented in this study represent a significant advancement in the analysis of vEM data. By alleviating the laborious process of manual segmentation, these tools enhance the efficiency and throughput of vEM imaging, thereby enabling comprehensive studies of cellular structures and functions. The adaptability of the segmentation models to different tissues and organelles underscores their versatility and potential for widespread application in biological research. Overall, the study provides a robust framework for accurate and effective quantitative analysis of vEM data, offering unprecedented insights into mammalian cellular biology.

1284

AI-driven microscopy for analysis of xenotransplantation models

Dr Courtney Wright[1], Professor Deniz Kirik[1]
[1]Brain Repair and Imaging in Neural Systems (B.R.A.I.N.S), Department of Experimental Medicine, Lund University, Sweden, Lund, Sweden

Poster Group 1

Background and Aims
Accurate visualization and quantification of immunohistochemical data is critically important in biological applications, particularly when requiring nuance within disease models and paradigms. Manual and single threshold methods are prone to bias, inaccuracy and are wholly inefficient over a large scale. The increased demand for accurate analysis of high throughput data acquisition becomes even more critical when modelling disease as results can influence the development of treatments and new therapeutics. Therefore, the aims of this work were to develop a highly accurate pipeline for image analysis of xenografted human cells to determine how pathology may develop in Parkinson's disease (PD) mouse models, utilizing AI-driven machine learning to accomplish these aims.
Methods
Immunofluorescent stained mouse tissue grafted with human derived cells were imaged using a widefield slide-scanner solution to train a deep neural network (DNN). Individual slides were loaded and scanned automatically using a 20x overview and target cells manually labelled to create initial training datasets. Of these datasets, 80% were used to train the DNN and 20% used for internal validation. Utilising instance segmentation with the ResNet50/FasteRCNN DNN we generated, this first trained iteration was applied over new datasets for automated tissue and cell detection with manual approval/quality control checks. Additional training and optimisation of the DNN was applied until a level of accuracy and acceptability was reached with low (<5%) errors detected.
Results
All grafts within scanned tissue were able to be accurately detected and cells of interest quantified. Initial training had accuracy at approximately 84% and required alterations to the scanning parameters to ensure high quality input data was used to train and improve the DNN accuracy. The developed DNN was additionally able to provide several critical readouts important for the analysis of pathophysiology as it relates to xenotransplantation models in PD. Area and size of grafts, migration of cells from the injection site, phenotyping and quantification of cells within the graft were able to be automatically detected and accurately analysed with the developed DNN.
Conclusion
Development of this AI driven microscopy solution for analysis of grafted cells within the brain has allowed for greater efficiency, accuracy and decreased bias within this animal model. By developing and training the above DNN, we were able to efficiently and accurately provide robust commentary on large dataset using a mouse model of human disease, improving our confidence in the results. This method could be applied widely to other models and similarly improve the accuracy and efficiency of data analysis as it applied to biological questions and potential downstream therapeutic development.

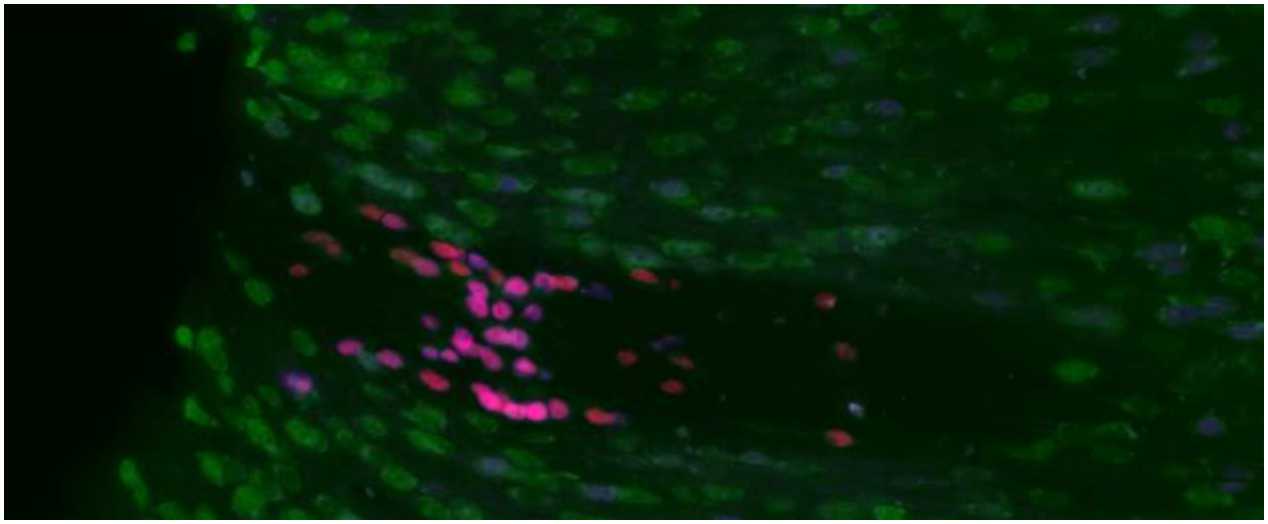

Keywords:

DNN AI xenotransplantation immunofluorescence widefield

1315

DELiVR: An end-to-end deep-learning pipeline for cleared-brain cell annotation

Moritz Negwer[1], Doris Kaltenecker[2], Rami Al-Maskari[2], Ali Ertürk[2]
[1]Radboudumc Nijmegen, Donders Institute for Brain, Behavious and Cognitionn, Nijmegen, Netherlands, [2]Institute for Tissue Engineering and Regenerative Medicine, Helmholtz Munich, Neuherberg, Germany

Poster Group 1

Background:
Automated detection of specific cells in three-dimensional datasets such as whole-brain light-sheet image stacks is challenging. Deep learning is a promising method for light-sheet image analysis, but only is as good as the training data for this specific dataset.

Methods:
We realized that virtual reality (VR) is an ideal approach to generate custom deep-learning training data. We found that VR-generated training data leads to better model performance, but more importantly is also generated much faster. We built DELiVR, a broadly applicable processing pipeline to segment arbitrarily labelled cells in light-sheet image stacks of cleared mouse brains.
We have open-sourced the entire pipeline, docker containers, FIJI plugin, and training data at https://discotechnologies.org/DELiVR/ .

Results:
Here, we present DELiVR, a virtual reality-trained deep-learning pipeline for detecting c-Fos+ cells as markers for neuronal activity in cleared mouse brains. Virtual reality annotation substantially accelerated training data generation, enabling DELiVR to outperform state-of-the-art cell-segmenting approaches. Our pipeline is available in a user-friendly Docker container that runs with a standalone Fiji plugin. DELiVR features a comprehensive toolkit for data visualization and can be customized to other cell types of interest, as we did here for microglia somata, using Fiji for dataset-specific training. We applied DELiVR to investigate cancer-related brain activity, unveiling an activation pattern that distinguishes weight-stable cancer from cancers associated with weight loss.

Conclusion:
Overall, DELiVR is a robust deep-learning tool that does not require advanced coding skills to analyze whole-brain imaging data in health and disease.

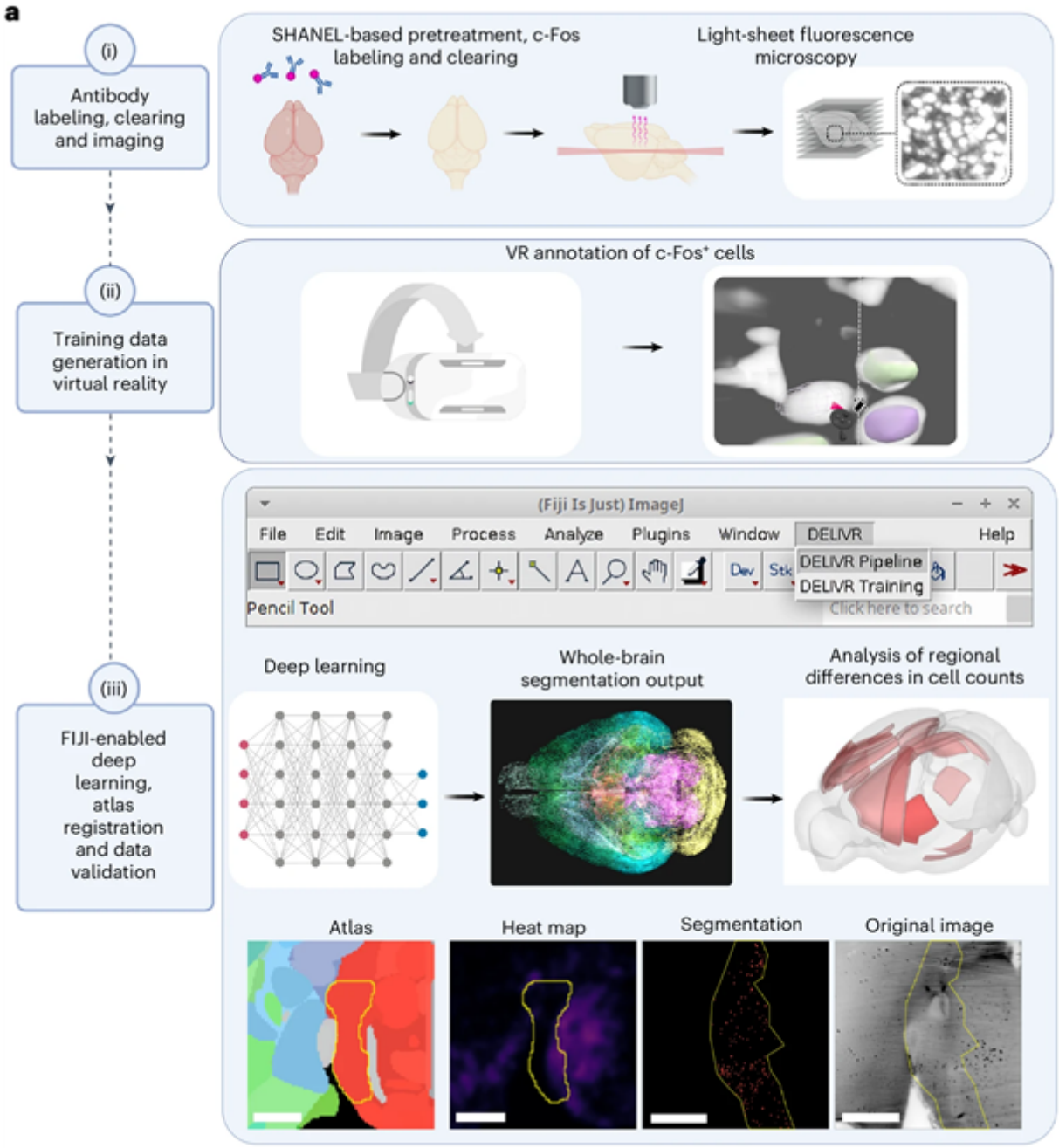

Keywords:

light-sheet, deep-learning, VR, virtual reality

Reference:

Kaltenecker, D., Al-Maskari, R., Negwer, M. et al. Virtual reality-empowered deep-learning analysis of brain cells. Nat Methods 21, 1306–1315 (2024). https://doi.org/10.1038/s41592-024-02245-2

1318

A pipeline for classification and segmentation of 3D quasi-ordered patterns rmormo

Dr. Luca Curcuraci[2], Konrad Handrich[1], Dr. Ronald Seidel[1], Dr. Peter Fratzl[2], Dr. Richard Weinkammer[2], Dr Luca Bertinetti[1]
[1]Technische Universität Dresden, Dresden, Germany, [2]Max Planck Institute of Colloids and Interfaces, Potsdam, Germany

Poster Group 1

Background incl. aims
Biological materials are of spectacular beauty and source of inspiration for principles of material design and synthesis. They are composed of a remarkable small number of simple building blocks which are often organized, at different length scales, in patches of periodic or quasi periodic units. Prominent examples are the cases of trabeculae in bone or skeletal elements of echinoderms, color-bearing photonics crystals structures in arthropods and pore systems in cuticular materials or bone. The structural features (3D texture) and orientation of the periodic/quasiperiodic units largely dictate the properties of the materials to which they belong. Yet, segmenting and classifying these regions in large 3D datasets --a prerequisite for a complete understanding of the material's properties-- is incredibly challenging. In fact, while it is relatively simple to obtain a binarized volume of the component these structures are made of (e.g. trabeculae, pores or channels etc...), it is not trivial to segment different regions with similar 3D organization and orientation or, even more so, recognize and classify those regions that exhibit the same texture but that are differently oriented with respect to each other.
Methods
To address this, we propose a pipeline that, with minimal supervision and without user bias, extracts, classifies and learns, in reciprocal space, 3D textural features from tomographic datasets. The learned features can then be used to segment out, in the real space, regions which differ by their structural regularity and spatial periodicity. Also, the proposed pipeline allows to easily identify regions of the dataset that are equivalent by rotation and quantitatively compare textural properties of different datasets.
Results
Using this pipeline, we were able to segment large tomographic datasets (in the order of 10^{10} voxels) of several different biological materials with minimal memory and storage imprint and user supervision. As an example, the graphic shows how the pipeline allows an unbiased and automatic segmentation of textural features in a sea urchin test plate (µCT dataset $4 \cdot 10^9$ voxels, top), lacuno-canalicular network in bone ($1.8 \cdot 10^9$ voxels, laser scanning confocal microscopy, bottom left) and a photonic crystal in weevils scales (FIB/SEM dataset $1.5 \cdot 10^9$ voxels, bottom right).
A segmentation of about 10^9 voxels dataset can be run in a few hours on a desktop PC with a small GPU (8GB of RAM) and 32 GB RAM.
Conclusion
The pipeline presented in this work allows the segmentation of large volumetric datasets that exhibit quasi-periodic features and is particularly useful in those cases where the aim of the imaging is to establish relationships between the structure and the function of the investigated.

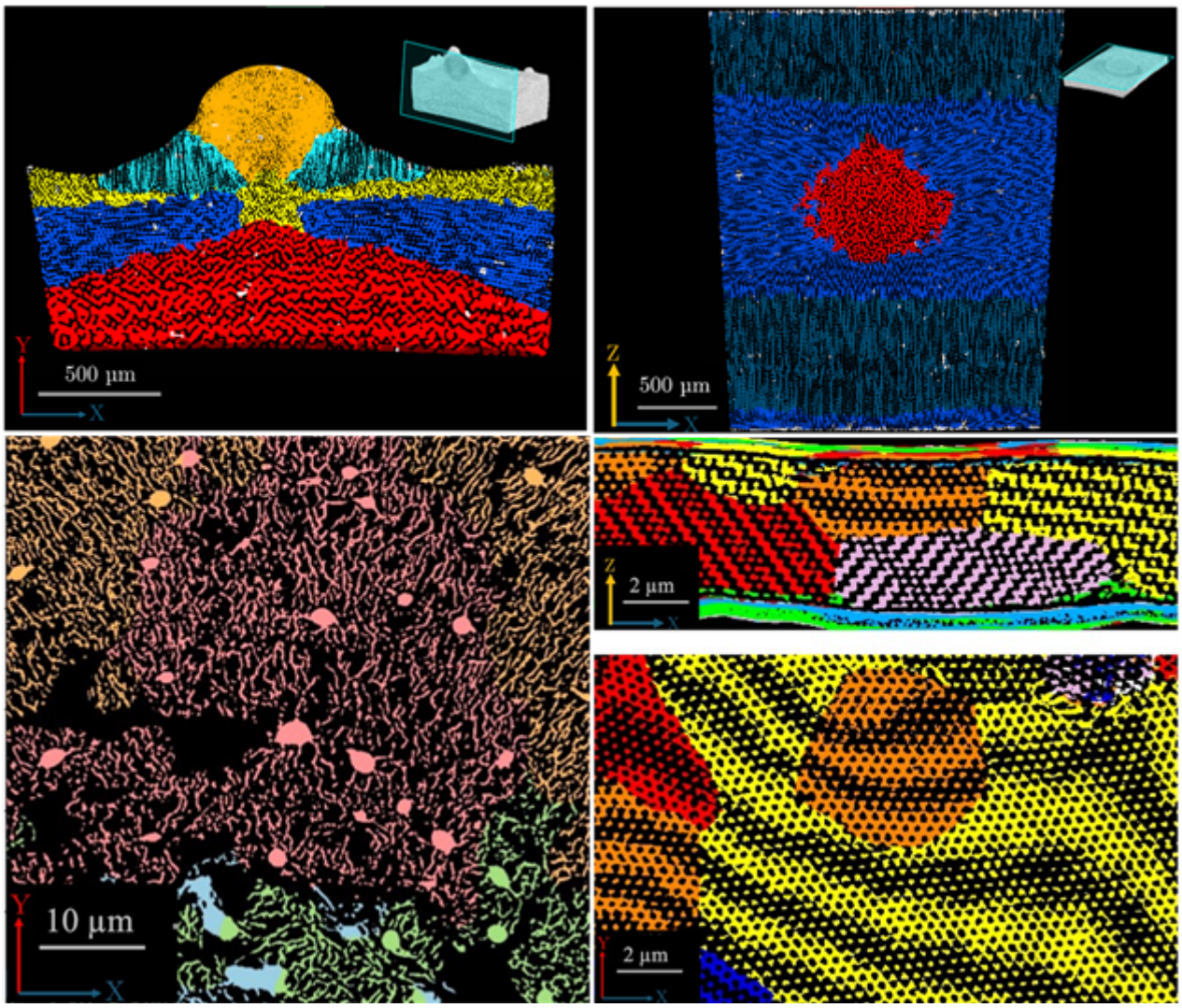

Keywords:

Tomography, machine-learning, segmentation, biological materials

1324

Advancements in Quantifying Neuroinflammation: Leveraging AI-Based Microscopy for Enhanced In Vivo Analysis in pharmaceutical studies

Dr Emilie Tresse-Gommeaux[1], Franziska Wichern[1], Lotte Frederiksen[1], Marie Barkai[1], Dr Morten Skott Thomsen Lindskov[1]
[1]Lundbeck, Valby, Denmark

Poster Group 1

Background
In the field of pharmaceutical research, accurately quantifying imaging data is essential. This precision is crucial for assessing neuroinflammation, a key factor in numerous neurological disorders. However, powered in vivo studies, especially for pharmacokinetics (PK) and pharmacodynamics (PD) evaluations, require utilizing large cohorts of animals. Additionally, recent technological advancements have significantly increased the capacity for multiplexing, allowing for more comprehensive data collection. This increase in data complexity poses new challenges for analysis.

Methods and Results
In our current studies investigating neuroinflammation, to manage and analyze the extensive data generated, we employ AI-based microscopy analysis. This innovative approach enables automated evaluation of drug efficiency in vivo, providing a robust and scalable solution for high-throughput studies. Our findings demonstrate the potential of AI-driven methodologies to streamline the analysis process, thereby enhancing the accuracy and efficiency of neuroinflammation assessments.

Conclusions
By integrating these advanced technologies, we pave the way for more in-depth research and faster, more precise therapeutic developments. The implications of our work extend beyond neuroinflammation, offering a framework for the application of AI in various bioimaging research areas. This approach not only improves the reliability of data interpretation but also significantly reduces the time and resources required for comprehensive analysis, ultimately accelerating the drug development pipeline and improving outcomes for patients.

Keywords:

neuroinflammation, histology, AI-based

1336

High throughput automated SEM imaging and feature identification using AI/ML models

Mr. Aloshious Lambai[1], Mr. Zeb Akhtar[1], Dr. Araujo Cesar[1], Dr. Supriya Nandy[1], Dr. Elina Huttunen-Saarivirta[1], Dr. Marko Mäkipää[1]
[1]VTT Technical Research Centre of Finland Ltd, , Finland

Poster Group 1

Background

Accelerated materials development requires integrating automation with Artificial intelligence (AI)/Machine learning (ML) based workflows along selection of material composition, production, characterization, and testing [1]. Each stage possesses unique possibility of incorporating automation and AI/ML models, supporting efficient experimental activities and ultimately computational modelling, and reducing time and cost. Materials Acceleration Platforms (MAPs) [2] address these possibilities. MAPs concept involves developing the methods for predicting optimal alloy compositions, the automation of manufacturing processes, and the implementation of advanced materials characterization techniques. Among these, the field of high-throughput characterization remains the least developed.

This work focuses on developing protocols for the automated imaging and defect detection in High-entropy alloys (HEA), through automated SEM imaging and AI/ML based models. The developed protocols are then extended to automated fatigue fracture surface analysis of 316L stainless steels and the detection of features such as facets, dimples, and striations.

Methods

Automated imaging was performed with a Zeiss Ultra plus SEM at an accelerating voltage of 15 kV. This developed facility allows imaging of random fields of HEA samples at the desired magnification using in-house developed code and SmartSEM macro functions. The collected images were segmented to identify defects and background information using a DeepLab-v3+ encoder-decoder architecture for semantic segmentation. The encoder extracts information from the input image through convolutional layers, while the decoder refines the segmentation results, thus capturing fine details and improving the localization of object edges. A dataset of 160 images (1024 x 768 pixels each) with annotated masks was utilized with 70%, 15%, and 15%, respectively, as training, validation, and test sets.

The developed SEM automation and AI/ML protocols in HEAs were subsequently applied to the fatigue fracture surfaces of fatigue of 316L stainless steels samples. Rather than inputting random fields in the case HEAs, user-defined feature selection from overview images and comprehensive fracture surface mapping of 316L stainless steels were utilized. Figure 1 illustrates the method employed for automated fracture surface imaging. Additionally, the ML algorithm developed for void detection are being refined to identify fatigue fracture surface features.

Results

With this guided automatic image acquisition, over 1000 images were captured at a rate of ~60 images per hour using SEM from multiple samples within 24 hours without human intervention. The AI/ML model predictions on the collecte data set demonstrated highly accurate segmentation of defects in images, with only minor deviations in a few instances, achieving scores of 0.994 for IoU (intersection over union) and 0.003 for dice loss, respectively. The predicted masks, generated within seconds, provide detailed information about the size, shape, and location of defects in the SEM

images, thereby aiding in the analysis and decision-making process for alloy optimization and characterization.

Conclusion and outlook

Integrating automation and AI/ML models facilitates rapid material development by streamlining the traditionally tedious workflows required for optimizing material properties. We developed techniques for high-entropy alloys (HEAs) and extended them to fracture surface analysis through automated SEM image acquisition and feature identification using AI/ML models. This approach minimizes human intervention, accelerates analysis, and significantly reduces the costs and time associated with these activities.

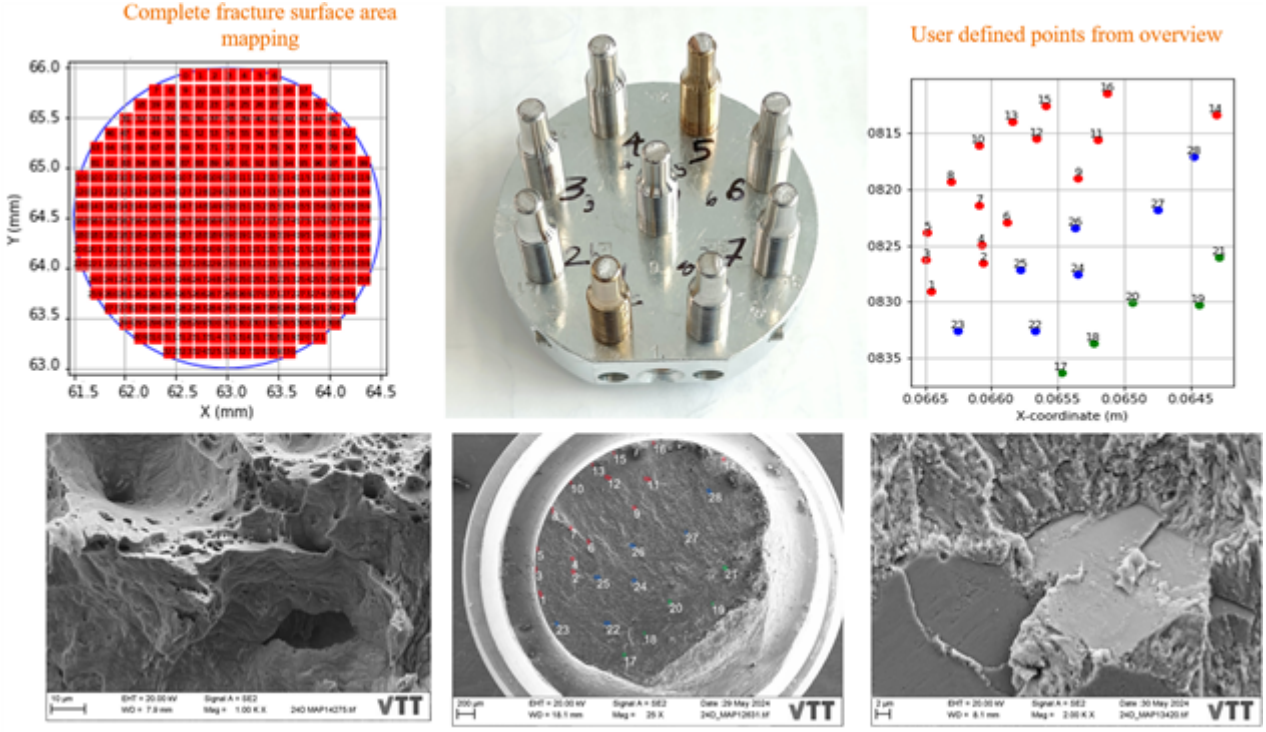

Keywords:

SEM, Alloys, Fracture surface, Automation

Reference:

1. E.O. Pyzer-Knapp, J.W. Pitera, P.W.J. Staar, S. Takeda, T. Laino, D.P. Sanders, J. Sexton, J.R. Smith and A. Curioni, Accelerating materials discovery using artificial intelligence, high performance computing and robotics. npj Comput. Mater., 2022, 8

2. Antikainen, A., Jokiaho, T., Kaunisto, K, Lambai, A., Laukkanen, A., Lindroos, T., Linnala, L., Mäkipää, M., Nandy, S., Pakarinen, J., Pinomaa, T., Tahkola, M. and Zeb, A. SOLID-MAP: development of a materials acceleration platform (MAP) for high entropy alloys (HEA) Under review. 2024